Title

Transforming a Macromolecular Therapeutic Factor into Small Molecules that Target its Transmembrane Receptors

Permalink

https://escholarship.org/uc/item/35q241wh

Author

Cheng, Guo

Publication Date

2015

Peer reviewed|Thesis/dissertation

UNIVERSITY OF CALIFORNIA

Los Angeles

Transforming a Macromolecular Therapeutic Factor into Small Molecules

that Target its Transmembrane Receptors

A dissertation submitted in partial satisfaction of the requirements

for the degree Doctor of Philosophy in

Molecular, Cellular, and Integrative Physiology

by

Guo Cheng

2015

ABSTRACT OF THE DISSERTATION

**Transforming a Macromolecular Therapeutic Factor into Small Molecules
that Target its Transmembrane Receptors**

By

Guo Cheng

Doctor of Philosophy in Molecular, Cellular, and Integrative Physiology

University of California, Los Angeles, 2015

Professor Hui Sun, Chair

Pigment Epithelium-Derived Factor (PEDF) is a natural factor with surprisingly diverse

therapeutic functions. Since its identification more than 20 years ago, PEDF has been recognized

as a neurotrophic factor, a stem cell niche factor, an anti-inflammatory factor, an anti-angiogenic

factor, a tumor inhibitor, and a protein with declined expression in aging. This secreted factor has

been demonstrated to have diverse therapeutic value in inhibiting the pathogenesis of several

major diseases such as diverse cancer types including melanoma, neuroblastoma, osteosarcoma,

hepatoblastoma, Lewis lung carcinoma, chondrosarcoma, gastric carcinoma, glioma, Wilm's

tumor, prostate cancer, and pancreatic cancer and several major blinding diseases including

ischemia-induced retinopathy, diabetic retinopathy, retinitis pigmentosa, and age-related macular

degeneration. Although this multifunctional factor has drawn increasing attention, its therapeutic potential is greatly hampered by the lack of knowledge on PEDF's signaling mechanism. Despite considerable efforts in academia and industry, the cell-surface receptors that transduce PEDF signal eluded identification since the 1990s.

To transform the high therapeutic value of PEDF to potent and efficient therapeutic agents to treat human diseases, we aimed to achieve three general goals. The first is to identify and characterize the cell-surface receptors for PEDF. The second is to investigate the mechanism of PEDF signaling through these receptors. The third is to screen small molecules that mimic PEDF functions by targeting its receptors. Receptors are ideal therapeutic targets due to their specificity in changing cell behaviors and small molecule drugs targeting receptors account for the largest fraction of drugs used clinically in treating human diseases.

After many years of effort and trying many strategies, we identified the long-sought PEDF cell-surface receptors as PLXDC1 and PLXDC2, two single transmembrane domain proteins that do not belong to well-known receptor families. We found that these two homologous transmembrane receptors not only confer cell-surface binding to PEDF but also mediate diverse PEDF functions such as promoting IL-10 secretion in macrophage, inducing endothelial cell death and protecting neuronal cell in a cell-type specific manner. We also found unique

mechanisms of interaction between PEDF and its receptors, such as receptor-induced PEDF dimerization through a disulfide bond. To identify compounds that specifically target these receptors, we have developed a novel cell-based, fluorescence-based and high-throughput screening strategy that color-codes receptor-expressing cells. Using this strategy, we have identified potent lead compounds that mimic PEDF actions such as causing cell death in a receptor-specific manner. These compounds are potential first-in-class drugs in treating diseases.

In summary, identification of PEDF receptors allows further investigation of the molecular mechanism of PEDF signaling and provides novel therapeutic targets. By developing a novel cell-based screening technique, we have identified chemical compounds that specifically and potently target the PEDF receptors and mimic PEDF actions.

The dissertation of Guo Cheng is approved.

David Williams

Lily Wu

Yousang Gwack

Hui Sun, Committee Chair

University of California, Los Angeles

2015

DEDICATION

THIS DISSERTATION IS DEDICATED TO MY PARENTS AND FAMILY FOR THEIR

LOVE, SUPPORT, INSPIRATION AND ENCOURAGEMENT

谨以此论文献给我的父母和家人

TABLE OF CONTENTS

LIST OF TABLES

LIST OF FIGURES

ACKNOWLEDGEMENTS

(cross-disciplinary scholars in science and technology).

Biographic Sketch

Education

PhD. Candidate   **2010-present**

Molecular , Cellular and Integrative Physiology (MCIP) graduate program   Los Angeles,
University of California, Los Angeles   CA, U.S.

Master of Clinic Medicine (7-year Program)   **2003-2010**

School of Medicine, Zhejiang University   Zhejiang, China

Professional Experience

Graduate Student Researcher, 2010-present
David Geffen School of Medicine, University of California, Los Angeles
Studying the newly identified, cell-surface receptors of PEDF, a protein factor with multiple
therapeutic value:

    Characterized the biological function of the receptors in three distinct cell models.
    Revealed the novel mechanism of the interaction between PEDF and its receptors.
    Performed high-throughput screening for small molecules that target PEDF receptors.

Organizer of MCIP Distinguished Speaker Seminar, 2014,
University of California, Los Angeles
Inviting distinguished speaker, advertising and programming the event.

Teaching Assistant, 2012, University of California, Los Angeles
Teaching the labs of Life Science Core Curriculums independently.
Teaching tasks including presentation, leading discussion, supervising students and grading.

Clinic Resident Training, 2009-2010, the 2nd Affiliated Hospital of Zhejiang University
Taking charge of the overall management of patients under the supervision from senior
doctors, including disease diagnosing, treatment and doctor-patient communication.

Organizing Committee Member, 2008, 2009, Zhejiang University
Organizing Gastrointestinal Endoscopy Conference. My tasks including summarizing and
presenting cases, and organizing the event.

Clinic Internship, 2008-2009, Affiliated Hospitals of Zhejiang University
Practicing medical knowledge and skills in the following departments: internal medicine, surgery, pediatrics, obstetrics and gynecology, oncology, ophthalmology, emergency, pathology and radiology.

Visiting scholar, 2008, University of California, Los Angeles
Cross-disciplinary Scholars in Science and Technology Summer Research program
Participating in the project of characterizing the cell-surface receptor for retinol binding protein (RBP):

Purified the holo-RBP/transthyretin complex and holo-RBP from human serum.

Publications

1. **Cheng, G**.*, Zhong, M.*, Kawaguchi, R.*, Kassai, M., Al-Ubaidi, M., Deng, J., Ter-Stepanian, M., and Sun, H. (2014) Identification of PLXDC1 and PLXDC2 as the transmembrane receptors for the multifunctional factor PEDF, *eLife 3:*e05401. *Equal contribution

2. Kawaguchi, R., Yu, J., Ter-Stepanian, M., Zhong, M., **Cheng, G.**, Yuan, Q., Jin, M., Travis, G.H., Ong, D., and Sun, H. (2011) Receptor-Mediated Cellular Uptake Mechanism that is Coupled to Intracellular Storage. ***ACS Chemical Biology*** 6:1041-51 .

Awards

Superior Oral Presentation, MCIP Retreat, UCLA	2015
China Scholarship Council (CSC) Scholarship	2010-2014
Excellent Master's Graduate, Zhejiang University	2010
First Prize of Excellent Undergraduate Scholarship (5%), Zhejiang University	2008
Third Prize of Excellent Undergraduate Scholarship, Zhejiang University	2007
Second Prize of Excellent Undergraduate Scholarship, Zhejiang University	2006
First Prize of Excellent Undergraduate Scholarship (5%), Zhejiang University	2005
Second Prize of Excellent Undergraduate Scholarship, Zhejiang University	2004

Chapter 1 Introduction

1.1 Introduction to signaling receptors

Cells communicate with the environment and with other cells. Cells depend on receptors to relay extracellular signals into cells to change cell behavior. Cell-surface receptors are transmembrane proteins that transduce signals from the outside of the cell into the cytoplasm. Ligands for cell-surface receptors include hormones, chemicals and light. Intracellular receptors are transcription factors inside the cell nucleus that perceive membrane permeable small molecules and are mostly receptors that sense steroids hormones.

There are many classes of cell-surface receptors. Two examples of well-characterized cell-surface receptors are G-protein coupled receptors (GPCRs) and receptor tyrosin kinases. GPCRs have seven transmembrane domains and transduce the most variety of extracellular signals and regulate many physiological processes. When extracellular ligands bind to GPCRs, GPCRs undergo conformational change and activate G proteins which relay signals to downstream signaling molecules (Alberts et al., 2001). Receptor tyrosine kinases are single transmembrane receptors. Upon ligand binding, receptor tyrosine kinase dimerizes and phosphorylates each other at the intracellular phosphorylation sites. The downstream

RAS-MAPK cascade is then triggered. A lot of growth hormones such as fibroblast growth factor (FGF), and platelet-derived growth factor (PDGF) are the ligands of this type of receptors (Alberts et al., 2001). For intracellular hormone receptors, hydrophobic molecules permeate the plasma membrane and bind to and activate their nuclear receptors. The activated receptors regulate gene expression. Sex hormones and retinoids signal through this mechanism (Alberts et al., 2001).

Not all receptors have been discovered. Ligands without receptors are called orphan ligands. Similarly, the ligands of many receptors are still unknown. These receptors are called orphan receptors. In my project, I studied an orphan ligand with diverse biological activities and its newly discovered cell-surface receptors that do not belong to any known families and use novel mechanism to transduce signals.

1.2 Introduction to PEDF

There exists a natural factor that can inhibit pathogenesis of several major diseases and has surprisingly diverse therapeutic value. This factor is called Pigment Epithelium-Derived Factor (PEDF) (Tombran-Tink et al., 1991; Dawson et al., 1999; Tombran-Tink and Barnstable, 2003). The 418 amino acids protein PEDF is a widely expressed secreted protein that belongs to the

non-inhibitory serpin protease inhibitor (serpin) family (Minkevich et al., 2010). The potent and broad biological functions of PEDF have been gradually revealed since its initial identification more than 20 years ago. The biological functions of PEDF are introduced below.

1.2.1 PEDF is a neurotrophic factor

PEDF was first reported in 1991 as a strong protective factor for neurons. PEDF was purified from the medium conditioned by human retinal pigmented epithelial (RPE) cells. The purified PEDF, at 1 nM concentration, effectively induced fast growing Y79 retinoblastoma cells to differentiate into non-proliferating cells. The differentiated cells showed outgrowing neurites, attached substrate better and expressed neuronal markers (Tombran-Tink et al., 1991). Other than RPE, PEDF is secreted by the ciliary epithelium, and is detected in ganglion cells and outer retina (Tombran-Tink and Barnstable, 2003). The intraocular PEDF maintains RPE functions of being a barrier and synthesizing melanin (Abul-Hassan et al., 2000; Ho et al., 2006). It also preserves outer segment of photoreceptors cells (Jablonski et al., 2000), protects retinal ganglion cell against hypoxia mediated damage (Uterlauft et al., 2014) and maintains Müller cell glutamate expression (Jablonski et al., 2001). Outside the eye, PEDF is able to promote the survival of cerabella neurons (Taniwaki et al., 1995; Araki et al., 1998) and hippocampus neurons (Decoster et al., 1999). It can induce spinal cord motor neurons growth and trigger neuronal process formation upon damage (Houenou et al.,1999; Batista et al., 2014). PEDF also

acts on glial cells. For example, it promotes Schwann cell growth at a concentration as low as 1nM (Crawford et al., 2001).

1.2.2 PEDF is a stem cell niche factor

PEDF exists in a stem cell niche, the subventricular zone (SVZ), in adult human brain. SVZ is a neurogenic, restricted region where adult neuronal stem cells (NSC) are localized, self-renew and/or differentiate. Ependymal cell and endothelial cell are two major components in SVZ. PEDF is expressed by both cell types, contributing to the microenvironment of NSC (Urban. et al., 2014). As a stem cell niche factor, PEDF increases NSC sphere number *in vivo* and induces NSC multipotentiality marker expression. This suggests that PEDF is actively involved in NSC self-renewal and maintenance (Ramirez-Castillejo et al., 2006). PEDF promotes NSC self-renewal by interacting with Notch pathway which is important in maintaining stemness in various stem cell niche. It is proposed that PEDF acts through $NF\kappa B$ pathway and intensifies Notch-dependent transcription. The changes then result in symmetrical division of neuronal stem cell to two daughter stem cells, rather than one stem cell and one differentiated cell (Andreu-Agullo et al., 2009).

Other evidence also suggests that PEDF directly influences stem cells. PEDF secreted by human embryo stem cell-derived RPE (hESC-RPE) increases retinal progenitor cell (RPC) proliferation

and protects them from apoptosis (Zhu et al., 2011). In a large-scale gene expression study on fibroblasts, feeder cells of human embryonic stem cell (hESC), PEDF stood out as a secreted factor that maintained the proliferation and stemness of hESCs. (Anisimov et al., 2011). In addition, an unbiased proteomic study identified PEDF in the secretome of adipose tissue to regulate mesenchymal stem cell. PEDF tunes the balance of mesenchymal stem cell differentiation to between adipogenensis and osteogenesis (Chiellini et al., 2008).

1.2.3 PEDF has anti-inflammatory activity

Inflammation is a self-protective effect of our bodies against harmful stimuli, such as infection, tissue damage, or foreign irritants. Blood vessels, immune cells, cytokines and complements all contribute to the initiation, maintenance, regulation and cessation of inflammation. Dysregulated inflammation is an important and/or essential component in the pathophysiological process of many diseases, such as auto-immune disorders, asthma, cancers, metabolic disorder and retinopathy. The role of PEDF to regulate inflammation has emerged recently. It is shown that PEDF injection in rat eye decreased blood vessels permeability. The administration of PEDF inhibited the LPS endotoxin-induced inflammation in the ear (Zamiri et al. 2006). One of the anti-inflammatory mechanisms is that PEDF modulates macrophage behavior, induces anti-inflammatory factor IL10 secretion but suppresses pro-inflammatory factor IL-12 and NO production. In fact, PEDF suppresses pro-inflammatory cytokine secretion in many disease

models such as oxygen induced retinopathy (Park et al., 2011) , diabetic retinopathy (Zhang et al., 2006), retinal degeneration (Wang et al., 2013), prostate cancer (Nelius et al., 2014), and metabolic syndrome (Gattu et al., 2014).

1.2.4 PEDF and metabolism

Metabolism is an essential process that sustains life and involves many organ systems such as the endocrine system, adipose tissue, liver, skeleton muscle, immune system and nervous system. PEDF is secreted by adipocytes (Famullar et al., 2011), hepatocytes (Matsumoto et al., 2004) and skeletal myocytes (Norheim et al., 2011). The proposal that PEDF is a metabolic regulatory protein is supported by a number of epidemiology studies. They suggest that PEDF is positively associated with several metabolic risk factors such as body mass index, waist circumference, fasting triglyceride, glucose and insulin. However, PEDF is negatively correlated with "good" cholesterol, high density lipoprotein (HDL) (Carnagarin et al., 2015). Cross-sectional studies found that PEDF is associated with a series of metabolic disorders, such as obesity (Nakamura et al., 2009), type 2 diabetes (Jenkins et al,. 2008), metabolic syndrome (Chen et al., 2010), coronary artery disease (Wang et al., 2013; Nozue et al., 2015) and polycystic ovarian syndrome (Yang et al., 2011).

It is worth noting that these epidemiology studies cannot address whether PEDF is the causal of the metabolic disorder or a protective response to the impaired metabolism. However, bench-side evidence is conflicting and cannot answer the question yet. In one study, administration of exogenous PEDF in lean mice reduced insulin sensitivity (Crowe et al., 2009). In another study, however, injecting PEDF to PEDF knock-out mice suppressed the proinflammatory metabolites, reduced hyperglycemia and restored insulin sensitivity in liver (Gattu et al., 2014). In summary, although PEDF plays a role in metabolism, its exact function is still not clear.

1.2.5 Blood vessels and disease

The most prominent function of PEDF is its anti-angiogenic activities, as explained in detail below. The roles of blood vessels in health and diseases are introduced in this section. Blood vessels supply oxygen and essential nutrients to all the tissues physiologically. They also provide gateways for immune surveillance, deliver endocrine signals and remove wastes. Blood vessel growth is essential in fetal development, in wound healing and female menstruation cycle. Dysregulated blood vessel growth contributes significantly in pathological process of many diseases such as tumor and blindness.

Blood vessel growth starts from vasculogenesis, which is *de novo* establishment of primitive vascular labyrinth by the differentiation of endothelial precursors during embryonic stage

(Yancopoulos et al., 2000; Syed et al., 2004; Carmeliet and Jain, 2011; Potente et al., 2011). Further expansion of vascular network relies on angiogenesis. Angiogenesis refers to the sprouting of new vessels from existing ones, and the branching and intussuscepting of new vessels (Potente, Gerhardt et al., 2011). Newly grown sprouts and vessels are then stabilized by mural cells and remodeled into visible and mature vessels.

Angiogenesis acts as an important complement for vasculogenesis in the embryo state and is the predominant form of blood vessel growth in postnatal stage. In the postnatal stage, the majority of endothelial cells remain quiescent. With angiogenic stimulation from the environment, angiogenesis occurs and new blood vessel forms. The angiogenic process starts with the activation of quiescent endothelial cells, degradation of pre-existing basement membrane followed by proliferation and migration of endothelial cells, endothelial tube formation, enclosure of endothelial tubes by basement membrane as well as mural cells, and the return of endothelial cells to quiescence (Carmeliet and Jain, 2011). The dynamic angiogenic process is delicately regulated by proangiogenic versus anti-angiogenic stimuli. The finely tuned balance is essential for blood vessels to grow with appropriate structure, in appropriate volume, at the appropriate place and time. Disrupted balance, on the other hand, leads to abnormalities in blood-vessel structure and function and in turn to diverse human diseases. For example, inadequate blood vessel maintenance or growth significantly contributes to myocardial infarction,

stroke, neurodegeneration and other ischemic disorders. On the contrary, excessive and abnormal vascularization promotes eye diseases (such as age-related macular degeneration and diabetic retinopathy), cancers and inflammatory diseases (such as rheumatoid arthritis and psoriasis) (Syed, Sanborn et al.s 2004; Carmeliet and Jain, 2011; Potente et al., 2011; Gerhardt et al., 2011). Vascular endothelium growth factor (VEGF) and basic fibroblast growth factor (bFGF) are well known examples of proangiogenic factors. They are upregulated in many pathological conditions, such as tumor development, metastasis and retinopathy. Angiostatin, endostatin, thrombospontin-1, and PEDF are anti-angiogenic factors.

1.2.6 PEDF is an anti-angiogenic factor

PEDF was first reported to inhibit ocular vascularization in 1999 (Dawson et al.,1999). In this unbiased search for new antiangiogenic factors, PEDF was purified from the extract of cornea and vitreous which are blood vessel-free structures. Purified PEDF inhibited endothelial cell migration in the presence of VEGF and impeded blood vessel growing into cornea in the presence of bFGF. PEDF was so potent that it counteracted VEGF and bFGF at a concentration as low as 2nM and 8 nM respectively. In fact, PEDF potency was ranked first in comparison with other known anti-angiogenic factors such as angiostatin, endostatin, and thrombospontin-1 (Dawson et al. 1999).

The role of PEDF to regulate blood vessel growth has been demonstrated in both *in vitro* and *in vivo* studies. It is shown that PEDF counteracts proangiogenic factors and suppresses microvascular endothelial cell proliferation, migration and tube formation (Crawford et al., 2001, Kanda et al,. 2005). In PEDF deficient mice, blood vessel density dramatically increases in retina, prostate, kidney and pancreas compared to wide type (Doll et al., 2003). In the pancreas, excessive blood vessels are dilated, and have thickened media (Doll et al., 2003; Stellmach et al., 2003). Several disease models show that PEDF treatment reduces microvascular density in a variety of malignancy including pancreatic adenocarcinoma, melanoma, neuroblastoma, prostate cancer, cervical cancer, lung cancer and Wilm's tumor (Ek. et al., 2006; Becerra et al., 2013).

1.2.7 PEDF is an anti-tumor factor

The anti-tumor mechanism of PEDF is multifaceted. PEDF can directly induce tumor cell apoptosis or differentiation. It also suppresses tumor growth through its anti-angiogenic effect as discussed above, and anti-metastatic effect. PEDF acts on tumor cells directly. At nanomolar concentration, PEDF induces the differentiation of neuroblastoma and retinoblastoma cells manifested by neurite growth or expression mature cell-surface marker *in vitro* (Crawford et al., 2001, Tombran-Tink et al., 1991). PEDF also promotes apoptosis in glioma cells (Guan et al., 2004), osteosarcoma cells (Takenaka et al., 2005), melanoma cells (Garcia et al., 2004; Fernandez-Garcia et al., 2007), lung adenocarcinoma cells (Li et al.,2014), and prostate cancer

cells (Filleur et al., 2005; Doll et al., 2003). It is suggested that the apoptosis induced by PEDF is dependent on FAS/FASL pathway (Li et al., 2014; Fernandez-Garcia et al., 2007). In addition, PEDF also sensitizes breast cancer cells to tamoxinfen treatment (Jan et al., 2012) and sensitizes lung cancer to radiation therapy (Xu et al., 2015).

Metastasis and invasion are advancement of most primary tumors that eventually lead to organ failure and death. PEDF has the ability to restrict tumor metastasis. Previous studies report that PEDF inhibits the migration of melanoma cells (Garcia et al., 2004) and breast cancer cells (Hong et al., 2014) *in vitro*. PEDF also prevents osteosarcoma from locally invading cartilages (Quan. et al., 2002). One possible mechanism to explain the anti-metastasis effect of PEDF is that PEDF inhibits matrix metalloproteinase 9 (MMP-9) which is upregulated in tumor. MMP9 cleaves extracellular matrix and paves the route for tumor cells to migrate. PEDF suppress MMP-9 activity and restrains tumor cells from migration and invasion (Guan et al., 2004).

1.2.8 The age-dependent loss of PEDF

PEDF seems to be widely expressed throughout fetal and adult tissues, including adult brain, spinal cord, eye, liver, plasma, bone, heart and lung. However, it was suggested that fibroblast cells lose PEDF expression when they become senile (Pignolo et al., 1993). Examine of human skin tissue found that PEDF expression declines from young age to old age (Francis et al., 2004).

PEDF levels were also found to decrease with age in human eyes (Ogata et al., 2004; Smith and Steinle, 2007; Steinle et al., 2008). The age-dependent loss of PEDF expression may play a role in many diseases. PEDF level was also found to decrease in many pathological conditions. A significant decrease of PEDF level in the eyes has been observed in patients with age-related macular degeneration and diabetic retinopathy, two major blinding diseases characterized by neovascularization (Ogata et al., 2001; Spranger et al., 2001; Holekamp et al., 2002; Ogata et al., 2002; Boehm et al., 2003). PEDF expression has been inversely related to metastasis in a variety of cancer types such as glioma (Guan et al., 2003), lymphangioma (Sidle et al., 2005), hepatoma (Matsumoto et al., 2004), melanoma (Orgaz et al., 2009), lung cancer (Zhang et al., 2006a), pancreatic cancer (Uehara et al., 2004), and prostate cancer (Halin et al., 2004).

1.2.9 Summary of the biological roles of PEDF

In summary, PEDF is a neurotrophic factor, a stem cell niche factor, an anti-inflammatory factor, an anti-angiogenic factor, and an anti-tumor factor. PEDF is broadly expressed and its expression is lost during aging. **Table 1-1** lists the cell types that respond to PEDF. **Table 1-2** summarizes the diseases that potentially benefit from PEDF treatment.

As shown in **Table 1-1** and **Table 1-2,** the important and broad functions of PEDF potentially make it a valuable therapeutic agent. As an extracellular protein factor, PEDF influences a

variety of cell types. Employing physiological signaling pathways to impede pathological processes has been a fruitful approach in developing effective therapeutics for human disease. However, the cell surface signaling mechanism of PEDF has not been elucidated for more than 20 years. My thesis project aims to investigate the mechanism of how cells respond to PEDF and specifically the identity and mechanism of its cell surface receptors.

1.3 Identification of PEDF receptors

As commented by Dr. Michael Boulton a few years ago, the search of PEDF receptors is very challenging: "Although an as yet unidentified receptor remains a possibility, considerable research effort in academia and industry has surprisingly failed to identify such a receptor, suggesting that PEDF may signal via a nonclassical route." Two proteins have been claimed as PEDF receptor candidates in the literature. They are phospholipase A2 (also called PNPLA2, adipose triglyceride lipase or PEDFR) (Notari. et al., 2006) and laminin receptor (LaminR, also called 40S ribosomal protein SA) (Bernard. et al., 2009). Phospholipase A2 belongs to an enzyme family. It regulates lipid droplet biogenesis by catalyzing key steps in fatty acid hydrolysis (Guijas et al., 2014). Its mutations cause neutral lipid storage disease with myopathy (Fischer et al., 2007). Base on its well established cellular location (in ER) and its enzymatic function, phospholipase A2 is unlikely to be PEDF receptor. Ribosomal protein SA is a

ubiquitously expressed component of the small subunit of the ribosome that is involved in preribosomal RNA processing and completely lacks any transmembrane domain (O'Donohue et al., 2010, Ben-Shem et al., 2011). There has been no explanation as to how an intracellular ribosomal protein without a transmembrane domain can transduce extracellular signals. In addition, endothelial cells are known to use integrins as the laminin receptor. Besides, the two proposed PEDF receptor candidates were identified based on intracellular interaction using the yeast two-hybrid assay. However, the first requirement of a cell-surface receptor is to confer cell-surface binding to the ligand. Therefore, the well-known enzyme that catalyzes the hydrolysis of fatty acid and the well-defined component of the ribosome are very unlikely to be PEDF receptor. Another group claimed that low-density lipoprotein receptor-related protein 6 (LRP6) is a cell surface binding protein for PEDF. LRP6 is a component of receptor complex for Wnt3a. It was suggested that the interaction of PEDF with LRP6 blocked Wnt signaling. However, no evidence have shown that LRP6 directly mediates PEDF signaling, which does not support LRP6 as a receptor for PEDF. Actually, in the numerous binding assays that we have done, we did not detect any cell-surface binding to PEDF for these three proteins, although we detected robust binding to our receptor candidates, as mentioned later.

To identify PEDF receptors, our lab tried three strategies. The first strategy we tried was to purify the receptors from native tissues or cells lines. Using PEDF as a bait protein, we tried to

unbiasedly identify its interacting membrane proteins by protein affinity purification. The purified proteins were analyzed by mass spectrometry. Animal tissues or cells lines that we used included mouse brain, mouse lung, bovine retina extract, bovine lung, human placenta, primary human endothelial cells and mouse endothelial cells. However, we failed to find PEDF receptor using this strategy. The possible explanations could be that the native receptors are extremely low in abundance and thus are invisible to current detection method after several rounds of purification. In addition, PEDF and its receptor interaction may involve complex mechanism that cannot be detected by purification. The second strategy that we tried is expression cloning. The strategy also failed because only half of the human gene pool was available and the functional assay for evaluating cell-surface binding is not robust enough for high throughput screening. The third strategy that we used is to test PEDF binding to orphan receptors (receptors without known ligand). Using this strategy, we found that two membrane proteins confer PEDF binding to live cell surface. They are two transmembrane proteins called plexin domain containing protein 1 (PLXDC1) and plexin domain containing protein 2 (PLXDC2).

PLXDC1 and PLXDC2 are homologous, single-transmembrane proteins that had not been characterized mechanistically before our study. For a membrane protein to qualify ligand receptor, it should meet two criteria. First, it confers cell-surface binding of the extracellular ligand. Second, it mediates signal transduction into cells from the extracellular ligand. I will

present the evidence that PLXDC1 and PLXDC2 meet those two criteria in Chapter 2. My thesis

focuses on the validation PLXDC1 and PLXDC2 as PEDF receptors; the unique interaction

mechanism between PEDF and its receptors, and the identification of chemical compounds that

mimic PEDF actions by developing a novel receptor-specific high-throughput technique.

Table 1-1. Biological effects of PEDF on multiple cell types.

	Cell Types	PEDF Effects	References
Eye	Retinal Pigmented epithelial cell (RPE)	Promotes differentiation	Malchiodi-albedi et al., 1998
		Promotes melanin synthesis and accumulation	Abul-Hassan et al.,2000
		Preserves barrier function of RPE against H_2O_2	Ho et al., 2006
	Photoreceptor cells	Promotes retina development	Jablonski et al., 2000
		Protects cell morphology and subcellular ultrastructure	
		Maintains outer segment assembly and opsin expression	
	Retina neuron	Protects against H_2O_2 induced cytotoxicity	Cao et al., 1999
	Retina ganglion cell	Protects against hypoxia induced apoptosis	Uterlauft et al.,2014
	Müller cell	Maintains adherent junction with photoreceptors	Jablonski et al., 2001
		Preserves glutamine synthase expression	
		Inhibits VEGF and proinflammatory cytokines production	Zhang et al., 2005
Neuronal Cells	Cerebella granule neuron	Prevents serum-deprivation induced apoptosis	Taniwaki et al., 1995; Araki et al.,1998
		Protects against glutamate induced cell damage	Taniwaki et al., 1997
	Hippocampus neuron	Protects against glutamate induced cell damage	Decoster et al., 1999
	Spinal cord motor neuron	Promotes cell survival and neurite outgrowth	Houenou et al.,1999
		Triggers neuroplasticity	Batista et al., 2014
		Increases neural processes formation	
		Protects against glutamate induced cell damage	Bilak et al., 1999
	Schwann cell	Promotes Schwann cell survival and growth	Crawford et al.,2001
	Astrocyte	Inhibits proliferation	Sugita et al., 1997
	Microglial cell	Increases metabolic activity	Sugita et al., 1997
		Inhibits proliferation	

	Cell Types	PEDF Effects	References
Endlthelial cells	Human dermal microvascular endothelial cell (HDMEC)	Induces apoptosis	Stellmach et al., 2001
		Inhibits migration in the presence of PDGF, VEGF, IL-8, bFGF	Dawson et al., 1999; Holekamp et al., 2002
	Human umbilical vascular endothelial cell (HUVEC)	Inhibits cell proliferation	Wang et al., 2003; Hase et al.,2005; Matsumoto et al., 2004
		Inhibits migration	Garcia et al., 2004, Filleur et al., 2005; Hase et al., 2005; Wang et al., 2003; Matsumoto et al.,2004
		Induces cell apoptosis	Filleur et al., 2005
		Inhibits tube formation	Wang et al., 2003
		Suppresses proinflammatory cytokine secretion	Matsui et al., 2013
	Porcine retinal endothelial cell (PREC)	Decreases permeability	Sheikpranbabu et al., 2010
		Reduces ROS production	
		Inhibits PREC proliferation	
		Inhibits tube formation	
		Inhibits migration	
	Bovine retinal capillary endothelial cell	Decreases permeability	Zhang et al., 2005
Stem cells	Human Embryonic Stem cell	Promotes growth	Anisimov et al., 2011
	Retinal Progenitor cell	Promotes survival and proliferation	Zhu et al., 2011
	Neural Stem cell	Promotes self-renewal and expansion	Ramírez-Castillejo et al.,2006; Mirochnik et al.,2009
		Induces differentiation to neuronal cells	
		Regulates symmetric and asymmetric division	Andreu-Agulló et al., 2009
	Mesenchymal stem cell	Regulates differentiation	Chiellini et al. 2008

Cell Types	PEDF Effects	References
Prostate cancer epithelium cell (LNCaP and PC-3)	Induces cell apoptosis	Filleur et al., 2005; Doll et al., 2003
	Induces cell neuroendocrine differentiation	Filleur et al., 2005; Nelius et al.,2014
	Inhibits cell proliferation	Nelius et al., 2014
Ovarian epithelium cell (IOSE-29, OSE-397, Caov-3, Skov-3)	Inhibits cell proliferation and survival	Cheung et al., 2006
Neuroblastoma cell (SK-N-BE2 , SH-SY5Y)	Induces cell differentiation, neurite outgrowth	Crawford et al.,2001
Retinoblastoma cell (Y79)	Induces cell differentiation and neurite formation	Tombran-Tink et al. 1991; Steele., et al., 1993; Filleur et al., 2005
Breast cancer cell (MDA-MB-231, KBR3)	Inhibits migration	Hong et al., 2014
Breast cancer cell (MCF-7:5C, MCF-7:2A)	Sensitizes tumor cells to tamoxifen therapy	Jan et al., 2012
Osteosarcoma cell (Saos-2, SJSA-1)	Induces apoptosis	Broadhead et al,.2011
	Inhibits proliferation	
	Enhances adhesion to Collagen I	
Osteosarcoma cell (MG63)	Suppresses VEGF expression Induces cell apoptosis	Takenaka et al., 2005
Lung cancer cell (A549, calu-3)	Induces cell apoptosis	Li et al,. 2014
Human Melanoma cell (UCD-Mel-N)	Inhibits cell migration	Garcia et al., 2004
	Induces apoptosis	
Macrophage	Induces anti-inflammatory cytokine	Zamiri et al. 2006
	Suppress pro-inflammatory cytokine	
Endometrial Stromal cell	Induces apoptosis	Sun et al., 2012
	Suppresses VEGF expression	
Hepatocyte	Reduces proinflammatory cytokine IL-1β mediated stress	Gattu et al., 2014

(The first group of rows, from "Prostate cancer epithelium cell" through "Human Melanoma cell", is labeled **Cancer cells**; the last group of rows, from "Macrophage" through "Hepatocyte", is labeled **Others**.)

Table 1-2. Diseases potentially benefit from PEDF treatment

Diseases	PEDF Effects	References
Age-related retinopathy Diabetic retinopathy Retinitis pigmentosa	Delays photoreceptor apoptosis Reduces proinflammatory cytokines production Reduces vascular permeability Inhibits neovascularization	Park et al., 2011 Wang et al., 2013 Semkova et al., 2002 Sheikpranbabu et al., 2010 Zhang et al., 2005 Stellmach et al., 2001, etc
Glaucoma	Preserves retinal ganglion cells Protects optic nerve	Haurigot et al., 2012 Miyazaki et al., 2011 Zhou et al., 2009
Spinal cord injury	Prevents spinal cord motor neuron death and atrophy Triggers neuroplasticityromotes motor neuron Increase processes formation	Houenou et al.,1999 Batista et al., 2014
Neuroblastoma Glioma Melanoma Prostate cancer Breast cancer Pancreatic cancer Cervical cancer Hepatocellular cancer Lung cancer Osteosarcoma Wilm's tumor Mesothelioma	Induces tumor cell apoptosis Inhibits tumor cell proliferation Inhibits angiogenesis Inhibits tumor metastasis Suppresses inflammation Sensitizes tumor cells to endocrine therapy (if appliable)	Streck et al,. 2005 Guan et al., 2003 Abe et al., 2004 Garcia et al., 2004 Shi et al., 2013 Nelius et al., 2014 Hong et al., 2014 Hase et al., 2005 Hosomichi., 2005 Matsumoto et al., 2004 Li et al., 2014 Xu et al., 2015 Mahtabifard et al.,2003 Merrit et al.,2004 Abramson et al., 2003 Broadhead et al,.2011, etc.
Psoriasis	Suppresses inflammation Inhibits angiogenesis	Nakajima et al.,2013 Abe et al., 2010
Metabolic Syndrome Type II diabetes	Modifies inflammatory cytokine profile Changes insulin sensitivity Affects metabolic homeostasis	Crowe et al., 2009 Sunderland et al., 2012 Gattu et al., 2014, etc.
Endometriosis	Reduces volumes of endometrial transplants Inhibits angiogenesis	Chuderland et al., 2013 Sun et al., 2012

References

Abe, R., Yamagishi, S.-i., Fujita, Y., Hoshina, D., Sasaki, M., Nakamura, K., Matsui, T., Shimizu, T., Bucala, R., and Shimizu, H. (2010) Topical application of anti-angiogenic peptides based on pigment epithelium-derived factor can improve psoriasis, *Journal of Dermatological Science 57*, 183-191.

Abramson, L. P., Stellmach, V., Doll, J. A., Cornwell, M., Arensman, R. M., and Crawford, S. E. (2003) Wilms' tumor growth is suppressed by antiangiogenic pigment epithelium-derived factor in a xenograft model, *Journal of Pediatric Surgery 38*, 336-342.

Abul-Hassan, K., Walmsley, R., Tombran-Tink, J., and Boulton, M. (2000) Regulation of tyrosinase expression and Activity in cultured human retinal pigment epithelial cells, *Pigment Cell Research 13*, 436-441.

Alberts, B., Johnson, A., Lewis, J., Raff M., Roberts, K., Walter, P. (2001), *Molecula Biology of the Cell.,* 4th edition.

Andreu-Agullo, C., Morante-Redolat, J. M., Delgado, A. C., and Farinas, I. (2009) Vascular niche factor PEDF modulates Notch-dependent stemness in the adult subependymal zone, *Nat Neurosci 12*, 1514-1523.

Andreu-Agullo, C., J. M. Morante-Redolat, et al. (2009). "Vascular niche factor PEDF modulates Notch-dependent stemness in the adult subependymal zone." **12**(12): 1514-1523.

Anisimov, S. V., Christophersen, N. S., Correia, A. S., Hall, V. J., Sandelin, I., Li, J.-Y., and Brundin, P. (2011) Identification of molecules derived from humanfibroblast feeder cells that support theproliferation of human embryonic stem cells, *Cellular & Molecular Biology Letters 16*, 79-88.

Araki, T., Taniwaki, T., Becerra, S. P., Chader, G. J., and Schwartz, J. P. (1998) Pigment epithelium-derived factor (PEDF) differentially protects immature but not mature cerebellar granule cells against apoptotic cell death, *Journal of Neuroscience Research 53*, 7-15.

Batista, C. M., Bianqui, L. L. T., Zanon, B. B., Ivo, M. M. A. A., de Oliveira, G. P., Maximino, J. R., and Chadi, G. (2014) Behavioral Improvement and Regulation of Molecules Related to Neuroplasticity in Ischemic Rat Spinal Cord Treated with PEDF, *Neural Plasticity 2014*, 451639.

Bernard, A., Gao-Li, J., Franco, C. A., Bouceba, T., Huet, A., and Li, Z. (2009) Laminin receptor involvement in the anti-angiogenic activity of pigment epithelium-derived factor, *J Biol Chem 284*, 10480-10490.

Ben-Shem, A., Garreau de Loubresse, N., Melnikov, S., Jenner, L., Yusupova, G., and Yusupov, M. (2011) The structure of the eukaryotic ribosome at 3.0 A resolution, *Science* 334, 1524-1529.

Bilak, M. M., Corse, A. M., Bilak, S. R., Lehar, M., Tombran-Tink, J., and Kuncl, R. W. (1999) Pigment epithelium-derived factor (PEDF) protects motor neurons from chronic glutamate-mediated neurodegeneration, *Journal of Neuropathology & Experimental Neurology 58*, 719-728.

Boehm, B. O., Lang, G., Volpert, O., Jehle, P. M., Kurkhaus, A., Rosinger, S., Lang, G. K., and Bouck, N. (2003) Low content of the natural ocular anti-angiogenic agent pigment epithelium-derived factor (PEDF) in aqueous humor predicts progression of diabetic retinopathy, *Diabetologia 46*, 394-400.

Broadhead, M. L., Dass, C. R., and Choong, P. F. M. (2011) Systemically administered PEDF against primary and secondary tumours in a clinically relevant osteosarcoma model, *British Journal of Cancer 105*, 1503-1511.

Cao, W., Tombran-Tink, J., Chen, W., Mrazek, D., Elias, R., and McGinnis, J. F. (1999) Pigment epithelium-derived factor protects cultured retinal neurons against hydrogen peroxide-induced cell death, *Journal of Neuroscience Research 57*, 789-800.

Carnagarin, R., Dharmarajan, A. M., and Dass, C. R. (2015) PEDF-induced alteration of metabolism leading to insulin resistance, *Mol Cell Endocrinol.* 401:98-104

Cayouette, M., Smith, S. B., Becerra, S. P., and Gravel, C. (1999) Pigment epithelium-eerived factor delays the death of photoreceptors in mouse models of inherited retinal degenerations, *Neurobiology of Disease 6*, 523-532.

Chen, C., Tso, A. W. K., Law, L. S. C., Cheung, B. M. Y., Ong, K. L., Wat, N. M. S., Janus, E. D., Xu, A., and Lam, K. S. L. (2010) Plasma level of pigment epithelium-derived factor is independently associated with the development of the metabolic syndrome in Chinese men: A 10-year prospective study, *The Journal of Clinical Endocrinology & Metabolism 95*, 5074-5081.

Chiellini, C., O. Cochet, et al. (2008). "Characterization of human mesenchymal stem cell secretome at early steps of adipocyte and osteoblast differentiation." Bmc Molecular Biology **9**.

Chuderland, D., Hasky, N., Ben-Ami, I., Kaplan-Kraicer, R., Grossman, H., and Shalgi, R. (2013) A physiological approach for treating endometriosis by recombinant pigment epithelium-derived factor (PEDF), *Human Reproduction 28*, 1626-1634.

Crawford, S. E., Stellmach, V., Ranalli, M., Huang, X., Huang, L., Volpert, O., De Vries, G. H., Abramson, L. P., and Bouck, N. (2001) Pigment epithelium-derived factor (PEDF) in neuroblastoma: a multifunctional mediator of Schwann cell antitumor activity, *J Cell Sci 114*, 4421-4428.

Crowe, S., Wu, L. E., Economou, C., Turpin, S. M., Matzaris, M., Hoehn, K. L., Hevener, A. L., James, D. E., Duh, E. J., and Watt, M. J. (2009) Pigment epithelium-derived factor contributes to insulin resistance in obesity, *Cell Metabolism 10*, 40-47.

DeCoster, M. A., Schabelman, E., Tombran-Tink, J., and Bazan, N. G. (1999) Neuroprotection by pigment epithelial-derived factor against glutamate toxicity in developing primary hippocampal neurons, *Journal of Neuroscience Research 56*, 604-610.

Doll, J. A., Stellmach, V. M., Bouck, N. P., Bergh, A. R., Lee, C., Abramson, L. P., Cornwell, M. L., Pins, M. R., Borensztajn, J., and Crawford, S. E. (2003) Pigment epithelium-derived factor regulates the vasculature and mass of the prostate and pancreas, *9*, 774-780.

Filleur, S., Volz, K., Nelius, T., Mirochnik, Y., Huang, H., Zaichuk, T. A., Aymerich, M. S., Becerra, S. P., Yap, R., Veliceasa, D., Shroff, E. H., and Volpert, O. V. (2005) Two functional epitopes of pigment epithelial-derived factor block angiogenesis and Induce differentiation in prostate cancer, *Cancer Research 65*, 5144-5152.

Fischer, J., Lefevre, C., Morava, E.,Mussini, J. M., Laforet, P., Negre-Salvayre, A., Lathrop, M., and Salvayre, R. (2007) The gene encoding adipose triglyceride lipase (PNPLA2) is mutated in neutral lipid storage disease with myopathy, *Nat Genet 39*, 28-30.

Francis, M. K., Appel, S., Meyer, C., Balin, S. J., Balin, A. K., and Cristofalo, V. J. (2004) Loss of EPC-1/PEDF Expression During Skin Aging In Vivo, *J Investig Dermatol 122*, 1096-1105.

Garcia, M., Fernandez-Garcia, N. I., Rivas, V., Carretero, M., Escamez, M. J., Gonzalez-Martin, A., Medrano, E. E., Volpert, O., Jorcano, J. L., Jimenez, B., Larcher, F., and Del Rio, M. (2004) Inhibition of xenografted human melanoma growth and prevention of metastasis development by dual antiangiogenic/antitumor activities of pigment epithelium-derived factor, *Cancer Research 64*, 5632-5642.

Gattu, A. K., Birkenfeld, A. L., Iwakiri, Y., Jay, S., Saltzman, M., Doll, J., Protiva, P., Samuel, V. T., Crawford, S. E., and Chung, C. (2014) Pigment epithelium-derived factor (PEDF) suppresses IL-1-Mediated c-Jun N-Terminal Kinase (JNK) activation to improve hepatocyte insulin signaling, *Endocrinology 155*, 1373-1385.

Guan, M., Yam, H. F., Su, B., Chan, K. P., Pang, C. P., Liu, W. W., Zhang, W. Z., and Lu, Y. (2003) Loss of pigment epithelium derived factor expression in glioma progression, *Journal of Clinical Pathology 56*, 277-282.

Guan, M., Pang, C. P., Yam, H. F., Cheung, K. F., Liu, W. W., and Lu, Y. (2004) Inhibition of glioma invasion by overexpression of pigment epithelium-derived factor, *Cancer Gene Ther 11*, 325-332.

Guijas, C., Rodriguez, J. P., Rubio, J. M., Balboa, M. A., and Balsinde, J. (2014) Phospholipase A2 regulation of lipid droplet formation, *Biochim Biophys Acta 1841*, 1661-1671.

Halin, S., Wikstrom, P., Rudolfsson, S. H., Stattin, P., Doll, J. A., Crawford, S. E., and Bergh, A. (2004) Decreased Pigment Epithelium-Derived Factor Is Associated with Metastatic Phenotype in Human and Rat Prostate Tumors, *Cancer Research 64*, 5664-5671.

Hase, R., Miyamoto, M., Uehara, H., Kadoya, M., Ebihara, Y., Murakami, Y., Takahashi, R., Mega, S., Li, L., Shichinohe, T., Kawarada, Y., and Kondo, S. (2005) Pigment epithelium-derived factor gene therapy inhibits human pancreatic cancer in mice, *Clin Cancer Res 11*, 8737-8744.

Ho, T.-C., Yang, Y.-C., Cheng, H.-C., Wu, A.-C., Chen, S.-L., and Tsao, Y.-P. (2006) Pigment epithelium-derived factor protects retinal pigment epithelium from oxidant-mediated barrier dysfunction, *Biochemical and Biophysical Research Communications 342*, 372-378.

Holekamp, N. M., Bouck, N., and Volpert, O. (2002) Pigment epithelium-derived factor is deficient in the vitreous of patients with choroidal neovascularization due to age-related macular degeneration1, *American Journal of Ophthalmology 134*, 220-227.

Hosomichi, J., Yasui, N., Koide, T., Soma, K., and Morita, I. (2005) Involvement of the collagen I-binding motif in the anti-angiogenic activity of pigment epithelium-derived factor, *Biochemical and Biophysical Research Communications 335*, 756-761.

Houenou, L. J., D'Costa, A. P., Li, L., Turgeon, V. L., Enyadike, C., Alberdi, E., and Becerra, S. P. (1999) Pigment epithelium-derived factor promotes the survival and differentiation of developing spinal motor neurons, *The Journal of Comparative Neurology* 412, 506-514.

Jablonski, M. M., Tombran-Tink, J., Mrazek, D. A., and Iannaccone, A. (2000) Pigment epithelium-derived factor supports normal development of photoreceptor neurons and opsin expression after retinal pigment epithelium removal, *J Neurosci 20*, 7149-7157.

Jablonski, M. M., Tombran-Tink, J., Mrazek, D. A., and Iannaccone, A. (2001) Pigment epithelium-derived factor supports normal müller cell development and glutamine synthetase expression after removal of the retinal pigment epithelium, *Glia* 35,14-25.

Jan, R., Huang, M., and Lewis-Wambi, J. (2012) Loss of pigment epithelium-derived factor: a novel mechanism for the development of endocrine resistance in breast cancer, *Breast Cancer Research : BCR 14*, R146-R146.

Jenkins, A., Zhang, S. X., Gosmanova, A., Aston, C., Dashti, A., Baker, M. Z., Lyons, T., and Ma, J.-X. (2009) Increased serum pigment epithelium derived factor levels in type 2 diabetes patients, *Diabetes Research and Clinical Practice 82*, e5-e7.

Kanda S., Mochizuki Y, Nakamura T, Miyata Y, Matsuyama T, Kanetake H. (2005) Pigment epithelium-derived factor inhibits fibroblast-growth-factor-2-induced capillary morphogenesis of endothelial cells through Fyn. *J Cell Sci.* Mar 1;118(Pt 5):961-70

Kozaki K, Miyaishi O, Koiwai O, Yasui Y, Kashiwai A, Nishikawa Y, Shimizu S, Saga S (1998) Isolation, purification, and characterization of a collagen-associated serpin, caspin, produced by murine colon adenocarcinoma cells. *J Biol Chem* 273:15125–15130

Lattier, J., Yang, H., Crawford, S., and Grossniklaus, H. (2013) Host pigment epithelium-derived factor (PEDF) prevents progression of liver metastasis in a mouse model of uveal melanoma, *Clinical & Experimental Metastasis 30*, 969-976.

Li, L., Yao, Y.-C., Fang, S.-H., Ma, C.-Q., Cen, Y., Xu, Z.-M., Dai, Z.-Y., Li, C., Li, S., Zhang, T., Hong, H.-H., Qi, W.-W., Zhou, T., Li, C.-Y., Yang, X., and Gao, G.-Q. (2014) Pigment epithelial-derived factor (PEDF)-triggered lung cancer cell apoptosis relies on p53 protein-driven fas ligand (Fas-L) up-regulation and fas protein cell surface translocation, *Journal of Biological Chemistry 289*, 30785-30799.

Mahtabifard, A., Merritt, R. E., Yamada, R. E., Crystal, R. G., and Korst, R. J. (2003) In vivo gene transfer of pigment epithelium-derived factor inhibits tumor growth in syngeneic murine models of thoracic malignancies, *J Thorac Cardiovasc Surg 126*, 28-38.

Malchiodi-albedi, F., Feher, J., Caiazza, S., Formisano, G., Perilli, R., Falchi, M., Petrucci, T. C., Scorcia, G., and Tombran-tink, J. (1998) Pedf (Pigment epithelium-derived Factor) promotes increase and maturation of pigment granules in pigment epithelial cells in neonatal albino rat retinal cultures, *International Journal of Developmental Neuroscience 16*, 423-432.

Matsumoto, K., Ishikawa, H., Nishimura, D., Hamasaki, K., Nakao, K., and Eguchi, K. (2004) Antiangiogenic property of pigment epithelium-derived factor in hepatocellular carcinoma, *Hepatology 40*, 252-259.

Merritt, R. E., Yamada, R. E., Wasif, N., Crystal, R. G., and Korst, R. J. Effect of inhibition of multiple steps of angiogenesis in syngeneic murine pleural mesothelioma, *The Annals of Thoracic Surgery 78*, 1042-1051.

Minkevich, N. I., Lipkin, V. M., and Kostanyan, I. A. (2010) PEDF - A noninhibitory serpin with neurotrophic activity, *Acta Naturae 2*, 62-71.

Mirochnik, Y., Aurora, A., Schulze-Hoepfner, F. T., Deabes, A., Shifrin, V., Beckmann, R., Polsky, C., and Volpert, O. V. (2009) Short pigment epithelial-derived factor-derived peptide inhibits angiogenesis and tumor growth, *Clinical Cancer Research 15*, 1655-1663.

Miyazaki, M., Ikeda, Y., Yonemitsu, Y., Goto, Y., Kohno, R.-i., Murakami, Y., Inoue, M., Ueda, Y., Hasegawa, M., Tobimatsu, S., Sueishi, K., and Ishibashi, T. (2008) Synergistic neuroprotective effect via simian lentiviral vector-mediated simultaneous gene transfer of human pigment epithelium-derived factor and human fibroblast growth factor-2 in rodent models of retinitis pigmentosa, *The Journal of Gene Medicine 10*, 1273-1281.

Miyazaki M, Ikeda Y, Yonemitsu Y, Goto Y, Murakami Y, Yoshida N, et al. (2011); Pigment epithelium-derived factor gene therapy targeting retinal ganglion cell injuries: neuroprotection against loss of function in two animal models. *Human gene therapy*. 22(5):559-65.

Mònica Sabater, J. M. M.-N., Francisco José Ortega, Gerard Pardo, Javier Salvador, Wifredo Ricart, Gema Frühbeck, and José Manuel Fernández-Real. (2010) Circulating pigment epithelium-derived factor levels are associated with insulin resistance and decrease after weight loss, *The Journal of Clinical Endocrinology & Metabolism 95*, 4720-4728.

Nakajima, H., Nakajima, K., Tarutani, M., and Sano, S. (2013) The role of pigment epithelium-derived factor as an adipokine in psoriasis, *Archives of Dermatological Research 304*, 81-84.

Nakamura, K., Yamagishi, S.-i., Adachi, H., Kurita-Nakamura, Y., Matsui, T., and Inoue, H. (2009) Serum levels of pigment epithelium-derived factor (PEDF) are positively associated with visceral adiposity in Japanese patients with type 2 diabetes, *Diabetes/Metabolism Research and Reviews 25*, 52-56.

Nelius, T., Martinez-Marin, D., Hirsch, J., Miller, B., Rinard, K., Lopez, J., de Riese, W., and Filleur, S. (2014) Pigment epithelium-derived factor expression prolongs survival and enhances the cytotoxicity of low-dose chemotherapy in castration-refractory prostate cancer, *Cell Death Dis 5*, e1210.

Norheim, F., Raastad, T., Thiede, B., Rustan, A. C., Drevon, C. A., and Haugen, F. (2011) Proteomic identification of secreted proteins from human skeletal muscle cells and expression in response to strength training, *American Journal of Physiology - Endocrinology and Metabolism 301*, E1013-E1021.

Notari, L., Baladron, V., Aroca-Aguilar, J. D., Balko, N., Heredia, R., Meyer, C., Notario, P. M., Saravanamuthu, S., Nueda, M. L., Sanchez-Sanchez, F., Escribano, J., Laborda, J., and Becerra, S. P. (2006) Identification of a lipase-linked cell membrane receptor for pigment epithelium-derived factor, *J Biol Chem 281*, 38022-38037.

Nozue, T., Yamagishi, S.-i., Hirano, T., Yamamoto, S., Tohyama, S., Fukui, K., Umezawa, S., Onishi, Y., Kunishima, T., Hibi, K., Terashima, M., and Michishita, I. (2015) Pigment epithelium-derived factor is associated with necrotic core progression during statin therapy, *Coronary Artery Disease 26*, 107-113.

O'Donohue, M. F., Choesmel, V., Faubladier, M., Fichant, G., and Gleizes, P. E. (2010) Functional dichotomy of ribosomal proteins during the synthesis of mammalian 40S ribosomal subunits, *J Cell Biol 190*, 853-866.

Ogata, N., Tombran-Tink, J., Nishikawa, M., Nishimura, T., Mitsuma, Y., Sakamoto, T., and Matsumura, M. (2001) Pigment epithelium-derived factor in the vitreous is low in diabetic retinopathy and high in rhegmatogenous retinal detachment, *American Journal of Ophthalmology 132*, 378-382.

Ogata, N., Nishikawa, M., Nishimura, T., Mitsuma, Y., and Matsumura, M. (2002) Inverse levels of pigment epithelium-derived factor and vascular endothelial growth factor in the vitreous of eyes with rhegmatogenous retinal detachment and proliferative vitreoretinopathy, *American Journal of Ophthalmology 133*, 851-852.

Ogata, N., Matsuoka, M., Imaizumi, M., Arichi, M., and Matsumura, M. (2004) Decrease of pigment epithelium-derived factor in aqueous humor with increasing age, *American Journal of Ophthalmology 137*, 935-936.

Orgaz, J. L., Ladhani, O., Hoek, K. S., Fernandez-Barral, A., Mihic, D., Aguilera, O., Seftor, E. A., Bernad, A., Rodriguez-Peralto, J. L., Hendrix, M. J. C., Volpert, O. V., and Jimenez, B. (2009) /`Loss of pigment epithelium-derived factor enables migration, invasion and metastatic spread of human melanoma/', *Oncogene 28*, 4147-4161.

Park, K., Jin, J., Hu, Y., Zhou, K., and Ma, J.-x. (2011) Overexpression of pigment epithelium-derived factor inhibits retinal inflammation and neovascularization, *The American Journal of Pathology 178*, 688-698.

Pignolo RJ1, Cristofalo VJ, Rotenberg MO (1993). Senescent WI-38 cells fail to express EPC-1, gene induced in young cells uponentry into the G0 state. J Biol Chem. Apr 25;268(12):8949-57

Quan GM, Ojaimi J, Nadesapillai AP, Zhou H, Choong PF (2002) Resistance of epiphyseal cartilage to invasion by osteosarcoma is likely to be due to expression of antiangiogenic factors. *Pathobiology* 70:361–367

Ramirez-Castillejo, C., Sanchez-Sanchez, F., Andreu-Agullo, C., Ferron, S. R., Aroca-Aguilar, J. D., Sanchez, P., Mira, H., Escribano, J., and Farinas, I. (2006) Pigment epithelium-derived factor is a niche signal for neural stem cell renewal, *Nat Neurosci 9*, 331-339.

Semkova, I., Kreppel, F., Welsandt, G., Luther, T., Kozlowski, J., Janicki, H., Kochanek, S., and Schraermeyer, U. (2002) Autologous transplantation of genetically modified iris pigment epithelial cells: A promising concept for the treatment of age-related macular degeneration and other disorders of the eye, *Proceedings of the National Academy of Sciences 99*, 13090-13095.

Sheikpranbabu, S., Haribalaganesh, R., Lee, K.-j., and Gurunathan, S. (2010) Pigment epithelium-derived factor inhibits advanced glycation end products-induced retinal vascular permeability, *Biochimie 92*, 1040-1051.

Sheikpranbabu, S., Ravinarayanan, H., Elayappan, B., Jongsun, P., and Gurunathan, S. (2010) RETRACTED: Pigment epithelium-derived factor inhibits vascular endothelial growth factor-and interleukin-1beta-induced vascular permeability and angiogenesis in retinal endothelial cells, *Vascular Pharmacology 52*, 84-94.

Shi, H.-s., Yang, L.-p., Wei, W., Su, X.-q., Li, X.-p., Li, M., Luo, S.-t., Zhang, H.-l., Lu, L., Mao, Y.-q., Kan, B., and Yang, L. (2013) Systemically administered liposome-encapsulated Ad-PEDF potentiates the anti-cancer effects in mouse lung metastasis melanoma, *Journal of Translational Medicine 11*, 86-86.

Sidle, D. M., Maddalozzo, J., Meier, J. D., Cornwell, M., Stellmach, V., and Crawford, S. E. (2005) ALtered pigment epithelium-derived factor and vascular endothelial growth factor levels in lymphangioma pathogenesis and clinical recurrence, *Archives of Otolaryngology-head & Neck Surgery 131*, 990-995.

Smith, C. P., and Steinle, J. J. (2007) Changes in growth factor expression in normal aging of the rat retina, *Experimental Eye Research 85*, 817-824.

Spranger, J., Osterhoff, M., Reimann, M., Mohlig, M., Ristow, M., Francis, M. K., Cristofalo, V., Hammes, H.-P., Smith, G., Boulton, M., and Pfeiffer, A. F. H. (2001) Loss of the Antiangiogenic Pigment Epithelium-Derived Factor in Patients With Angiogenic Eye Disease, *Diabetes 50*, 2641-2645.

Steele, F. R., Chader, G. J., Johnson, L. V., and Tombran-Tink, J. (1993) Pigment epithelium-derived factor: neurotrophic activity and identification as a member of the serine protease inhibitor gene family, *Proceedings of the National Academy of Sciences of the United States of America 90*, 1526-1530.

Steinle, J. J., Sharma, S., and Chin, V. C. (2008) Normal Aging Involves Altered Expression of Growth Factors in the Rat Choroid, *The Journals of Gerontology Series A: Biological Sciences and Medical Sciences 63*, 135-140.

Stellmach, V., Crawford, S. E., Zhou, W., and Bouck, N. (2001) Prevention of ischemia-induced retinopathy by the natural ocular antiangiogenic agent pigment epithelium-derived factor, *Proceedings of the National Academy of Sciences* 98, 2593-2597.

Streck, C. J., Zhang, Y., Zhou, J., Ng, C., Nathwani, A. C., and Davidoff, A. M. (2005) Adeno-associated virus vector-mediated delivery of pigment epithelium-derived factor restricts neuroblastoma angiogenesis and growth, *Journal of Pediatric Surgery 40*, 236-243.

Sugita, Y., Becerra, S. P., Chader, G. J., and Schwartz, J. P. (1997) Pigment epithelium-derived factor (PEDF) has direct effects on the metabolism and proliferation of microglia and indirect effects on astrocytes, *Journal of Neuroscience Research* 49, 710-718.

Sunderland, K. L., Tryggestad, J. B., Wang, J. J., Teague, A. M., Pratt, L. V., Zhang, S. X., Thompson, D. M., and Short, K. R. (2012) Pigment epithelium-derived factor (PEDF) varies with body composition and insulin resistance in healthy young people, *The Journal of Clinical Endocrinology & Metabolism 97*, E2114-E2118.

Sun, Y., Che, X., Zhu, L., Zhao, M., Fu, G., Huang, X., Xu, H., Hu, F., and Zhang, X. (2012) Pigment epithelium derived factor inhibits the growth of human endometrial implants in nude mice and of ovarian endometriotic stromal cells in vitro, *Plos One* 7, e45223.

Takenaka, K., Yamagishi, S., Jinnouchi, Y., Nakamura, K., Matsui, T., and Imaizumi, T. (2005) Pigment epithelium-derived factor (PEDF)-induced apoptosis and inhibition of vascular endothelial growth factor (VEGF) expression in MG63 human osteosarcoma cells, *Life Sciences 77*, 3231-3241

Taniwaki, T., Becerra, S. P., Chader, G. J., and Schwartz, J. P. (1995) Pigment epithelium-derived factor is a survival factor for cerebellar granule cells in culture, *Journal of Neurochemistry 64*, 2509-2517.

Taniwaki, T., Hirashima, N., Becerra, S. P., Chader, G. J., Etcheberrigaray, R., and Schwartz, J. P. (1997) Pigment epithelium-derived factor protects cultured cerebellar granule cells against glutamate-induced neurotoxicity, *Journal of Neurochemistry 68*, 26-32.

Tombran-Tink, J., Chader, G. G., and Johnson, L. V. (1991) PEDF: A pigment epithelium-derived factor with potent neuronal differentiative activity, *Experimental Eye Research 53*, 411-414.

Uehara, H., Miyamoto, M., Kato, K., Ebihara, Y., Kaneko, H., Hashimoto, H., Murakami, Y., Hase, R., Takahashi, R., Mega, S., Shichinohe, T., Kawarada, Y., Itoh, T., Okushiba, S., Kondo, S., and Katoh, H. (2004) Expression of Pigment Epithelium-Derived Factor Decreases Liver Metastasis and Correlates with Favorable Prognosis for Patients with Ductal Pancreatic Adenocarcinoma, *Cancer Research 64*, 3533-3537.

Unterlauft, J. D., Claudepierre, T., Schmidt, M., Müller, K., Yafai, Y., Wiedemann, P., Reichenbach, A., and Eichler, W. Enhanced survival of retinal ganglion cells is mediated by Müller glial cell-derived PEDF, *pp* 206-214.

Urban, N., and Guillemot, F. (2014) Neurogenesis in the embryonic and adult brain: same regulators, different roles, *Front Cell Neurosci 8*, 396.

Wang, F., Ma, X., Zhou, M., Pan, X., Ni, J., Gao, M., Lu, Z., Hang, J., Bao, Y., and Jia, W. (2013) Serum pigment epithelium-derived factor levels are independently correlated with the presence of coronary artery disease, *Cardiovascular Diabetology 12*, 56-56.

Wang, L., Schmitz, V., Perez-Mediavilla, A., Izal, I., Prieto, J., and Qian, C. (2003) Suppression of angiogenesis and tumor growth by adenoviral-mediated gene transfer of pigment epithelium-derived factor, *Mol Ther 8*, 72-79.

Wang, Y., Subramanian, P., Shen, D., Tuo, J., Becerra, S., and Chan, C.-C. (2013) Pigment epithelium-derived factor reduces apoptosis and pro-inflammatory cytokine gene expression in a murine model of focal retinal degeneration, *Asnneuro5*, e00126.

Xu, Z., Dong, Y., Peng, F., Yu, Z., Zuo, Y., Dai, Z., Chen, Y., Wang, J., Hu, X., Zhou, Q., Ma, H., Bao, Y., Gao, G., and Chen, M. (2015) Pigment epithelium-derived factor enhances tumor response to radiation through vasculature normalization in allografted lung cancer in mice, *Cancer Gene Ther 22*, 181-187.

Yamaji, Y., Yoshida, S., Ishikawa, K., Sengoku, A., Sato, K., Yoshida, A., Kuwahara, R., Ohuchida, K., Oki, E., Enaida, H., Fujisawa, K., Kono, T., and Ishibashi, T. (2008) TEM7 (PLXDC1) in neovascular endothelial cells of fibrovascular membranes from patients with proliferative diabetic retinopathy, *Investigative Ophthalmology & Visual Science 49*, 3151-3157.

Yang, S., Li, Q., Zhong, L., Song, Y., Tian, B., Cheng, Q., Qing, H., Xia, W., Luo, M., and Mei, M. (2011) Serum pigment epithelium-derived factor is elevated in women with polycystic ovary syndrome and correlates with insulin resistance, *The Journal of Clinical Endocrinology & Metabolism 96*, 831-836.

Zamiri, P., S. Masli, et al. (2006). "Pigment epithelial growth factor suppresses inflammation by modulating macrophage activation." *Investigative Ophthalmology & Visual Science 47(9)*: 3912-3918.

Zhang, L. J., Chen, J. F., Ke, Y., Mansel, R. E., and Jiang, W. G. (2006) Expression of pigment epithelial derived factor is reduced in non-small cell lung cancer and is linked to clinical outcome, *International Journal of Molecular Medicine 17*, 937-944.

Zhang, S. X., Wang, J. J., Gao, G., Shao, C., Mott, R., and Ma, J.-x. (2005) Pigment epithelium-derived factor (PEDF) is an endogenous antiinflammatory factor, *The FasebJournal*.

Zhang, S. X., J. J. Wang, et al. (2006). "Pigment epithelium-derived factor (PEDF) is an endogenous antiinflammatory factor." *Faseb Journal 20(2)*: 323-325.

Zhou, X., Li, F., Kong, L., Chodosh, J., and Cao, W. (2009) Anti-inflammatory effect of pigment epithelium-derived factor in DBA/2J mice, *Molecular Vision 15*, 438-450.

Zhu, D., Deng, X., Spee, C., Sonoda, S., Hsieh, C.-L., Barron, E., Pera, M., and Hinton, D. R. (2011) Polarized secretion of PEDF from human embryonic stem cell-derived RPE promotes retinal progenitor cell survival, *Investigative Ophthalmology & Visual Science 52*, 1573-1585.

Chapter 2 Characterizing PEDF receptors PLXDC1 and PLXDC2

2.1 Introduction

The receptor of PEDF has eluded identification for 20 years despite of considerable effort in academia and industry. We started the search eight years ago and tried several strategies as mentioned in the previous chapter. Eventually, we identified two homologous membrane proteins, PLXDC1 and PLXDC2, as PEDF receptors. Human PLXDC1 (500 amino acids) and PLXDC2 (529 amino acids) are encoded by genes *plxdc1* and *plxdc2* respectively. They localize on the cell surface with a very large extracellular domain at N-terminus, a single transmembrane domain and a relatively small intracellular domain at the C-terminus (**Figure 2-1**). Neither of them has been categorized into any known protein family or receptor family.

Studying PEDF receptors requires robust and accessible cellular assays for gain and loss of function studies. We used three cell types that respond robustly and reproducibly to PEDF as the cellular models to study PEDF receptors. They are macrophage cell RAW267.4, endothelial cell SVEC4-10, and neuronal cell 661W. These three cell types represent three distinct cellular targets of PEDF. We found that both PLXDC1 and PLXDC2 are expressed in these three cellular models, consistent with previous knowledge (Wang et al., 2005; Gaultier et al.,2010; Cheng et al., 2014).

For a membrane protein to qualify as a receptor, it should meet two criteria. First, it confers cell-surface binding to the extracellular ligand. Second, it mediates signal transduction into cells from the extracellular ligand. In this chapter, I will present the evidence supporting PLXDC1 and PLXDC2 as PEDF receptors that meet both criteria. We found that PLXDC1 and PLXDC2 confer PEDF binding to cell surface by interacting through their extracellular domains. In addition, we found that PLXDC1 and PLXDC2 mediate distinct effects of PEDF in three cell models described above in a cell-type specific manner. Although PLXDC1 and PLXDC2 mediate the PEDF induced interleukin 10 (IL-10) secretion in macrophages; PLXDC2 alone is responsible for the PEDF induced endothelial cell death and PLXDC1 alone mediates the neuronal protection effect of PEDF. The findings presented in this chapter have been published (Cheng et al., 2014).

2.2 Materials and methods

2.2.1 Material

Reagents, cell lines, and equipment used for the experiments described in this chapter are listed in **Table 2-1**. Three cell models (RAW267.4 cell, endothelial cell SVEC4-10, and neuronal cell 661W) all express both PLXDC1 and PLXDC2 as shown in **Figure 2-2**. Monoclonal anti-Rim antibody is against Rim tag, a strand of peptide with 14 amino acids (NETYDLPLHPRTAG) generated by Dr. Robert Molday's lab at University of British Columbia (Illing et al.,1997).

2.2.2 Engineering cDNAs for PLXDC1, PLXDC2 and PEDF.

PLXDC1, PLXDC2 and PEDF genes were engineered into PRK5 vector with proceeded secretion signal for alkaline phosphatase (AP). The HA tag was added after the secretion signal for AP and before the N-terminus of PEDF to produce N-terminal HA-tagged PEDF (HA-PEDF). We created receptors without cytoplasmic tail (PLXDC1-dC: 19-454; PLXDC2-dC: 31-482). PLXDC1 extracellular fragment with Rim tag at the N-terminus (19-426, Rim-PLXDC1-ECD) and its N-terminus truncated short version (126-426, Rim-PLXDC1-sECD) were also engineered. We also created chimeras containing the transmembrane domain (TM) of another single transmembrane protein DCC (Stein and Tessier-Lavigne, 2001) and the C-terminus of the receptors. The DCC transmembrane domain was fused to the secretion signal of AP and Rim tag at the N-terminus and the cytoplasmic tail of PLXDC1 or PLXDC2 at the C-terminus. The most likely positions of phosphorylation sites in the cytoplasmic domains of human PLXDC1 and PLXDC2 were identified through PhosphoSite Plus, a bioinformatics resource to identify potential protein phosphorylation sites (http://www.phosphosite.org/staticUsingPhosphosite.do). Residue numbers are according to human isoform 1.

cDNA was transfected into cells by jetPRIME reagent following the manufacturer's protocol. Cells were split 16 hours before transfection so that they reached 40-50% confluency during transfection. cDNA to be transfected was mixed with jetPRIME buffer, vortexed for 10 sec and

spun down. jetPRIME reagent was added and the mixture was vortexed for 10 sec and spun down. The jetPRIME-DNA mixture was incubated at room temperature (RT) for 10 min and was gently added to cells. Six hours after transfection, cell medium was changed to fresh medium.

2.2.3 PEDF purification from conditioned media.

We found in previous experiments that adding tag to PEDF at either N-terminus or C-terminus impairs the biological activity of PEDF. Therefore, we produced untagged PEDF for functional assays. PEDF is naturally present in several isoforms as revealed by isoelectric focusing (Tombran-Tink et al., 1995). Not all PEDF isoforms are equally active (Duh et al., 2002; Subramanian et al., 2012). Consistent with previous reports (Duh et al., 2002; Subramanian et al., 2012), we found that more negatively charged PEDF isoforms are more biologically active. PEDF produced by mammalian cells are purified by chromatography. Because negatively charged PEDF isoforms are more biologically active, we purified PEDF from cell conditioned medium using sequential anion exchange chromatography, a combination of Q sepharose and polyethyleneimine column.

To produce PEDF, we performed large-scale (5-10 plates of petri dish) transfection of human PEDF cDNA into HEK293T cells using jetPRIME reagent. Six hours after transfection, the cells were washed twice with Hank's Balanced Salt Solution (HBSS) and cultured in serum free

Dulbecco's Modified Eagles medium (SFM). Conditioned SFM was harvested 24, 48, or 72 hours. One volume of SFM was dialyzed against 50 volumes of binding buffer (20 mM Tris, pH 7.5 and 50 mM NaCl) overnight at 4°C. Dialyzed medium was then applied to Q sepharose pre-equilibrated with 20 bed volumes of the binding buffer. The column was washed with 10 bed volumes of binding buffer. Elution was performed using a series of elution buffer containing 20 mM Tris, pH 7.5 with 100, 200, 300, or 400 mM NaCl. Two bed volumes of elution buffer was used for each fraction.

High performance liquid chromatography (HPLC) using polyethyleneimine column was performed to further purify PEDF. Briefly, buffer exchange for the Q fraction containing PEDF was performed for three times by diluting with 10 volumes of column buffer (25 mM Tris, pH 8.4) and concentrating in an Ultracentrifugal filter with a spin at 3.4k g for 20 min. Equilibrated Q fraction was then loaded onto the HPLC system. HPLC was performed using the Agilent 1100 series liquid chromatography system with a diode-array detector. Proteins were separated on polyethyleneimine column using column buffer with increasing NaCl concentrations as the mobile phase (from 0 to 1.8 M in 8 min and the 1.8 M sodium concentration was maintained for another 4 min). The flow speed of mobile phase was 0.5 ml/min, and four fractions were collected every minute. Elution fractions with significant A280 value were saved. Buffer exchange was performed for three times by diluting with 10 volumes of phosphate buffered

saline (PBS) and concentrating in an Ultracentrifugal filter. The final volume of each concentrated elution was 0.5 ml.

The presence of PEDF was confirmed by both total gel staining. Briefly after protein samples were resolved in SDS-PAGE gel by electrophoresis, total proteins in the gel were stained by Sypro Ruby. The gel was fixed twice (30 min incubation each time) by fixation buffer (50% methanol, 10% acetic acid in distilled water) at RT. Sypro Ruby was used to stain the gel overnight in dark. The next day, Sypro Ruby staining reagent was removed. The gel was washed twice (30 min incubation each time) by wash buffer (10% methanol, 7% acetic acid in distilled water) at RT before being visualized under UV light. Protein was sterilized by filtering through Ultrafree Durapore 0.22 μm filter with a spin at 12k g for 1 min.

2.2.4 Gene expression analysis at mRNA level

Gene expression levels were analyzed by reverse transcription polymerase chain reaction (RT-PCR). Total RNA was extracted from cells using Qiagen RNA purification kit. Total RNA concentration was measured by Nanodrop at 260 nm. We used SuperScript III Synthesis System to generate cDNA library from total RNA. Oligo dT provided in the kit was used as primer to anneal with mRNA. Equal amount of total RNA in weight for each condition was used for comparison. Nuclease free water was used to replace total RNA in control to rule

out RNA contamination. To evaluate receptor expression level, we used PCR to amplify a fragment of receptor gene from cDNA library. Mouse PLXDC1 was amplified by 5′-GGAGGCAGAAGGCAAGACATGCG-3′ and 5′-CGTGGAGGCCGAGCAGTGCTGA-3′. mouse PLXDC2 was amplified by 5′-CTGCCAGCCGGGATCTGTGGGTTAACATAGACC-3′ and 5′-GGGAAGTGGAGTCATCTCCACAGCTGAGATGTTGG-3′. Primer concentration is 0.5 μM. Anealing temperature was set at (55°C). To see a differentiated gene expression level between conditions before saturation, amplified DNA fragments were sampled when PCR reaction was paused at 28 cycles, 30 cycles, 32 cycles and 35 cycles. The amplified DNA fragments were analyzed by DNA gel electrophoresis.

2.2.5 siRNA -mediated knock-down

After screening many siRNA transfection reagents including X-tremeGENE, siTran, jetPRIME , RNAiMAX, and GenMute, we found that the most effective siRNA transfection reagent is RNAiMAX. Since the three cell types (RAW267.4, SVEC4-10 and 661W) used as cellular models to study PEDF receptors are all mouse cells, siRNAs targeting mouse genes were tested. For mouse PLXDC1, siRNAs tested included Dharmacon D-060224-01 (siRNA-1), Dharmacon D-060224-02 (siRNA-2), Dharmacon D-060224-03 (siRNA-3), Dharmacon D-060224-04 (siRNA-4), Invitrogen 4390771-s90877 (siRNA-5), Invitrogen 4390771-s90878 (siRNA-6), Dharmacon smart pool L-060224-01 (siRNA-7) and Origene 866091-SR46066C (siRNA-8). For

mouse PLXDC2, siRNAs tested included Dharmacon D-059538-01 (siRNA-1), Dharmacon D-059538-02 (siRNA-2), Dharmacon D-059538-03 (siRNA-3), Dharmacon D-059538-04 (siRNA-4), Invitrogen 4390771-n380220 (siRNA-5), Invitrogen 4390771-n380229 (siRNA-6), Dharmacon smart pool L-059538-01 (siRNA-7), and Origene 866094-SR416812C (siRNA-8).

We did two consecutive rounds of reverse transfection to achieve high transfection rate and effective knockdown. Briefly, siRNA oligo was diluted in opti-MEM medium and mixed with RNAiMAX according to protocol. The mixture was incubated for 10 min at RT. Cells were replated at 1:5 ratio in antibiotic free culture medium. The siRNA mixture was added to cells with a final siRNA concentration of 50 nM. 48 hours after transfection, the cells were reverse transfected again using the same siRNA for the second round of knockdown. Functional assays were performed 48 hours after the second round of reverse transfection.

2.2.6 Receptor binding assay

PEDF was biotinylated using sulfo-NHS-SS-biotin after overnight dialysis in PBS at 4°C. After biotinylation, free biotin was removed by further overnight dialysis in PBS at 4°C and the degree of biotinylation was assessed by the shift of molecular weight in SDS-PAGE gels after incubation with streptavidin. The advantage of biotinylation is that biotin is a tag much smaller than peptide tags or fusion protein tags and is less likely to interfere with biological activities. In addition, biotin is added after protein production and folding and allows sensitive detection.

However, excessive biotinylation can inactivate proteins due to the modification of key lysine residues. To prevent excessive biotinylation, the ideal degree of biotinylation is about 90%, as judged by shifting in molecular weight after binding to streptavidin. Biotinylated PEDF (20 nM) was added to transfected or control cells grown on a fibronectin-coated dish in HBSS with 10 mM HEPES, pH 7.5 and 2 mg/ml BSA at room temperature for 1 hour. After two continuous washes with HBSS, 10 mM HEPES, pH 7.5, the cells were fixed using freshly made 4% paraformaldehyde in HBSS, pH 7.5 for 20 min. The cells were heated in HBSS at 65°C for 1 hr to inactive endogenous AP activity. After blocking in 5 mg/ml BSA in PBS for 1 hour, the cells were incubated with streptavidin-AP diluted in 5 mg/ml BSA in PBS. After four washes using PBS, AP activity was visualized using NBT/BCIP.

2.2.7 Immunofluorescence

Control or receptor transfected HEK293T cells were incubated with polyclonal anti-receptor antibody in SFM and 0.5 mg/ml BSA at 37°C for 1 hour (anti-receptor antibody concentration 1:500 in volume). Cells were washed twice with HBSS before fixed in freshly made 4% paraformaldehyde in HBSS, pH 7.5 for 20 min at room temperature. Paraformaldehyde was washed away by two HBSS wash. Cells were incubated with anti-rabbit secondary antibody (concentration 1:1000) conjugated with Alexa Fluo 488 (AF488-anti-rabbit Ab) in dark at room temperature for 1 hour. Fluorescent signals representing cell surface expressed receptors were

observed and imaged by Nikon inverted microscope and quantified using Nikon NIS Elements AR Analysis software.

2.2.8 Cell coculture and protein copurification studies

NEK 293T cells were transfected with cDNA of HA-PEDF or Rim-tagged PLXDC1 constructs or control protein. Cells were harvested and replated in serum free medium (SFM) 24 hours after transfection. During replating, HA-PEDF transfected cells (split at 1:2 ratio) and PLXDC1 constructs or control protein transfected cells (split at 1:1 ratio) were mixed for coculture. Cell-conditioned medium was harvested 48 hours and purified using the monoclonal anti-Rim antibody conjugated to CNBr-activated Sepharose 4 Fast Flow beads. Briefly, conditioned medium was harvested and spun at 2,000×g for 5 min to remove cell debris. The medium was applied to anti-Rim antibody conjugated beads, and rotated for 4 hr at 2°C. The beads were washed two times using HBSS by spinning down at 2000×g for 30 s. Bound proteins were eluted by 0.1 M Glycine, pH = 2.3 for 15 min at room temperature and neutralized by 0.1 M Tris (pH 9.5). Elution was boiled with SDS and resolved in non-reducing SDS-PAGE gel and analyzed by Western Blotting. Rim-tagged proteins were detected by monoclonal anti-Rim antibody. HA-PEDF were detected using a polyclonal anti-HA antibody.

2.2.9 Protein electrophoresis and Western Blotting

Proteins were loaded onto 10% or 4-12% gradient SDS-PAGE gels and transferred to nitrocellulose membrane (10cm ×10cm). Membranes were blocked at RT for 1 hr in 10 ml 5% milk in Tris-Buffered Saline and Tween 20 (TBST). The membranes were incubated with primary antibody in 5% milk in TBST at RT for another 1 hr followed by three 5-min washes. Secondary antibody probing was performed in 10 ml 5% milk in TBST at RT for 1 hr followed by three 5-min washes. To detect weak signal, we did primary antibody probing in TBST with 5mg/ml BSA at RT for 1hr or at 4°C overnight.

We used two developing systems: the chemiluminescence system and Licor-infrared system. In chemiluminescence system, we used hydrogen peroxidase (HRP)-conjugated goat anti-mouse antibody (to probe monoclonal primary antibody，HRP-anti-mouse Ab), or HRP-conjugated goat anti-rabbit antibody (to probe polyclonal primary antibody, HRP-anti-rabbit Ab) as secondary antibody. To develop membranes, membranes were incubated with Luminata HRP substrate for 2min at RT. Then membranes were developed by Western blot detection system (Fujifilm, LAS-3000). In Licor-infrared system, we used Dylight 680-conjugated goat anti-mouse antibody (to amplify monoclonal primary antibody) or IRDye 800-conjugated goat anti-rabbit antibody (to amplify polyclonal primary antibody) as secondary antibody. Membranes were scanned by Licor Infrared Imager. In Licor-infrared system, the membrane can be probed by two primary antibodies from different species at the same time.

2.2.10 Endothelial cell death assay.

Mouse endothelial cell SVEC4-10 was used for this assay. The survival of SVEC4-10 with or without PEDF treatment was analyzed by the MTT assay. Briefly, SVEC4-10 cells were grown in Dulbecco's Modified Eagles Medium (DMEM) containing 10% FBS, penicillin and streptomycin at 37°C with 5% CO_2 until confluence. During splitting, SVEC4-10 were detached from the petri dish by 0.05% trypsin for 5 min at RT. Trypsin was neutralized by equal volume of trypsin inhibitor. Detached cells were collected by spinning down at 1200 rpm for 2min. Cells were then resuspended with serum free medium (SFM) containing 0.5mg/ml bovine serum albumin (BSA) and plated at 1:10 ratio. 20 nM PEDF was added at the same time as cell plating. Cell viability was assessed 24 hr after cell plating by MTT assay.

2.2.11 MTT assay

MTT assay was done by incubating cells with 100μl 100 μg/ml MTT reagent in SFM for 3 hours at 37°C. DMSO (50 μl) was added to each well after MTT reagent was removed. The absorbance of the purple color from the formazan formed was measured and quantified using POLARstar Omega at 570 nm. DMSO in empty well was used as blank control.

2.2.12 PEDF neurotrophic activity assay

PEDF neurotrophic effect on cone-derived 661W cells under hydrogen peroxide-mediated oxidative damage was evaluated. Basically, 661W cells were grown in 10% FBS, 40 μg/L of hydrocortisone 21-hemisuccinate, 40 μg/L of progesterone, 32 mg/L of putrescine, 40 μl/L of β-mercaptoethanol in DMEM containing penicillin and streptomycin and treated with 10 nM PEDF for 20 hours. Then 2.5 mM H_2O_2 was added to cells and incubated with cells for 1 hr (to achieve about 90% cell death in control cells the next day). After that the H_2O_2 containing media was replaced with fresh media and the cells were continuously grown for 24 hours. Cell survival was quantified using the MTT assay as described above. For siRNA transfected cells, 10 nM PEDF was added after two rounds of 48-hour transfection. For DNA transfection, the cells were split at 1:5 ratio 16 hr before transfection and were transfected using jetPRIME reagent. Four hours after transfection, the media was changed to fresh media and PEDF was added. All final assays were performed in 96-well plates in triplicate.

2.2.13 Macrophage IL-10 secretion assay

Macrophage cell line RAW267.4 was grown in RPMI1640 media with 10% FBS plus, penicillin and streptomycin. For DNA transfection, the cells were split at 1:6 ratio 16 hours before transfection and were transfected using jetPRIME reagent. Eight hours after transfection, the media was changed to fresh media while different concentration of PEDF was added. PEDF-induced IL-10 secretion from macrophages was assayed using mouse IL-10 ELISA kit

from Southern Biotech 18 hours after PEDF addition. For siRNA transfection, media was changed to fresh media and PEDF was added after two rounds of 48-hour transfection. All final assays were performed in 96-well plates in triplicate. We found that longer culture of RAW267.4 cells without cell replating leads to more responsiveness to PEDF. Since siRNA experiments need longer cell culture time, cells are consistently more responsive to PEDF than cells in DNA transfection experiments, which are done only 1 day after transfection.

2.3 Results

2.3.1 PLXDC1 and PLXDX2 confer cell-surface binding to PEDF

A prerequisite for a membrane protein to be receptor is the ability to confer extracellular ligand binding to cell surface. We performed biotinylated PEDF live cell surface binding assay using HEK293T cells heterologously expressing membrane proteins. We found that PLXDC1 or PLXDC2 confers extracellular PEDF binding to live cell surface (**Figure 2-3 A-C**). PLXDC1 and PLXDC2 without extracellular domain lose the ability to bind to PEDF, while a deletion of intracellular C-terminus does not affect binding (**Figure 2-3 D-F**). The cell surface expression of the membrane proteins is confirmed by live cell staining using anti-Rim antibody against the Rim tag engineered after the secretion signal at the N-terminus (**Figure 2-3 G-L**). These experiments demonstrated that PEDF binds to cell-surface transmembrane domain proteins

PLXDC1 and PLXDC2 through their extracellular domains. Previous claimed PEDF receptors phospholipase A2 and laminin receptor (LamininR) and PEDF interacting protein low-density lipoprotein receptor-related protein 6 (LRP6) do not confer PEDF binding to cell surface (**Figure 2-4**).

2.3.2 PLXDC1 copurifies with PEDF in immunopurification assay

We also performed co-immunoprecipitation assay to confirm direct interaction between PEDF and its receptor. HA-PEDF transfected HEK 293T cells were cocultured with Rim-PLXDC1-ECD, or Rim-PLXDC1-sECD or control transfected HEK 293T cells. After 48 hours of cell coculture, cell-conditioned medium was purified by anti-Rim antibody-conjugated sepharose beads. As shown in **Figure 2-5**, HA-PEDF was copurified with Rim-PLXDC1-ECD or with Rim-PLXDC1-sECD but not with control. The result supports that PEDF physically interacts with PLXDC1 extracellular domain.

The above evidence suggests that PLXDC1 and PLXDC2 physically interacts with PEDF and confer cell-surface binding to PEDF. To demonstrate that PLXDC1 or PLXDC2 meets the second criteria (transducing ligand signal), we adopted three cell models, macrophage cell RAW 267.4, endothelial cell SVEC4-10 and neuronal cell 661W, all of which express both PLXDC1 and PLXDC2 as introduced previously (**Figure 2-2**).

2.3.3 PEDF induces IL-10 secretion in macrophage through PLXDC1 or PLXDC2

In macrophage RAW267.4, PEDF is known to stimulate secretion of IL-10, an anti-inflammatory cytokine (Zamiri et al., 2006). We reproduced this result and measured IL-10 by ELISA. To illustrate if the PEDF-induced IL-10 secretion is receptor dependent, we created loss of function model and gain of function models. To perform loss of function studies, we screened for siRNAs that can effectively knockdown PLXDC1 or PLXDC2 expression in RAW267.4 cells (**Figure 2-6**). The most effective siRNA was used in subsequent functional assays. PLXDC1 or PLXDC2 cDNA was transfected into RAW267.4 cells for gain of function studies.

We found that knocking down of either PLXDC1 or PLXDC2 leads to a substantial decrease in PEDF response (**Figure 2-7A**). Conversely, transfection of either receptor into macrophages further augments PEDF-induced secretion of IL-10 without increasing basal activity (basal activity is defined as receptor activity without PEDF treatment) (**Figure 2-7 B**). Either receptor lacking the cytoplasmic domain no longer has this activity, consistent with role of the cytoplasmic domain in cellular signaling (**Figure 2-7 B**). Tyrosine 481 in human PLXDC1 is a highly conserved residue in the cytoplasmic domain and is a potential phosphorylation site (**Figure 2-8 C**). PLXDC1 with a mutation of this single residue in the cytoplasmic domain (Y481F) has highly enhanced PEDF-mediated response without increasing the basal activity of

the receptor (**Figure 2-7 D, E**). One potential mechanism is that phosphorylation of this residue dampens receptor signaling and the mutation prevents this inhibition. PLXDC1 transfected cell shows about 100% increased activity in response to 2 nM PEDF as compared to control cells, while PLXDC1-Y481F cells showed about 400% increased activity in response to PEDF (**Figure 2-7 D**). This profound stimulatory effect on PEDF signaling by mutating a single intracellular conserved residue in PLXDC1 supports its role in PEDF signaling.

2.3.4 PEDF inhibits SVEC4-10 endothelial cell death inthrough PLXDC2

Using endothelial cell SVEC4-10, we established a highly effective and reproducible assay to study PEDF-mediated endothelial cell death. We found that PEDF mediated cell death was completely suppressed by siRNA-mediated knockdown of PLXDC2, but there was no suppression by siRNA knockdown of PLXDC1 (**Figure 2-8 A**). Since the cytoplasmic domain of each receptor is expected to be involved in downstream signaling, we tested the effect of expression of the cytoplasmic domain fused to the transmembrane domain of another membrane protein (DCC) (Stein and Tessier-Lavigne, 2001) without the extracellular domain of each receptor. Interestingly, transfection of PLXDC2 cytoplasmic domain linked to the DCC transmembrane domain is sufficient to cause cell death independently of PEDF. In contrast, the cytoplasmic domain of PLXDC1 does not have this activity (**Figure 2-8 B**). We also found that mutations in two cytoplasmic residues that are potential phosphorylation sites in the PLXDC2

tail enhance the effect of PLXDC2 in causing cell death (**Figure 2-8 B**). These experiments

demonstrated that PLXDC2 is responsible for mediating PEDF-induced cell death in this cell

type, while there is no detectable role of PLXDC1. In addition, the cytoplasmic domain of the

PLXDC2 is sufficient to trigger downstream activity. SiRNA oligos for PLXDC1 or PLXDC2

were screened in SVEC 4-10 and the most effective siRNA oligo for either gene was used in the

above assay (**Figure 2-9**) .

2.3.5 PEDF protects neuronal cells via PLXDC1

To assay PEDF's neurotrophic activity, we used 661W cells, a neuronal cell line derived from

cone photoreceptors (Tan et al., 2004; Kanan et al., 2008). We found that PEDF treatment

effectively protects 661W cells against oxidative damage. Knocking down PLXDC1, but not

PLXDC2, in 661W cells abolishes the protective effect of PEDF (**Figure 2-10 A**). Conversely,

using gain of function analysis, we showed that transfection of PLXDC1 further enhances the

protective effect of PEDF and that transfection of the cytoplasmic domain of PLXDC1 protects

661W independent of PEDF (**Figure 2-10 B**). These experiments suggest that the cytoplasmic

domain of the receptor is responsible for triggering the intracellular events during receptor

activation. The dependence of 661W cell on PLXDC1 for the survival promoting effect of PEDF

is in contrast to the dependence of SVEC4-10 on PLXDC2 to mediate the cell death effect of

PEDF. SiRNA oligos for PLXDC1 or PLXDC2 were screened in 661W and the most effective

siRNA oligo for either gene was used in the above assay (**Figure 2-11**).

2.4 Discussion

In this chapter, we first show that PLXDC1 or PLXDC2 confers PEDF cell-surface binding on

live cells and directly interacts with PEDF. Second, through both loss of function and gain of

function studies, we demonstrate the PLXDC1- or PLXDC2-dependent response of PEDF in

three distinct cell models. In another word, PLXDC1 or PLXDC2 binds to PEDF on cell surface,

mediates PEDF signal transduction into cells. PLXDC1 or PLXDC2 are the only two proteins

meet the requirements as the cell-surface receptor for PEDF. Other known properties of

PLXDC1 and PLXDC2 such as tissue expression are also consistent with their roles as PEDF

receptors.

Most of the previous knowledge on the biological functions of these two membrane proteins was

obtained from gene expression studies. PLXDC1 expression was associated with blood vessels in

a disease specific pattern and may play a role in regulating endothelial behavior. PLXDC1 is also

called tumor endothelial marker 7 as it was originally identified to be a cell-surface protein

enriched in tumor blood vessels. A serial analysis of gene expression (SAGE) study which

evaluates mRNA quantity by analyzing the tag added on each transcripts revealed that PLXDC1 was specifically expressed in the endothelial cells from colorectal tumor tissue but not in endothelial cells from normal tissue of the same specimen (Croix et al., 2000). The tumor endothelium cell specific expression pattern of PLXDC1 has also been described in ovarian cancer (Lu et al., 2007) and glioblastoma (Beaty et al., 2007). All three findings are based on unbiased evaluation of transcripts quantity. Besides that, PLXDC1 was also found to be highly expressed in the endothelial cells of another human disease-diabetic retinopathy but not in endothelial cells in retina of other disease without involvement of angiogenesis (Yamaji et al., 2008). These studies suggest that PLXDC1 expression is highly specific to diseased blood vessels. Besides, PLXDC1 expression was found positively correlated with the vascular density in glioblastoma (Carpenter et al., 2015) and with invasion and progression of gastric cancer (Zhang et al., 2015) and osteogenic sarcoma (Fushs et al., 2007). An *in vitro* study illustrated that PLXDC1 expresses in mouse endothelial cell SVEC4-10 and promotes SVEC4-10 tube formation on fibrinogen in a serum-deprived condition (Wang et al., 2005). The identity of PLXDC1 as tumor endothelial cell marker that is highly expressed in tumor blood vessels is consistent with the function of PEDF in inhibiting tumor angiogenesis and tumor growth.

It is worth noting that PLXDC1 has a disease-specific expression in endothelial cell but it is not responsible for PEDF induced endothelial cell death in our model. Three explanations could

account for the finding. First, PEDF affects endothelial cell in multiple aspects. It probably induces endothelial cell death, suppresses migration and tube formation and controls blood vessel permeability via different signal pathways. As the interaction of PEDF and PLXDC2 triggers the signal pathway leading to cell death in our model, the interaction between PEDF and PLXDC1 could couple with other pathways and mediate other functions of PEDF. Second, PLXDC1 expression may be up-regulated in pathological condition that is not represented by our system. Thus in pathological conditions, PLXDC1 can outnumber PLXDC2 and plays a more dominant role than PLXDC2 does in mediating endothelial cell death. Third, PLXDC1 is not responsible for PEDF signaling in endothelial cells, possibly because its large extracellular domain interacts with other ligands that blocks PEDF binding. In fact, PLXDC1 has been proposed as a receptor for extracellular matrix protein Nidogen and facilitates cell spreading (Lee et al., 2006). Other research showed that PLXDC1 is also expressed on the macrophage cell surface (Gaultier et al., 2010) and is down-regulated by LDL receptor related protein 1 (LRP-1), a large membrane protein involved in endocytosis of a variety of cell surface receptors (Herz and Stickland, 2001). Our findings that PLXDC1 is responsible for PEDF mediated neuronal protection and for PEDF induced IL-10 secretion from macrophages contribute new knowledge of this protein.

On the other hand, PLXDC2 expression is likely associated with cell-cycle regulation. PLXDC2 is one of the target genes of E2F1, a transcriptional factor crucial in cell-cycle progression and tumorgenesis (Hallstrom et al., 2008). Besides, PLXDC2 is down-regulated during normal cell transformation to malignancy and perturbation of PLXDC2 increases tumor volume (McMurray et al., 2008). However, it is up-regulated while tumor cell enters senescence or undergoing apoptosis induced by drugs (Schwarze et al., 2005). In addition to the role in regulating cell cycle, PLXDC2 is also involved in stem cell biology. Microarray analysis identified PLXDC2 as an asymmetrical self-renewal associated marker in adult stem cells (Noh, 2006). Proteomic analysis also revealed PLXDC2 on the cell surface of human pluripotent stem cells (Boheler et al., 2014). PLXDC2 was also found as a mitogen for neuroprogenitors (Miller-Delaney et al., 2011). Consistent with these earlier reports, our study identified PLXDC2 as playing the dominant role in a PEDF-induced endothelial cell death model.

In summary, we found that PLXDC1 and PLXDC2 are PEDF cell surface receptors which confer PEDF live cell surface binding and tranduce PEDF signals into cells. None of previously reported PEDF receptor candidates satisfies one of these criteria. These two PEDF receptors have cell-type specific roles. In macrophage, both PLXDC1 and PLXDC2 mediate PEDF-induced IL-10 secretion. This suggests that both receptors are responsible in PEDF mediated anti-inflammatory function. PLXDC1, but not PLXDC2, plays a crucial role in the

neurotrophic effect of PEDF. In endothelial cell, PLXDC2, but not PLXDC1, is transducing the

cell death signal of PEDF.

Table 2-1. List of reagents, cell lines, and equipment.

	Materials/Equipment	Description	Manufacturer
Cell Lines	661W	Mouse cone derived cell	N/A
	COS-1	Monkey kidney fibroblast cells	ATCC
	HEK293T	Human embryo kidney 293 cell with T-antigen	ATCC
	RAW267.4	Mouse macrophage	ATCC
	SVEC4-10	Mouse endothelial cell	ATCC
Reagents	Affi-Gel	Affigel 10 Gel	Bio rad
	AF488-anti-rabbit Ab	Alexa 488 conjugated goat anti-rabbit antibody	Thermo Scientific
	Anti-Rim Ab	Monoclonal anti-Rim antibody	N/A
	β-mercaptoethanol	N/A	Sigma
	BSA	Bovine serum albumin fraction V	Santa cruz biotechnology
	AX-300	Polyethyleneimine column	Eprogen
	DMEM	Dulbecco's Modified Eagles Medium	Hyclone, GE Healthcare Life Sciences
	DMSO	Dimethyl sulfoxide	BDH solvent
	DTT	Dithiothreitol	Omnipur, Millipore
	Dylight 680 Ab	Dylight 680-conjugated goat anti-mouse antibody	Pierce, Thermo
	FBS	Fetal Bovine Serum	Hyclone, GE Healthcare Life Sciences
	FBS plus	Performance FBS	Gibco, ThermoFisher Scientific
	GenMute	SiRNA transfection reagent	SignaGen Laborotory
	HBSS	Hank's Balanced Salt Solution	Thermo Scientific
	HEPES	N/A	AMRESCO
	HRP-anti-mouse Ab	Goat anti-mouse Ig-HRP	SouthernBiotech
	HRP-anti-rabbit Ab	Goat anti-rabbit Ig-HRP	SouthernBiotech
	Hydrocortisone	Hydrocortisone 21-hemisuccinate	Sigma
	Hydrogen peroxide	N/A	ThermoFisher Scientific
	IL-10 ELISA Kit	Rat anti-mouse Interleukin-10 ELISA Set	SouthernBiotech
	IRDye 800CW Ab	IRDye 800-conjugated goat anti-rabbit antibody	Li-Cor
	JetPRIME	DNA transfection reagent	Polyplus-transfection
	Luminata HRP substrate	Luminata Forte Western HRP substrate	Millipore
	MCIB131	MCDB131 medium, no glutamine	Gibco, ThermoFisher Scientific
	MTT reagent	3-(4,5-Dimethylthiazol-2-yl)-2,5-Diphenyltetrazolium Bromide	AMRESCO Life Science Research Products
	MVGS	Microvascular growth supplement	Gibco, ThermoFisher Scientific

Materials/Equipment	Description	Manufacturer
NBT/BCIP	NBT/BCIP substrate solution	Thermo Scientific
Nitrocellulose membrane	N/A	Maine manufacturing
Opti-MEM	Reduced-Serum Medium, Improved Minimal Essential Medium	Gibco, ThermoFisher Scientific
Paraforamaldehyde	N/A	Acros Organics
PBS	Phosphate Buffered Saline	Corning cellgro
Penicillin/Streptomycin	Penicillin/Streptomycin solution 100X	Caissonlabs
Polyethyleneimine column	Polyethyleneimine column AX-301	Eprogen
Progesterone	N/A	Sigma
Protease inhibitor cocktail	Protease Inhibitor Single-Use Cocktail (100X)	Halt™, ThermoFisher Scientific
Putrescine	N/A	Sigma
Q sepharose	N/A	Amersham, GE Healthcare
Qiagen RNA purification kit	Rneasy Mini Kit	Qiagen
RNAiMAX	Lipofectamine RNAiMAX Transfection Reagent	ThermoFisher Scientific
RPMI1640 medium	PRIM 1640 medium	Hyclone, GE Healthcare Life Sciences
Sepharose beads	CNBr-activated Sepharose 5 Fast Flow beads	Amersham, GE Healthcare
SiTran	SiRNA transfection reagent	Origene
Streptavidin	N/A	Pierce
Streptavidin-AP	Alkaline Phosphotase conjugated streptavidin	Thermo Scientific
Sulfo-NHS-SS-biotin	N/A	Pierce
SuperScript III Synthesis System	RNA reverse transcription kit	Qiagen
Sypro Ruby Protein Gel Stain	N/A	ThermoFisher Scientific
Triton X-100	Triton X-100 surfactant	Omnipur, Millipore
Trypsin	0.05% trypsin	Hyclone, GE Healthcare Life Sciences
Trypsin Inhibitor	DTI, defined trypsin inhibitor	Gibco, Life Technology
X-tremeGENE	SiRNA transfection reagent	Roche

The left margin of the table is labeled **Reagents** (rotated).

	Materials/Equipment	Description	Manufacturer
Equipment	Fujifilm LAS 3000 imager	N/A	Fujifilm
	HPLC system	Agilent 1000 series	Agilent technology
	Li-Cor Infrared Imager	N/A	Li-Cor
	Nanodrop	N/A	Thermo Scientific
	Nikon inverted microscope	Nikon Eclipse Ti inverted microscope	Nikon
	POLARstar Omega	N/A	BMG Labtech
	Ultracentrifugal filter	15ml filter, membrane NMWL 10kDa	Millipore
	Ultrafree durapore filter	Ultrafree durapore 0.22 μm filter	Millipore
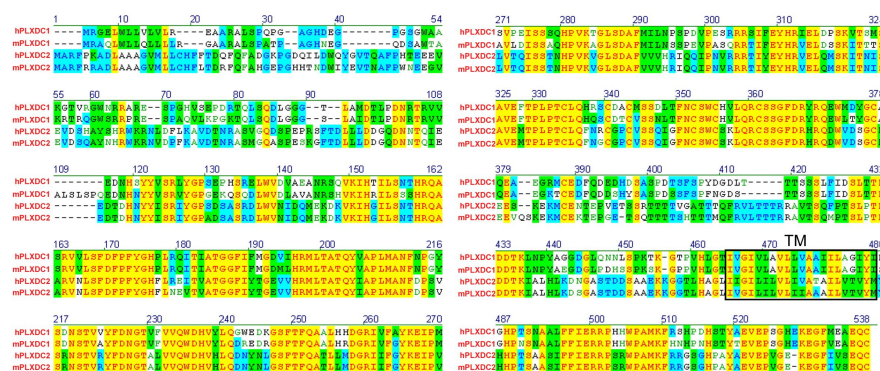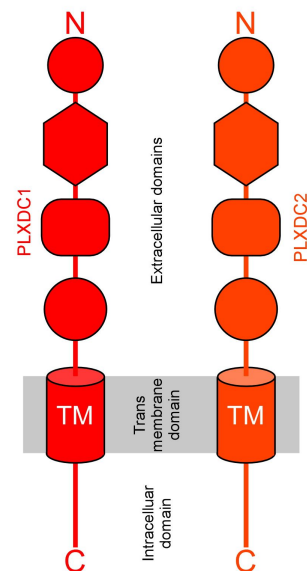
Figure 2-1. PLXDC1 and PLXDC2 protein sequences alignment.

(A) PLXDC1 and PLXDC2 share homology. Transmembrane domain (TM) is framed in black.

(B) Schematic diagrams of PLXDC1 and PLXDC2 showing the big extracellular domains, transmembrane domains and small intracellular domains.
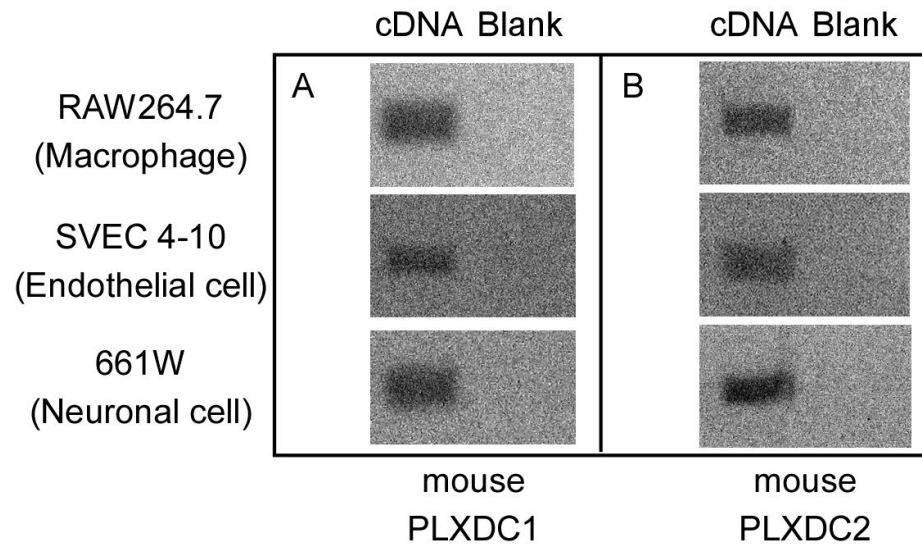
Figure 2-2. Expression of PLXDC1 and PLXDC2 in three cell models.

Total RNA was extracted from RAW 267.4, SVEC 4-10, and 661W cell respectively and reverse transcribed into cDNA. A fragment of PLXDC1 **(A)** or PLXDC2 **(B)** was amplified from the cDNA respectively by PCR using PLXDC1 or PLXDC2 specific primers. Nuclease free water was used as blank control.
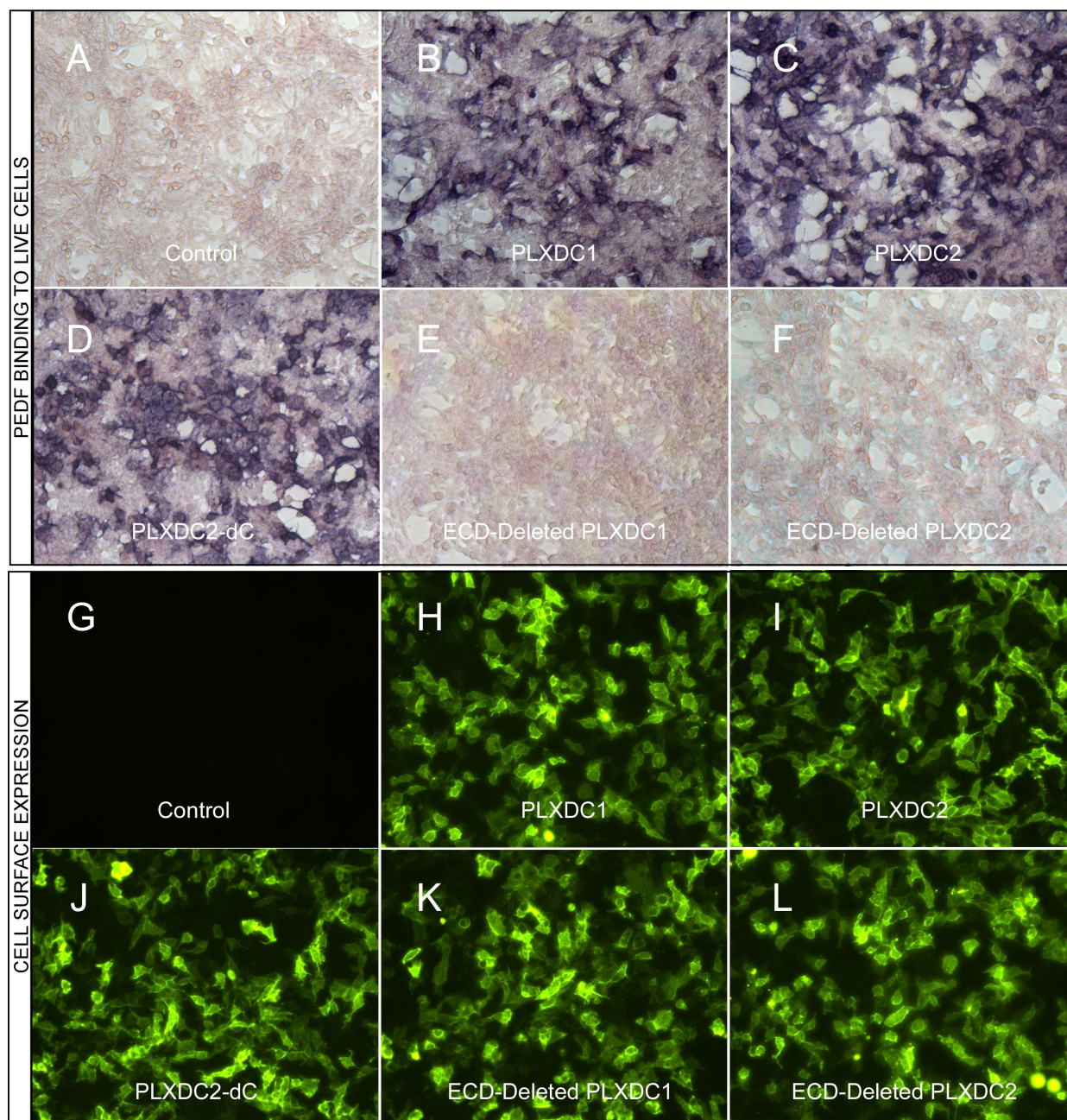
Figure 2-3. The binding of PEDF to PLXDC1 or PLXDC2 on live cell surface.

Upper panel: Binding of biotinylated PEDF to untransfected control HEK293T cells (**A**), HEK293T cells transfected with PLXDC1 (**B**) , PLXDC2 (**C**), intracelluar deleted PLXDC2

(PLXDC2-dCtail, **D**), extracelluar domain (ECD) deleted PLXDC1 (**E**) or ECD deleted PLXDC2 (**F**). Binding was detected by stretavidin-alkaline phosphatase, shown as deep purple color. Lower panel: Live cell staining of an Rim tag of control HEK293 cells **(G)** or HEK293 cells transfected with PLXDC1 **(H)**, PLXDC2 **(I)**, intracellular domain deleted PLXDC2 **(J**, PLXDC2-dC), ECD-deleted PLXDC1 (**K**), or ECD deleted PLXDC2 (**L**). All constructs have the Rim tag engineered after the secretion signal at the N-terminus.
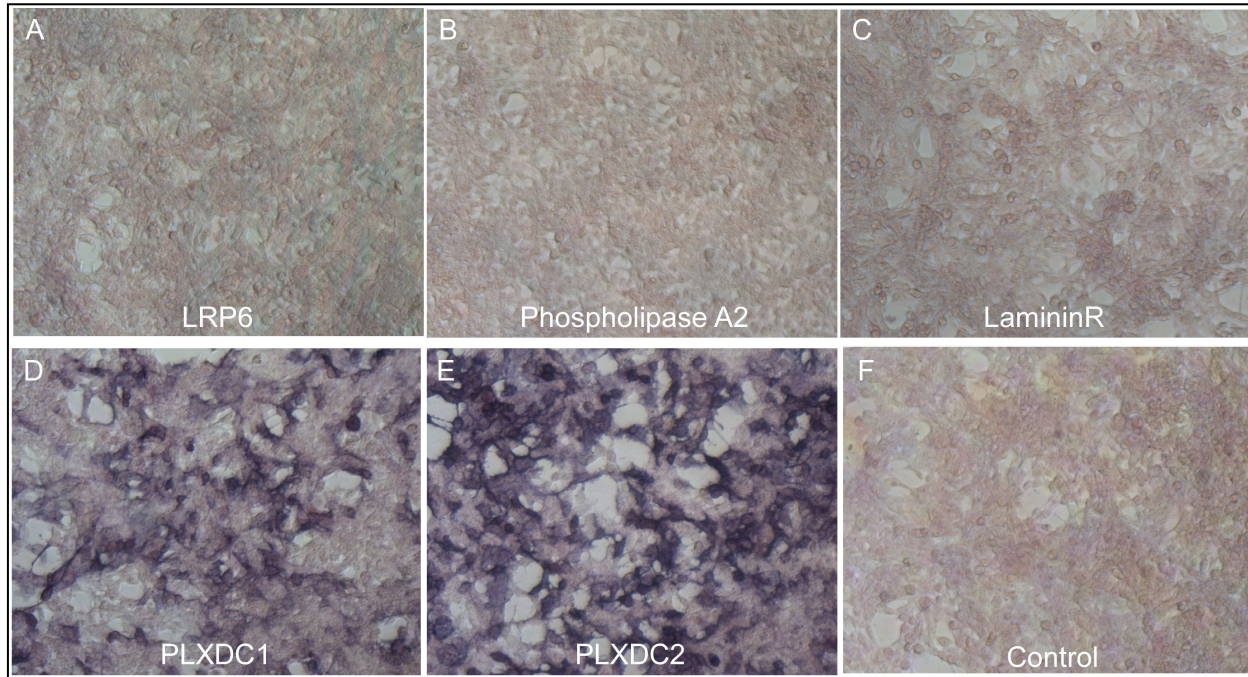
Figure 2-4. Binding of PEDF to cells expressing proposed PEDF receptors

Binding of biotinylated PEDF to HEK293T cells transfected with LRP6 **(A)**, phospholipase A2 **(B)**, laminin receptor (LamininR) **(C)**, PLXDC1 **(D)**, PLXDC2 **(E)** and untransfected control HEK293T cells **(F)**. Binding was detected by stretavidin-alkaline phosphatase, shown as deep purple color.
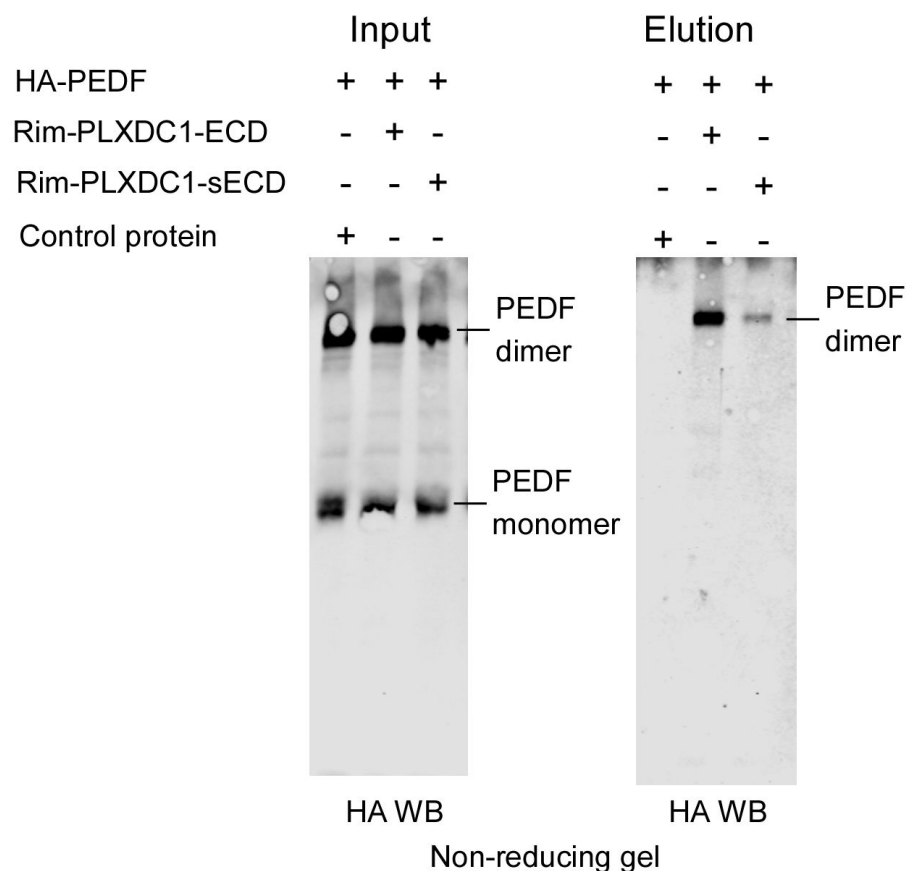
Figure 2-5. PEDF copurified with PLXDC1

HA-PEDF transfected HEK 293T cells were cocultured with Rim-PLXDC1-ECD, or Rim-PLXDC1-sECD or control transfected HEK 293T cells. A small fraction of cell-conditioned medium was directly resolved in SDS-PAGE gel as "Input" (left). The rest of medium was purified by anti-Rim antibody-conjugated sepharose beads. Purified proteins were analyzed as "Elution" (right). Proteins in both input and elution were probed by anti-HA antibody. As shown in the Western blot, HA-PEDF was copurified with Rim-PLXDC1-ECD or with Rim-PLXDC1-sECD but not with control. N-terminus is truncated in Rim-PLXDC1-sECD compared to Rim-PLXDC1-ECD. The formation of PEDF dimer is discussed in Chapter 3.
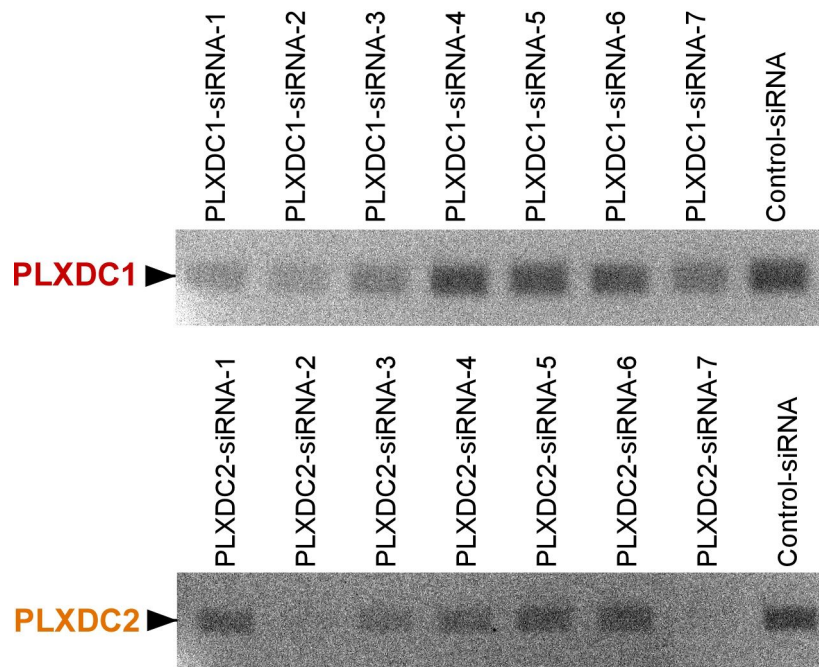
Figure 2-6. Unbiased screening for effective siRNAs in macrophage

We did unbiased screening for effective siRNAs that knock down PLXDC1 or PLXDC2 expression in macrophage cell RAW267.4. Above shows the expression of PLXDC1 and PLXDC2 at mRNA level after 48 hours of reverse transfection of 50nM siRNA of each kind. Messenger RNA was extracted from cells and reverse transcribed to cDNA. PLXDC1 or PLXDC2 copies in cDNA pool was detected by PCR. The siRNA definition is described in 2.2.5.
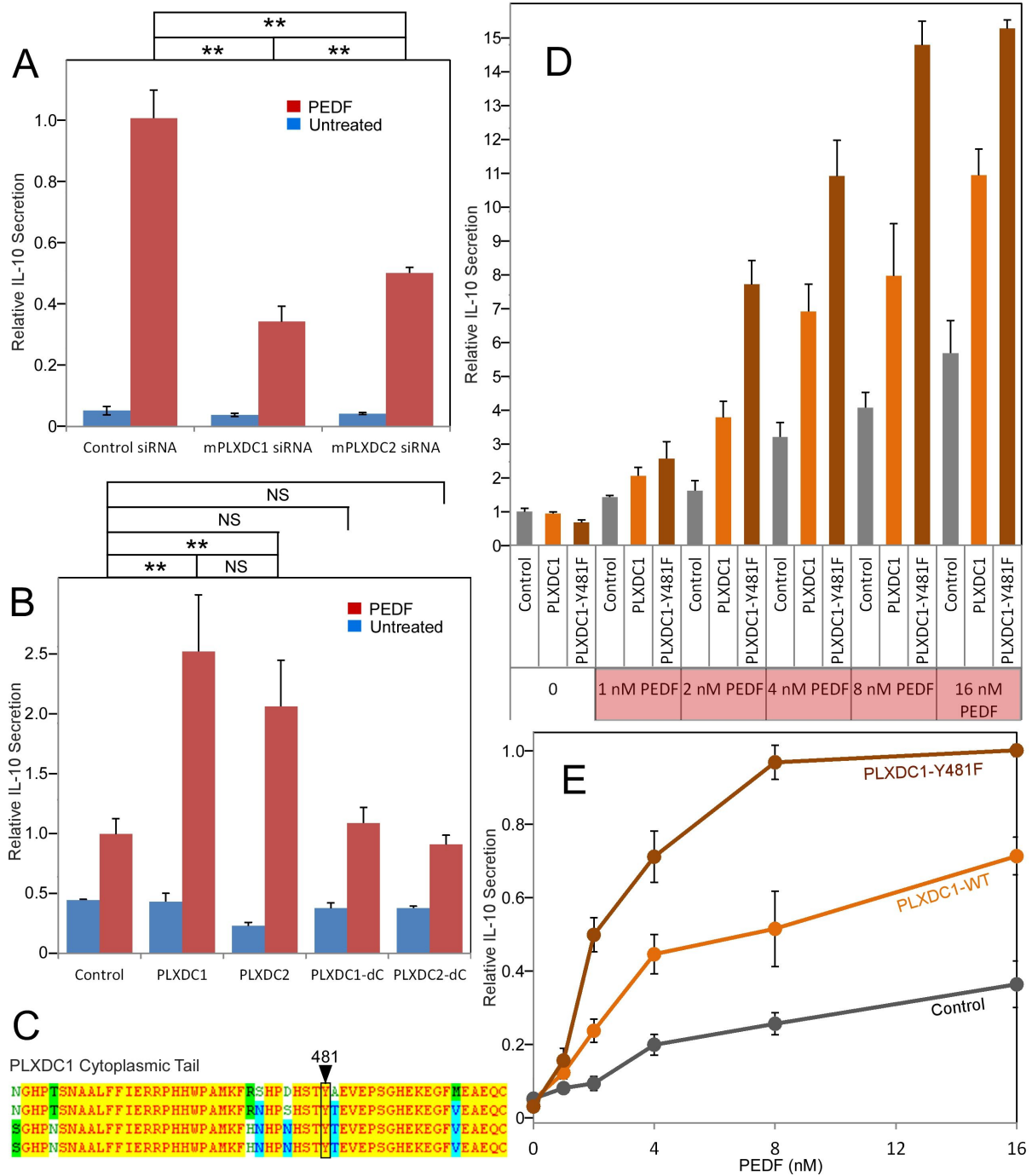
Figure 2-7. The roles of PLXDC1 and PLXDC2 in PEDF-induced IL-10 secretion

(**A**) siRNA-mediated knockdown of PLXDC1 or PLXDC2 substantially suppresses

PEDF-stimulated IL-10 secretion. Activity of control transfected cells with PEDF treatment is

defined as 1. ** = p < 0.01. (**B**) Transfection of either PLXDC1 or PLXDC2 cDNA enhances

PEDF-stimulated IL-10 secretion in RAW cell, while PLXDC1 or PLXDC2 lacking the

cytoplasmic domain (PLXDC1-dC or PLXDC2-dC) do not show significantly different secretion

from control EGFP transfection. Activity of control cells with PEDF treatment is defined as 1. **

= p < 0.01; NS = not significant. (**C**) Alignment of human, bovine, mouse, and rat PLXDC1

cytoplasmic tail and the location of the putative phosphorylated residue (residue number

according to human PLXDC1). (**D**) Comparing PEDF-induced IL-10 secretion by RAW267.4

transfected with PLXDC1 and PLXDC1-Y481F. Mutation Y481F on the cytoplasmic tail of

PLXDC1 greatly enhances its response to PEDF. Activity of control transfected cells without

PEDF treatment is defined as 1. (**E**) PEDF concentration-dependent stimulation of IL-10

secretion from control, PLXDC1, and PLXDC1-Y481F transfected cells (from D). Activity of

PLXDC1-Y481F cells at 16 nM PEDF is defined as 1.
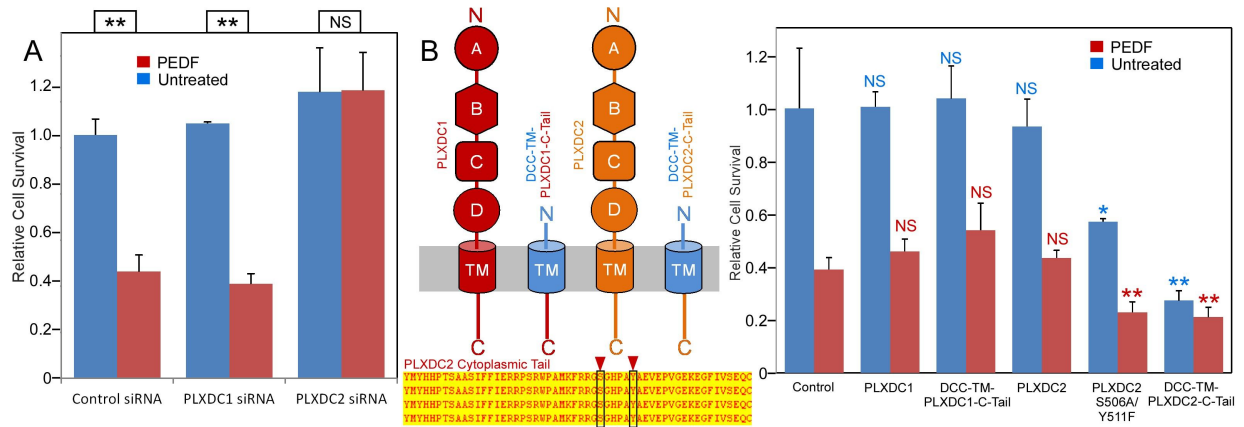
Figure 2-8. The PLXDC2 dependence of PEDF's effect on endothelial cell

(**A**) PEDF promoted-cell death of SVEC4-10 cells is suppressed by siRNA-mediated knockdown of PLXDC2, but not PLXDC1. Survival of control siRNA tranfected cells without PEDF treatment is defined as 1. Statistical significance is shown on the top. ** = p < 0.01, and NS = not significant. (**B**) Left panel: Schematic diagrams of full length receptors and the fusion proteins for the receptor cytoplasmic tails. The cytoplasmic tail of the receptor is fused to the TM domain of DCC, which is fused to the secretion signal of alkaline phosphase at the N-terminus. Alignment of human, mouse, rat and bovine PLXDC2 cytoplasmic tails shows complete conservation (bottom). Locations of potential phosphorylation sites are indicated. Right panel: Expression of cytoplasmic tail of PLXDC2, but not the cytoplasmic tail of PLXDC1 promotes SVEC4-10 cell death. PLXDC2 double mutant S506A/Y511F has greater activity. Survival of control EGFP transfected cells without PEDF treatment is defined as 1. Statistical significance of the comparison of cells without PEDF treatment (with the control cells without PEDF treatment)

is shown in blue. Statistical significance of the comparison of cells with PEDF treatment (with the control cells with PEDF treatment) is shown in red. * = p < 0.05, ** = p < 0.01, and NS = not significant.
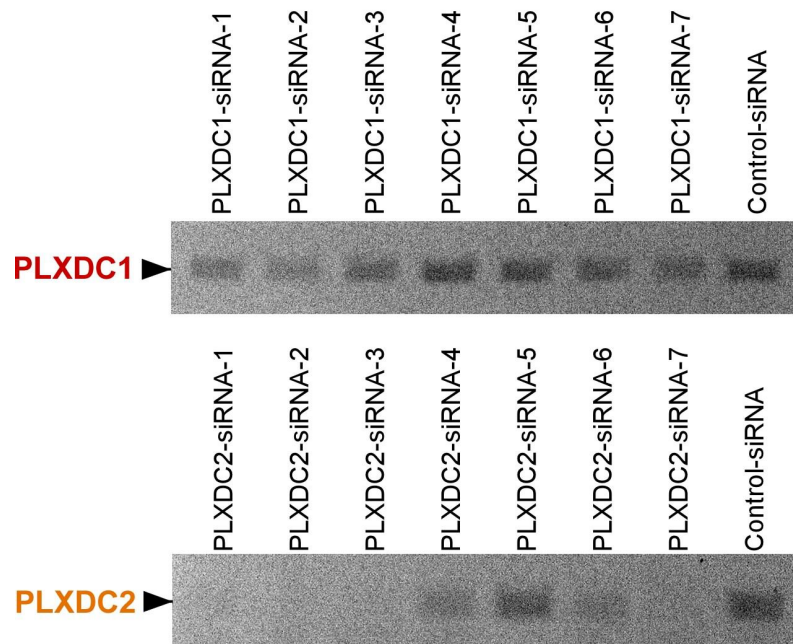
Figure 2-9. Unbiased screening for effective siRNAs in endothelial cell SVEC4-10

We did unbiased screening for effective siRNAs that knock down PLXDC1 or PLXDC2 expression in endothelial cell SVEC4-10. The expression of PLXDC1 and PLXDC2 at mRNA level after 48 hours of reverse transfection of 50nM siRNA of each kind is shown above. Messenger RNA was extracted from cells and reverse transcribed to cDNA. PLXDC1 or PLXDC2 copies in cDNA pool was detected by PCR. The siRNA definition is described in 2.2.5.
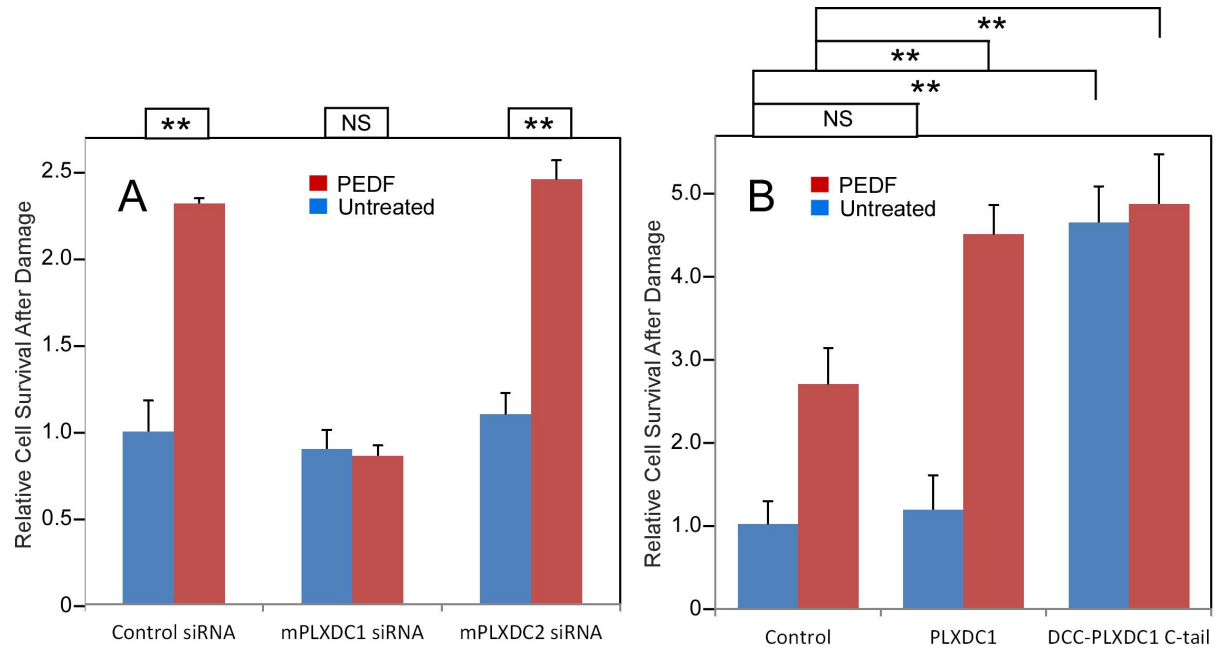
Figure 2-10. The neurotrophic effect of PEDF on 661W cells depends on PLXDC1

(**A**) PEDF treatment protects 661W cells against hydrogen peroxide-mediated oxidative damage. siRNA-mediated knockdown of PLXDC1, but not PLXDC2 abolishes the protective effect of PEDF. The survival of control siRNA transfected cell without treatment is defined as 1. (**B**) Transfection of PLXDC1 or the cytoplasmic domain of PLXDC1 fused to DCC's TM domain enhances protection of 661W cells against damage caused by hydrogen peroxide. The effect of DCC-PLXDC1 C-tail is independent of PEDF. Cell survival of transfected control is defined as 1. Statistical significance is shown on the top. ** = p < 0.01; NS = not significant.
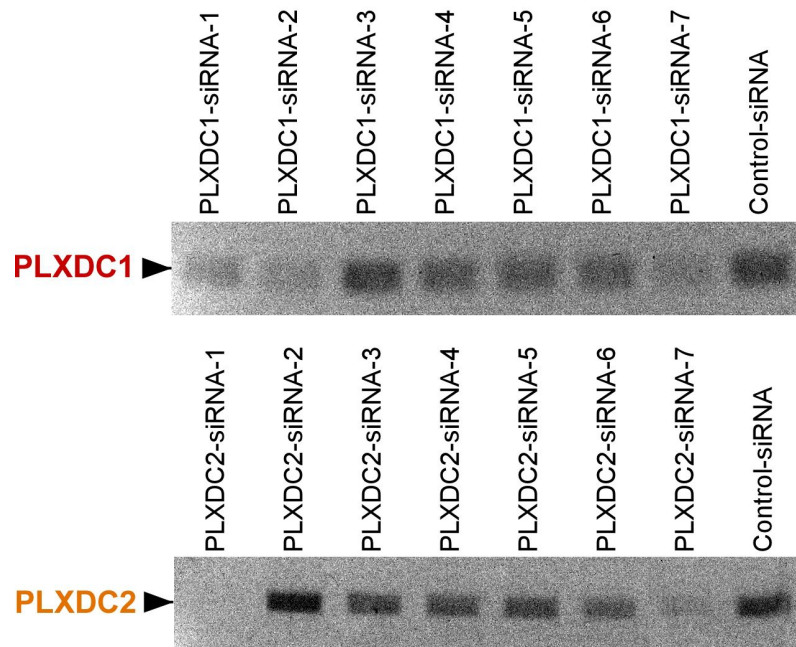
Figure 2-11. Unbiased screening for effective siRNAs in neuronal cell 661W

We did unbiased screening for effective siRNAs that knock down PLXDC1 or PLXDC2 expression in neuronal cell 661W. The expression of PLXDC1 and PLXDC2 at mRNA level after 48 hours of reverse transfection of 50nM siRNA of each kind is shown above. Messenger RNA was extracted from cells and reverse transcribed to cDNA. PLXDC1 or PLXDC2 copies in cDNA pool was detected by PCR. The siRNA definition is described in 2.2.5.

References

Beaty, R. M., Edwards, J. B., Boon, K., Siu, I. M., Conway, J. E., and Riggins, G. J. (2007) PLXDC1 (TEM7) is identified in a genome-wide expression screen of glioblastoma endothelium, *Journal of Neuro-Oncology 81*, 241-248

Boheler, K., Bhattacharya, S., Kropp, E., Chuppa, S., Riordon, D., Bausch-Fluck, D., Burridge, P., Wu, J., Wersto, R., Chan, G., Rao, S., Wollscheid, B., and Gundry, R. (2014) A human pluripotent stem cell surface N-Glycoproteome resource reveals markers, extracellular epitopes, and drug targets, *Stem Cell Reports 3*, 185-203.

Carpenter, R. L., Paw, I., Zhu, H., Sirkisoon, S., Xing, F., Watabe, K., Debinski, W., and Lo, H.-W. (2015) The gain-of-function GLI1 transcription factor TGLI1 enhances expression of VEGF-C and TEM7 to promote glioblastoma angiogenesis. *Oncotarget,* 6(26), 22653-2266

Cheng, G., Zhong, M., Kawaguchi, R., Kassai, M., Al-Ubaidi, M., Deng, J., Ter-Stepanian, M., and Sun, H. (2014) Identification of PLXDC1 and PLXDC2 as the transmembrane receptors for the multifunctional factor PEDF, *eLife 3:*e05401.

Croix, B. S., Rago, C., Velculescu, V., Traverso, G., Romans, K. E., Montgomery, E., Lal, A., Riggins, G. J., Lengauer, C., Vogelstein, B., and Kinzler, K. W. (2000) Genes expressed in human tumor endothelium, *Science* 289 1197-1202

Duh EJ, Yang HS, Suzuma I, Miyagi M, Youngman E, Mori K, Katai M, Yan L, Suzuma K, West K, Davarya S, Tong P, Gehlbach P, Pearlman J, Crabb JW, Aiello LP, Campochiaro PA, Zack DJ. 2002. Pigment epithelium-derived factor suppresses ischemia-induced retinal neovascularization and VEGF-induced migration and growth. *Investigative Ophthalmology & Visual Science* 43:821–829.

Gaultier, A., Simon, G., Niessen, S., Dix, M., Takimoto, S., Cravatt, B. F., III, and Gonias, S. L. (2010) LDL Receptor-related protein 1 regulates the abundance of diverse cell-signaling proteins in the plasma membrane proteome, *Journal of Proteome Research 9*, 6689-6695.

Greening, D. W., Kapp, E. A., Ji, H., Speed, T. P., and Simpson, R. J. (2013) Colon tumour secretopeptidome: Insights into endogenous proteolytic cleavage events in the colon tumour microenvironment, *Biochimica et Biophysica Acta (BBA) - Proteins and Proteomics, An Updated Secretome 1834*, 2396-2407.

Hallstrom, T. C., Mori, S., and Nevins, J. R. (2008) An E2F1-dependent gene expression program that determines the balance between proliferation and cell death, *Cancer Cell 13*, 11-22.

Herz, J., and Strickland, D. K. (2001) LRP: a multifunctional scavenger and signaling receptor, *Journal of Clinical Investigation 108*, 779-784.
Illing, M., Molday, L. L., and Molday, R. S. (1997) The 220-kDa Rim protein of retinal rod outer segments is a member of the ABC transporter superfamily, *Journal of Biological Chemistry 272*, 10303-10310.

Kanan, Y., Kasus-Jacobi, A., Moiseyev, G., Sawyer, K., Ma, J.-X., and Al-Ubaidi, M. R. (2008) Retinoid processing in cone and Muller cell lines, *Experimental Eye Research 86*, 344-354.

Lee, H. K., Seo, I. A., Park, H. K., and Park, H. T. (2006) Identification of the basement membrane protein nidogen as a candidate ligand for tumor endothelial marker 7 in vitro and in vivo, *Febs Letters 580*, 2253-2257.

Leighton, P. A., Mitchell, K. J., Goodrich, L. V., Lu, X., Pinson, K., Scherz, P., Skarnes, W. C., and Tessier-Lavigne, M. (2001) Defining brain wiring patterns and mechanisms through gene trapping in mice, *Nature 410*, 174-179.

Lu, C., Bonome, T., Li, Y., Kamat, A. A., Han, L. Y., Schmandt, R., Coleman, R. L., Gershenson, D. M., Jaffe, R. B., Birrer, M. J., and Sood, A. K. (2007) Gene alterations identified by expression profiling in tumor-associated endothelial cells from invasive ovarian carcinoma, *Cancer Research 67*, 1757-1768.

McMurray, H. R., Sampson, E. R., Compitello, G., Kinsey, C., Newman, L., Smith, B., Chen, S.-R., Klebanov, L., Salzman, P., Yakovlev, A., and Land, H. (2008) Synergistic response to oncogenic mutations defines gene class critical to cancer phenotype, *Nature 453*, 1112-1116.

Miller-Delaney, S. F. C. d., Lieberam, I., Murphy, P., and Mitchell, K. J. (2011) Plxdc2 is a mitogen for neural progenitors, *Plos One 6*.e14565.

Noh M. 2006. Self-renewal pattern-associated genes and their role in adult stem cell function: *Massachusetts Institute of Technology*.

Schwarze, S. R., Fu, V. X., Desotelle, J. A., Kenowski, M. L., and Jarrard, D. F. (2005) The identification of senescence-specific genes during the induction of senescence in prostate cancer cells, *Neoplasia 7*, 816-823.

Stein, E., and Tessier-Lavigne, M. (2001) Hierarchical organization of guidance receptors: silencing of netrin attraction by slit through a Robo/DCC receptor complex, *Science 291*, 1928-1938.

Tan, E., Ding, X.-Q., Saadi, A., Agarwal, N., Naash, M. I., and Al-Ubaidi, M. R. (2004) Expression of cone-photoreceptor-specific antigens in a cell line derived from retinal tumors in transgenic mice, *Investigative Ophthalmology & Visual Science 45*, 764-768.

Yamaji, Y., Yoshida, S., Ishikawa, K., Sengoku, A., Sato, K., Yoshida, A., Kuwahara, R., Ohuchida, K., Oki, E., Enaida, H., Fujisawa, K., Kono, T., and Ishibashi, T. (2008) TEM7 (PLXDC1) in neovascular endothelial cells of fibrovascular membranes from patients with proliferative diabetic retinopathy, *Investigative Ophthalmology & Visual Science 49*, 3151-3157.

Wang, X. Q., Sheibani, N., and Watson, J. C. (2005) Modulation of tumor endothelial cell marker 7 expression during endothelial cell capillary morphogenesis, *Microvasc Res 70*, 189-197.

Zhang, Z. Z., Hua, R., Zhang, J. F., Zhao, W. Y., Zhao, E. H., Tu, L., Wang, C. J., Cao, H., and Zhang, Z. G. (2015) TEM7 (PLXDC1), a key prognostic predictor for resectable gastric cancer, promotes cancer cell migration and invasion, *Am J Cancer Res 5*, 772-781.

Zamiri, P., Masli, S., Streilein, J. W., and Taylor, A. W. (2006) Pigment epithelial growth factor suppresses inflammation by modulating macrophage activation, *Invest Ophthalmol Vis Sci 47*, 3912-3918.

Chapter 3 Mechanism of PEDF-Receptor Interaction

3.1 Introduction

PEDF belongs to the non-inhibitory serine protease inhibitor (serpin) family (Minkevich et al.,2010). It shares around 27% homology to typical inhibitory serpins (Steel et at.,1993) and is 76% identical to the serpin essential spatial structure. PEDF also contains an exposed loop with an equal length of 17 amino acids to its counterpart, reactive center loop (RCL) in serpins. Unlike typical inhibitory serpins that inactivate proteases as suicide inhibitors, PEDF does not have the ability to inhibit proteases (Minkevich et al.,2010), most likely because the loop in PEDF lacks the characteristic of an alanine-rich sequence and threonine in positions 8 and 14 in RCL (Tombran-Tink et al., 2005). The mechanism of how PEDF interacts with its receptors is completely unknown.

PEDF's cell-surface receptors PLXDC1 and PLXDC2 are homologous proteins with similar structural characteristics. They all contain a large extracellular domain at the N-terminus, a transmembrane domain followed by a small intracellular domain. In addition, Nidogen-like domain and cysteine-rich plexin repeats domain are two conserved domains that exist in the extracellular regions of both receptors. Despite the fact that PLXDC1 and PLXDC2 have an

architecture reminiscent of membrane receptors with extracellular, transmembrane and intracellular domains, they do not belong to any well-characterized receptor families.

In this chapter, we performed further mechanistic studies to characterize PEDF/receptor interaction and found that their interaction is unlike any known ligand/receptor pair and has several unique characteristics. We found that PLXDC1 or PLXDC2 forms homooligomer. PEDF and receptor interaction leads to several dramatic consequences on either the ligand PEDF or the receptors. They include PEDF-induced dissociation of receptor homooligomer, receptor-induced PEDF dimer formation and receptor-induce cleavage of PEDF at its C-terminal exposed loop. PEDF-induced receptor dissociation is exactly the opposite of receptor tyrosine kinase, which is activated by ligand induced association. Receptor-induced PEDF dimer formation is mediated by the single cycteine that is burried in PEDF. This receptor catalyzed disulfade bond formation indicates dramatic conformational change of PEDF to expose the buried cysteine in PEDF. The cleavage of PEDF C-terminal loop, similar to the cleavage of RCL in serpins after protein interaction, suggests that PEDF still retains a property of serpins, although it no longer functions as a protease inhibitor.

3.2 Materials and methods

3.2.1 Materials

Reagents, cell lines, and equipment used for the experiments described in this chapter are listed in **Table 3-1**. More detailed information on antibodies is explained below.

Polyclonal antibody against the N-terminal peptide of human PLXDC1 (SPQPGAGHDEGPGSGWAAKGTVRG), polyclonal antibody against the N-terminal peptide of human PLXDC2 (KPGDQILDWQYGVTQAFPHTE) and polyclonal antibody against HA tag (YPYDVPDYA) were produced commercially by Genemed Synthesis. Briefly, peptides conjugated keyhole limpet hemocyanin (KLH) were injected into rabbit at multiple sites to elicit immune response. After 7 weeks, the immunized rabbit was bled and serum containing antibody was isolated from the blood. Antibodies were purified from rabbit crude sera by binding to corresponding peptide conjugated to Affi-Gel and eluted by 0.5 M peptide solution. The purified antibody underwent buffer exchange for three times by diluting with 10 volumes of phosphate buffered saline (PBS) and concentrating in an Ultracentrifugal filter. Information on monoclonal anti-Rim antibody is explained in Chapter 2.

3.2.2 Engineering cDNAs for PLXDC1 and PLXDC2

We used PLXDC1 as the major model and divided the the extracellular domain of PLXDC1 into four domains based on the conserved domains homologous to plexin and Nidogen. The domains for PLXDC1 were: domain A (19–127), domain B (128–242), domain C (243–292), and domain D (293–359) (**Figure 3-1**).

Based on the above definition, We made full length receptors and receptor constructs with different domain deletion. We also created a series of soluble PLXDC1 fragments such as full length PLXDC1 extracellular domain (19-426), individual domains, and fragments composed of various domain combinations. To purify and identify PEDF, or receptors or receptor fragments, we engineered Rim or HA tag to the protein. Rim tag is a 14-residue polypeptide (NETYDLPLHPRTAG) (Illing et al., 1997) and HA tag is a 9-residue polypeptide (YPYDVPDYA). To tag proteins at N-terminus, the tag is engineered after the secretion signal of alkaline phosphatase and before the protein sequence. To add tag to the C-terminus, the tag is inserted after the last amino acid of the construct followed by the stop codon. The schematic diagrams of some of the constructs are shown in **Figure 3-2**.

3.2.3 Copurification studies

Rim-tagged proteins were purified by anti-Rim antibody-conjugated to sepharose beads. Briefly, cells were washed once with HBSS and lysed in well with 1% Triton X-100 in Hank's Balanced Saline Solution (HBSS) with protease inhibitor cocktail for 10 min on ice. Cell lysate was harvested and spun at 16,000×g, 4°C for 10 min to remove insoluble materials. Cell lysate was applied to anti-Rim antibody-conjugated beads, and rotated for 4 hr at 2°C. The beads were washed twice using 0.1% Triton X-100 in HBSS by spinning down at 2000×g for 30 s and eluted in 0.1% Triton X-100 in 0.1 M Glycine, pH = 2.3 for 15 min at room temperature. Tris (pH 9.5)

was added to 0.1 M to neutralize the elution. Elution was boiled with SDS with or without DTT, resolved in SDS-PAGE gel and analyzed by Western blot. Rim-tagged proteins were detected by monoclonal anti-Rim antibody. HA-tagged proteins were detected using polyclonal anti-HA antibody. Untagged PEDF was detected by BioProduct's anti-PEDF polyclonal antibody. Untagged PLXDC1 or PLXDC2 was probed by polyclonal antibody against the N-terminal peptide of human PLXDC1 (SPQPGAGHDEGPGSGWAAKGTVRG) and polyclonal antibody against the N-terminal peptide of human PLXDC2 (KPGDQILDWQYGVTQAFPHTE) respectively.

To compare homooligomerization and heteroligomerization, anti-Rim purification was performed 24 hr after NEK293T cells were transfected with Rim-tagged PLXDC1 (20%), HA-tagged PLXDC1 (40%) and untagged PLXDC2 (40%) in one experiment and Rim-tagged PLXDC2 (20%), HA-tagged PLXDC2 (40%) and untagged PLXDC1 (40%) in another experiment. Copurification of PLXDC1 extracellular constructs with PEDF was performed using the conditioned media from NEK293T cells 48 hr after cotransfection of PLXDC1 constructs and PEDF constructs. Purification was performed at 4°C for 2 hr.

3.2.4 Incubation of PLXDC1 extracellular constructs with PEDF

N-terminal Rim-tagged PLXDC1 fragment containing domain A to C (Rim-PLXDC1-fABC) and PEDF constructs were transfected into NEK 293T cells at a 2:1 ratio. Cell medium was changed to serum free Dulbecco's Modified Eagles Medium (SFM) 6 hr after transfection. Cells were incubated at 37°C for 48 hours before cell conditioned medium was harvested. The conditioned medium was incubated at room temperature for overnight before being boiled with or without DTT and loaded on SDS-PAGE gel.

3.2.5 Receptor terminal cysteine crosslinking catalyzed by oxidizer

Membranes were prepared from HEK293 cells transfected with the receptors using Phosphate Buffer (PBS) and 5 mM EDTA, which helps to keep free cysteine residues in the reduced state. After one wash using PBS, the membrane was resuspended in PBS and incubated with or without PEDF for 3 hr at room temperature. Oxidation-induced disulfide bond formation was catalyzed by 0.5 mM Cu (II) 1,10-phenanthroline (Phe). After 5 min, EDTA was added to each reaction to 50 mM to stop the oxidation reaction. The membranes were spun down, resuspended and boiled in SDS loading buffer with or without DTT for loading onto a SDS-PAGE gel.

3.2.6 An assay to visualize receptor dissociation

We developed a live cell-based assay to study the ability of PEDF to dissociate receptor complexes. PLXDC1 extracellular domain with a Rim tag following the N-terminal secretion

signal of alkaline phosphatase was cotransfected into COS-1 cells with wild-type PLXDC1 with no tag. The Rim-tagged extracellular domain of PLXDC1 associated with the cell surface through its interaction with the extracellular domain of the full length PLXDC1. 1 day after transfection, the cells were washed once with HBSS and incubated overnight at 37°C in SFM with 5 mg/ml BSA with or without 50 nM PEDF. The next day cell surface associated Rim tagged protein was assessed through live cell staining by anti-Rim antibody by incubating with antibody diluted in SFM with 5 mg/ml BSA for 60 min at 37°C. After antibody binding, the cells were washed with HBSS and fixed in freshly made 4% paraformaldehyde in HBSS, pH 7.5 for 20 min. Rim antibody was detected through immunostaining using AF488 anti-mouse secondary antibody. Fluorescent signals were quantified using Nikon NIS Elements AR Analysis software.

3.2.7 Real-time analysis of PEDF-mediated receptor receptor dissociation

CFP and YFP proteins were fused to the C-terminus of PLXDC1 and PLXDC2 to detect oligomerization of PEDF receptors. Three glycine linkers were added between YFP/CFP and the C-terminal tail of PLXDC1 or PLXDC2. FRET analysis was performed similarly as described (Kawaguchi et al., 2011). Briefly, membranes were prepared from HEK293T cells that coexpress PLXDC1-CFP and PLXDC2-YFP. CFP-YFP FRET was measured in black flat bottom 96-well plates (Microfluor 2, Thermo Scientific) using simultaneous dual emission optics in POLARstar Omega with excitation filter 422-20 and emission filters 470-12 and 530-10. The background

signal of each reaction was measured before PEDF was added to the membrane suspension to initiate the reactions. The signal from each time point was the average of 20 measurements. After all the measurements were done, the signals were calculated as the ratio of emissions at 530 nm over emissions at 470 nm to observe the dynamic change in FRET. To crosslink the C-terminal free cysteine using BMOE, membrane preparations were made in PBS and 5 mM EDTA. BMOE was added to the membrane suspension at a concentration of 2 mM. The reaction was carried out at room temperature for 1 hour. Concentrated DTT solution was added to 5 mM to quench the reaction. After incubation at room temperature for 10 min, 1 ml of HBSS/HEPES (HBSS with 10 mM HEPES, pH 7.5) was added to the membrane suspension. After the membranes were pelleted down, the resulting membrane pellets were washed once and resuspended in HBSS/HEPES for FRET measurement.

3.3 Results

3.3.1 PLXDC1 and PEDF interaction requires domain B of the receptor

N-terminal HA-tagged PEDF (HA-PEDF) was cotrasnfected with each of PLXDC1 domain deletion series in NEK293T cell. Using Rim-tagged PLXDC1 domain deletion series to immunoprecipitate HA-PEDF, we found that PLXDC1 constructs with domain B deletion

significantly lose the affinity to PEDF. The experiment suggests that domain B is necessary for PLXDC1 to bind to PEDF (**Figure 3-3**).

3.3.2 PLXDC1 or PLXDC2 forms homooligomer

We hypothesized that PLXDC1 and PLXDC2 may form oligomer without PEDF activation. Since they are homologous proteins, they can from homooligomer or heterooligomer. To test this hypothesis and investigate which oligomer type is in favored of, we copurified N-terminal Rim-tagged PLXDC1 with N-terminal HA-tagged PLXDC1 and untagged PLXDC2 using antibody against Rim tag. HA-tagged PLXDC1 and untagged PLXDC2 would be detected by ant-HA antibody and anti-PLXDC2 antibody respectively if they were coprecipitated with Rim-tagged PLXDC1. It was found that Rim-tagged PLXDC1 only copurify HA-tagged PLXDC1 but not PLXDC2. In a similar experiment, we found that HA-tagged PLXDC2 but not untagged PLXDC1 copurified with Rim-tagged PLXDC2 (**Figure 3-4**). The above experiments suggest that both PLXDC1 and PLXDC2 preferentially form homooligomers. Using deletion series of the extracellular domains, we identified domain D as an important domain for oligomerization (**Figure 3-5**).

3.3.3 Studying receptor dimerization using cysteine crosslinking

We noticed that the last residue in the cytoplasmic domain of both PLXDC1 and PLXDC2 is a conserved cysteine. Since intracellular cysteines are in the reduced state, we tested whether copper phenanthroline-induced thiol oxidation (Zhou et al., 2009) could crosslink these cysteines. Indeed, we found that copper phenanthroline promoted the formation of covalent dimers, consistent with the close proximity of the two cysteines on the cytoplasmic domain (**Figure 3-6**). This covalent dimer can be cleaved under reducing conditions (**Figure 3-6**), consistent with its linkage through a disulfide bond catalyzed by copper phenanthroline. Interestingly, incubation with PEDF before copper phenanthroline treatment inhibited the formation of the dimer and promoted the formation of the monomer, indicating that the cytoplasmic tail is no longer in close contact with another cytoplasmic tail (**Figure 3-6**).

3.3.4 PEDF dissociates PLXDC1 oliogomer

To demonstrate the effect of PEDF on receptor oligomerization in live cells, we developed an assay to visualize PEDF-induced receptor dissociation on the cell surface. Epitope-tagged extracellular domain of PLXDC1 is associated with the cell surface through its binding to the coexpressed full length untagged PLXDC1 (**Figure 3-7**). Incubation of the cells with PEDF causes the dissociation of the extracellular domain and the loss of the epitope tag from the cell surface (**Figure 3-7**). This live cell-based assay again demonstrated the ability of PEDF to dissociate receptor oligomer.

To further observe the effect of PEDF on receptor oligomerization in real time, we developed a fluorescence resonance energy transfer (FRET)-based assay. We coexpressed PLXDC1 fused to a Cyan Fluorescent Protein (CFP) and PLXDC1 fused to a yellow fluorescent protein (YFP) at the C-terminus and observed a time-dependent decrease in FRET signals after addition of PEDF, but not a control extracellular protein nidogen (**Figure 3-8**). To show that the decrease in FRET signal was due to receptor dissociation, we crosslinked the cysteine residues on the cytoplasmic domain of PLXDC1 using sulfhydryl-specific crosslinker bismaleimidoethane (BMOE) before PEDF addition and found that this crosslinker prevents PEDF-dependent suppression of the FRET signal (**Figure 3-9**). However, mutation of the cysteine to serine (C500S) prevents the blocking effect of BMOE on PEDF. To conclude, the above results demonstrate that PLXDC1 or PLXDC2 forms homooligomer and PEDF's interaction with PLXDC1 dissociate the receptor oligomer. The results presented in **Figure 3-1** to **Figure 3-9** have been published (Cheng et al., 2014).

3.3.5 PEDF forms a dimer upon interaction with its receptor

In the investigation of the fate of PEDF during ligand-receptor interaction, we found something unexpected. When we copurified Rim-PLXDC1-fABC with untagged PEDF, we noticed that copurified PEDF migrated as a dimer in a non-reducing SDS-PAGE gel rather than as a monomer. The dimer signal, however, became remarkably weaker in a reducing gel. The results

suggest that PEDF, during the interaction with PLXDC1, form a dimer which is disulfide-bond dependent. More than that, both PEDF monomer and Rim-PLXDC1-fABC signals became barely visible in either non-reducing or reducing gel, when PEDF monomer and Rim-PLXDC1-fABC were copurified with each other (**Figure 3-10**). A likely explanation is that PLXDC1 and PEDF monomer became almost undetectable by the antibodies. The result suggests that dramatic conformational changes may occur and the epitopes become barely accessible to the antibodies.

3.3.6 PEDF dimerization depends on a disulfide bond

It is very uncommon for a secreted protein to contain an unpaired cycteine, however PEDF has one (cysteine 261). Crystal structure of PEDF reveals that the cycteine, with its side chain facing inside, is enclosed by other amino acids (**Figure 3-11A**). We thus speculated that the single cycteine in PEDF is not exposed unless dramatic conformational change occurs. And the disulfide bond formed by the two exposed cycteines from two PEDF is responsible for the dimer formation. To test this hypothesis, we mutated the single cycteine in PEDF to serine, namely PEDF-C261S. In a similar experiment setting, we copurified Rim-PLXDC1-fABC with PEDF-C261S, untagged PEDF, another PEDF mutant (PEDF-D299N), PEDF with 6×histidine on the C-terminus (PEDF-His), HA-PEDF and control protein. Cysteine to serine mutation

abolished PEDF dimer formation as shown in the non-reducing gel (**Figure 3-11B**). The result

supports the hypothesis that PEDF dimer is disulfide-bond dependent.

3.3.7 PLXDC1 domain B induces PEDF dimer formation

We went on to study which part in PLXDC1 induces PEDF dimer formation. PEDF copurified

with extracellular fragments of PLXDC1 with different domain deletion was analyzed by

non-reducing SDS-PAGE gel and Western Blotting. It was shown that PLXDC1 domain B is

sufficient in binding to PEDF and inducing PEDF dimer formation whereas domain B deletion

largely abolishes the ability. PLXDC1-fABC shows the strongest effect possibly because it is in

an optimal conformation in inducing PEDF complex formation (**Figure 3-12**).

3.3.8 PEDF loses C-terminal tail upon the interaction with the receptors

To further investigate the mechanism of PEDF dimer formation we coexpressed the C-terminal

HA-tagged PEDF (PEDF-HA) with Rim-tagged PLXDC1 extracellular constructs or EGFP in

HEK 293T cells. Those PLXDC1 constructs included Rim-PLXDC1-ECD, Rim-PLXDC1-fABC

and Rim-tagged PLXDC1 domain B (Rim-PLXDC1-fB). After 48 hours incubation, which

allowed secreted PEDF-HA and Rim-tagged PLXDC1 constructs to interact, coexpressed

proteins were purified by anti-Rim antibody. We used anti-PEDF antibody to probe PEDF-HA.

In the input, the majority of PEDF-HA remained as monomer with a small fraction forming

dimer. A downward shift of dimer band was observed specifically with the presence of PLXDC1 constructs but not EGFP control. PEDF-HA was copurified with PLXDC1 extracellular constructs primarily as dimer rather than as monomer. Copurified PEDF-HA dimer also showed a smaller molecular weight compared to the PEDF-HA coexpressed with EGFP in the input (**Figure 3-13**). The results agree with previous findings that PLXDC1 induces PEDF to form a dimer, and dimer is preferentially copurified with PLXDC1 than monomer. In addition, the downward shift of dimer band suggests a cleavage in PEDF and loss of PEDF tail. PLXDC1 domain B is sufficient to induce the cleavage.

We also compared the dimer signal of N-terminal HA-tagged PEDF (HA-PEDF) with C-terminal HA-tagged PEDF (PEDF-HA). Briefly, we coexpressed HA-PEDF or PEDF-HA respectively with Rim-PLXDC1-fABC or control protein in HEK293T cell. Cell conditioned medium was harvested, incubated and resolved in SDS-PAGE gel. HA-PEDF was detected by anti-HA antibody in a non-reducing gel either as a dimer after incubation with PLXDC1 or as a monomer after incubation with control protein. However, PEDF-HA became invisible either as a dimer or as a monomer in HA Western after its incubation with PLXDC1 (**Figure 3-14**). The finding highly suggests that PEDF-HA loses part of its C-terminus together with the HA tag, which results in the invisibility of PEDF-HA signal in Western. Based on the above information, we

hypothesize that PEDF is subject to a cleavage near C-terminus during the interaction with PLXDC1. The cleavage, consequently, leads to a loss of C-terminus tail of PEDF.

As a member of non-inhibitory serpin family, PEDF contains an exposed loop analogous to the reactive cencer loop (RCL) in typical serpins. The exposed loop near the C-terminus is prone to protease cleavage as RCL. Leucine 382 (L382) and Threonine 383 (T383) in PEDF are proposed as the cleavage site in the loop (Carrell 1987 et al., 1987; Becerra et al., 1995) (**Figure 3-15 A**). To test if PEDF is cleaved at site L382-T383 (LT) during its interaction with PLXDC1, we mutated L382 and T383 to two alanines in HA-PEDF (HA-PEDF-LTAA). HA-PEDF truncated at T383 without C-terminal tail was also created (HA-PEDF-dctail). The truncated HA-PEDF-dctail differs from wild type HA-PEDF by only 3.8 kDa in molecular weight. We found that HA-PEDF, HA-PEDF-LTAA and HA-PEDF-dctail all copurify in the form of dimer with Rim-PLXDC1-fABC or with Rim-PLXDC2-fABC. It suggests that LT mutation, or C-terminus deletion after LT site does not affect the interaction of PEDF with its receptor and the receptor-induced dimer formation. More than that, we found HA-PEDF dimer and HA-PEDF-dctail dimer migrate to the same position in SDS-PAGE gel, while HA-PEDF-LTAA dimer migrate to a slightly higher position as shown in **Figure 3-15 B**. It means that HA-PEDF and HA-PEDF-dctail probably have the same molecular weight but slightly smaller than HH-PEDF-LTAA. The evidence suggests that HA-PEDF, undergoes a cleavage at LT site, loses

the C-terminal tail after LT site and migrates to the same position as HA-PEDF-dctail dimer. However, LT to AA mutation destroys the cleavage site and migrates as an intact PEDF.

3.4 Discussion

In this chapter, we discussed the mechanism of the interaction between PEDF and its receptors. First, using three different techniques (visualization of receptor oligomers in SDS-PAGE, visualization of receptor oligomers on the cell surface, and tracking receptor interaction in real-time), we found that PEDF receptors self-associate to form homooligomers. And the PLXDC1 homooligomerization is dependent on domain D. PEDF has the ability to dissociate receptor homooligomers so that the cytoplasmic tails are no longer in contact with each other. In Chapter 2, we demonstrate that heterologously expressing membrane-tethered cytoplasmic tail leads to cell death in SVEC4-10 endothelial cells and provides protection against oxidative damage in 661W neuronal cells independent of PEDF. The membrane-tethered cytoplasmic tails do not contact with each other as full length receptor since they lack domain D. In another word, the free receptor cytoplasmic tail is active and triggers downstream pathways even without PEDF. Therefore, we speculate that PLXDC1 or PLXDC2 remain self-inhibited as homooligomer at basal state. PEDF binds to the receptor to dissociate the oligomer and liberates the receptor cytoplasmic tail, resulting in the activation of downstream signaling pathway.

Second, we created a domain deletion series of PLXDC1 and demonstrated that PLXDC1 interacts with PEDF via domain B which contains nidogen-like domain. We also showed that domain B is both necessary and sufficient for inducing PEDF dimerization and is sufficient to cause PEDF c-tail cleavage which is summarized below.

Third, the interaction between PEDF and receptor causes the unexpected formation of PEDF dimer that is linked by a disulfide bond. By cycteine mutagenesis, we proved that receptor-induced PEDF dimerization depends on disulfide bond. A receptor-induced conformational change of PEDF is a prerequisite for the exposure of the buried single cysteine in PEDF to form disulfide bond. Interestingly, PEDF not only forms a dimer after interacting with the receptor, it also becomes poorly recognized by its antibody in boiled samples for Western blot, again consistent with large conformational change.

Fourth, we found that the C-terminus of PEDF is cleaved off during the interaction of PEDF with the receptor. L382-T383 in the exposed loop of PEDF is likely the cleavage site. We showed that mutation of these two residues prevented receptor-induced cleavage of PEDF tail. As L382-T383 is a recognition site for proteases, it is important to distinguish two scenarios. The first scenario is that receptor directly cleaves PEDF; The second scenario is that receptor induces PEDF conformational change to expose this cleave site, making PEDF more prone to protease cleavage.

Further experiment will distinguish the two scenarios, both of which are consistent with the profound effect of receptor on PEDF after their interaction.

To summarize, we identified a novel mechanism of ligand-receptor interaction and characterized PLXDC1 or PLXDC2 as a new type of cell-surface receptor.

Table 3-1. List of reagents, cell lines, and equipment

		Materials/Equipment	Description	Manufacturer
Cell lines		COS-1	Monkey kidney fibroblast cells	ATCC
		HEK293T	Human embryo kidney 293 cell with T-antigen	ATCC
Reagents		AF488-α-mouse Ab	Alexa 488 conjugated goat anti-mouse antibody	Thermo Scientific
		Anti-PEDF Ab	Rabbit anti-PEDF antibody	BioProductMD
		Anti-PLXDC1 Ab	Polyclonal anti-PLXDC1 antibody	Genemed Synthesis
		Anti-PLXDC2 Ab	Polyclonal anti-PLXDC2 antibody	Genemed Synthesis
		Anti-Rim Ab	Monoclonal anti-Rim antibody	N/A
		BSA	Bovine serum albumin fraction V	Santa cruz biotechnology
		BMOE	Maleimide crosslinker	Pierce
		Cu(II) Phe	Copper (II) 1,10- phenanthroline	Sigma
		DMSO	Dimethyl sulfoxide	BDH solvent
		DTT	Dithiothreitol	Omnipur, Millipore
		Dylight 680 Ab	Dylight 680-conjugated goat anti-mouse antibody	Pierce, Thermo
		FBS	Fetal Bovine Serum	Hyclone, GE Healthcare Life Sciences
		HBSS	Hank's Balanced Salt Solution	Thermo Scientific
		HEPES	N/A	AMRESCO
		IRDye 800CW Ab	IRDye 800-conjugated goat anti-rabbit antibody	Li-Cor
		JetPRIME	DNA transfection reagent	Polyplus-transfection
		mAnti-HA Ab	Monoclonal anti-HA antibody	Covance Biolegend
		Nitrocellulose membrane	N/A	Maine manufacturing
		PBS	Phosphate Buffered Saline	Corning cellgro
		pAnti-HA Ab	Polyclonal anti-HA antibody	Genemed Synthesis
		Protease inhibitor cocktail	Protease Inhibitor Single-Use Cocktail (100X)	Halt™, ThermoFisher Scientific
		Sepharose beads	CNBr-activated Sepharose 5 Fast Flow beads	Amersham, GE Healthcare
		Triton X-100	Triton X-100 surfactant	Omnipur, Millipore
		Trypsin	0.05% trypsin	Hyclone, GE Healthcare Life Sciences
Equip -ment		Li-Cor Infrared Imager	N/A	Li-Cor
		POLARstar Omega	N/A	BMG Labtech
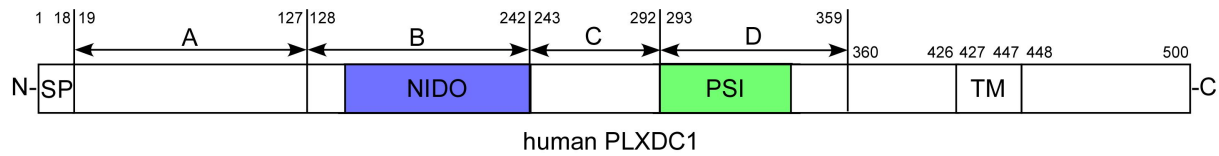
Figure 3-1. PLXDC1 domain definition

The extracelluar domain of PLXDC1 is arbitrarily divided into A, B, C, and D domains based on the conserved domains homologous to plexin and Nidogen. As shown above, domain B and domain D contain Nidogen-like domain (NIDO, blue block) and plexin repeats (PSI, green block) respectively. The Arabic numbers mark the positions of the amino acids. SP: signal peptide; TM: transmembrane domain.
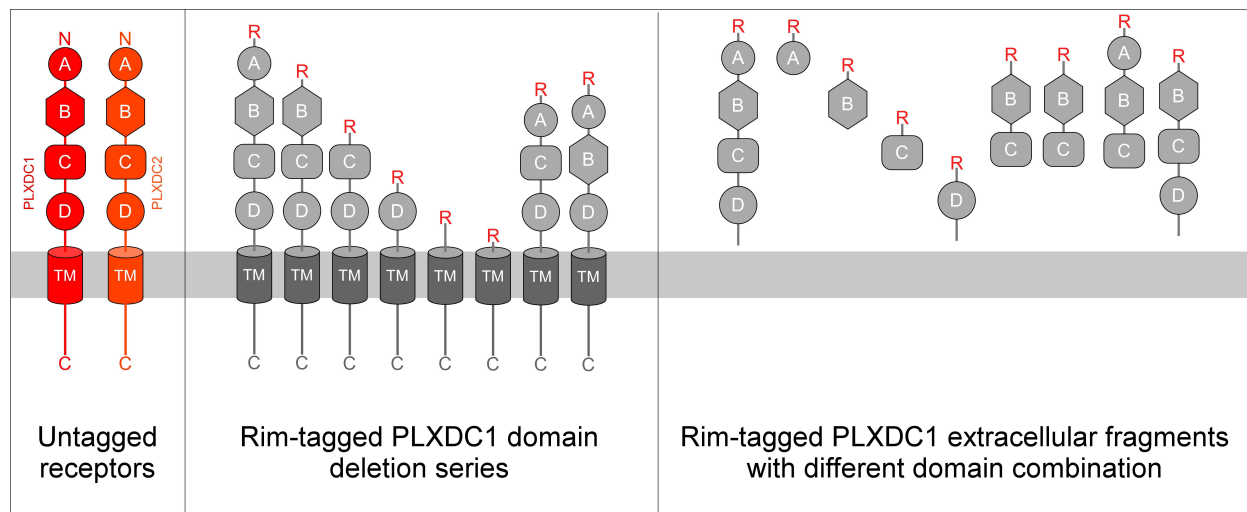
Figure 3-2. Schematic diagrams of the PLXDC1 and PLXDC2 constructs
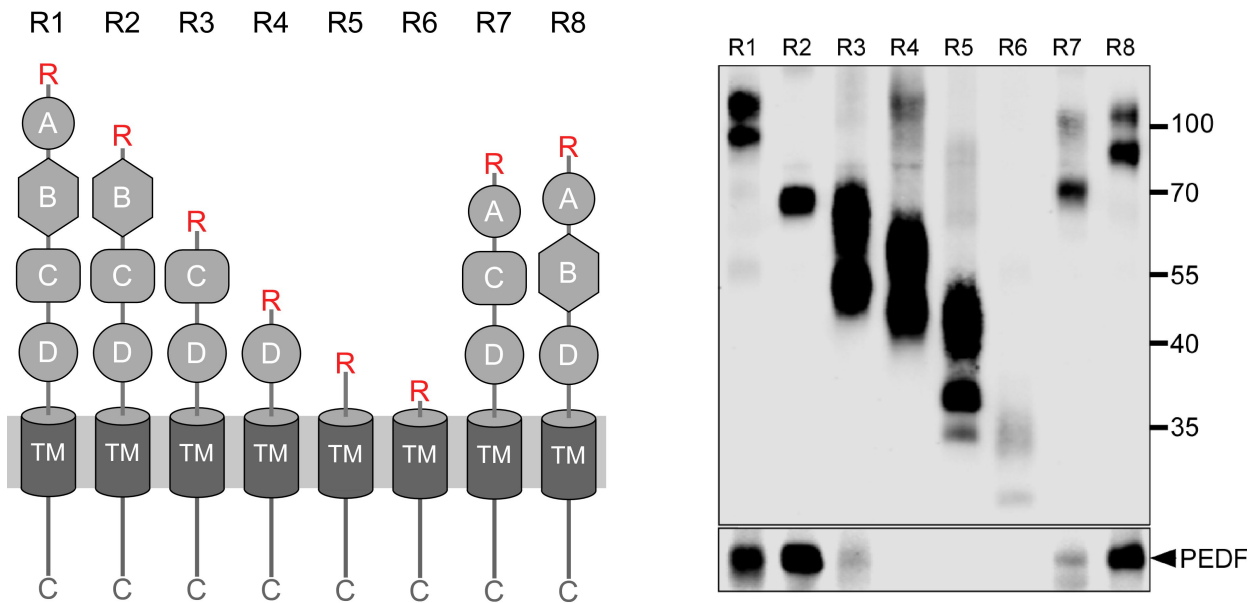
Figure 3-3. PLXDC1 and PEDF interaction requires domain B

PEDF with HA-PEDF is copurified with different deletion mutants of PLXDC1, which are all tagged with a Rim tag following the N-terminal secretion signal (diagrams on the left). Purification of the Rim-tagged proteins with HA-PEDF is shown on the right. The upper Western is the anti-Rim Western and the lower Western is anti-HA Western to detect HA-PEDF. Deletion of domain B largely abolishes the interaction between PLXDC1 and HA-PEDF.
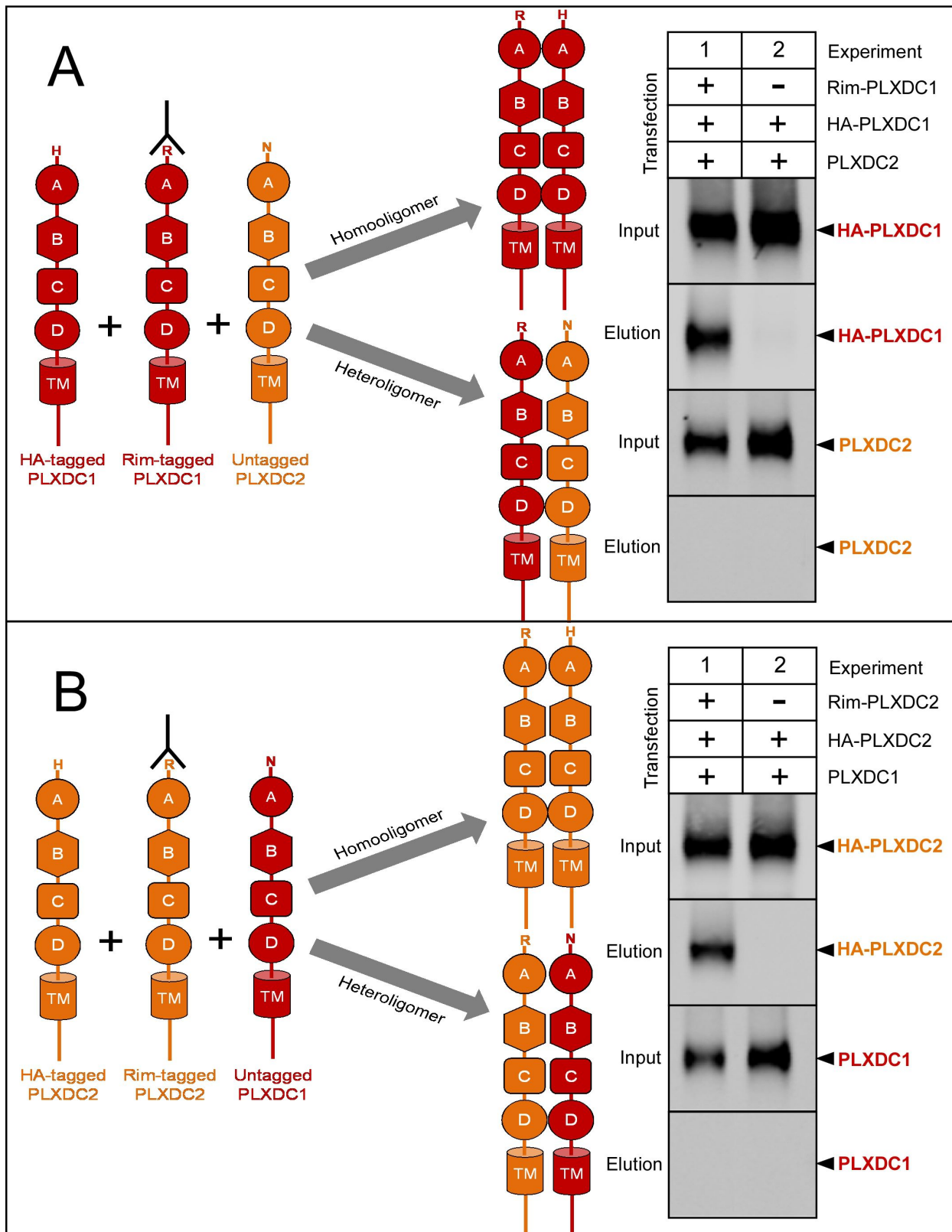
Figure 3-4. PLXDC1 or PLXDC2 homooligomer formation

(**A**) Purification of N-terminal Rim-tagged PLXDC1 with N-terminal HA-tagged PLXDC1 and untagged PLXDC2 by antibody against Rim tag (diagrams on the left). HA-tagged PLXDC1 and untagged PLXDC2 was probed by ant-HA antibody and anti-PLXDC2 antibody respectively as shown in the input and elution Western. Purification without Rim-tagged PLXDC1 served as blank control to exclude unspecific binding of proteins to anti-Rim antibody conjugated beads.

(**B**) Purification of N-terminal Rim-tagged PLXDC2 with N-terminal HA-tagged PLXDC2 and untagged PLXDC1 by antibody against Rim tag (diagrams on the left). HA-tagged PLXDC2 and untagged PLXDC1 was probed by ant-HA antibody and anti-PLXDC1 antibody respectively as shown in the input and elution Western. Purification without Rim-tagged PLXDC2 served as blank control to exclude unspecific binding of proteins to anti-Rim antibody conjugated beads.
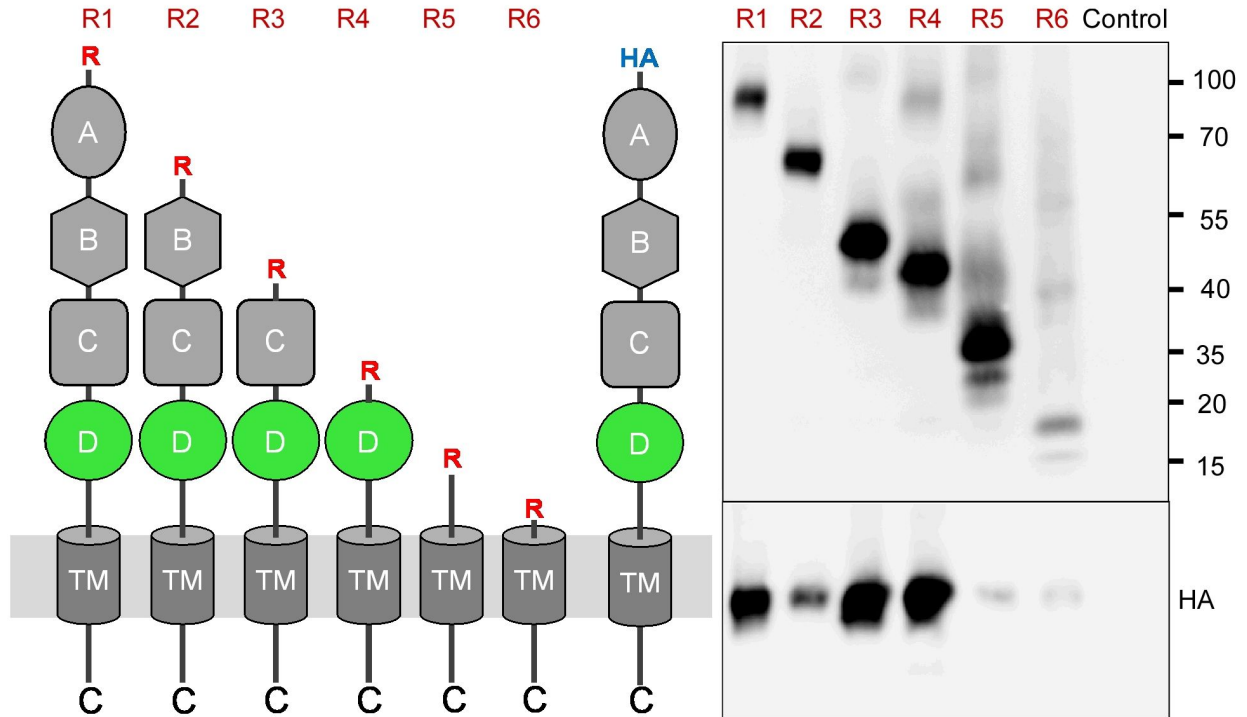
Figure 3-5. PLXDC1 oligomerization depends on domain D

PLXDC1 deletion series with a Rim tag following the N-terminal secretion signal were purified together with HA-tagged full length PLXDC1 by purifying the Rim tag (diagrams on the left). Anti-Rim Western is shown on the top and anti-HA Western is shown on the bottom for the elutions. HA-PLXDC1 no longer copurifies if domain D is deleted.
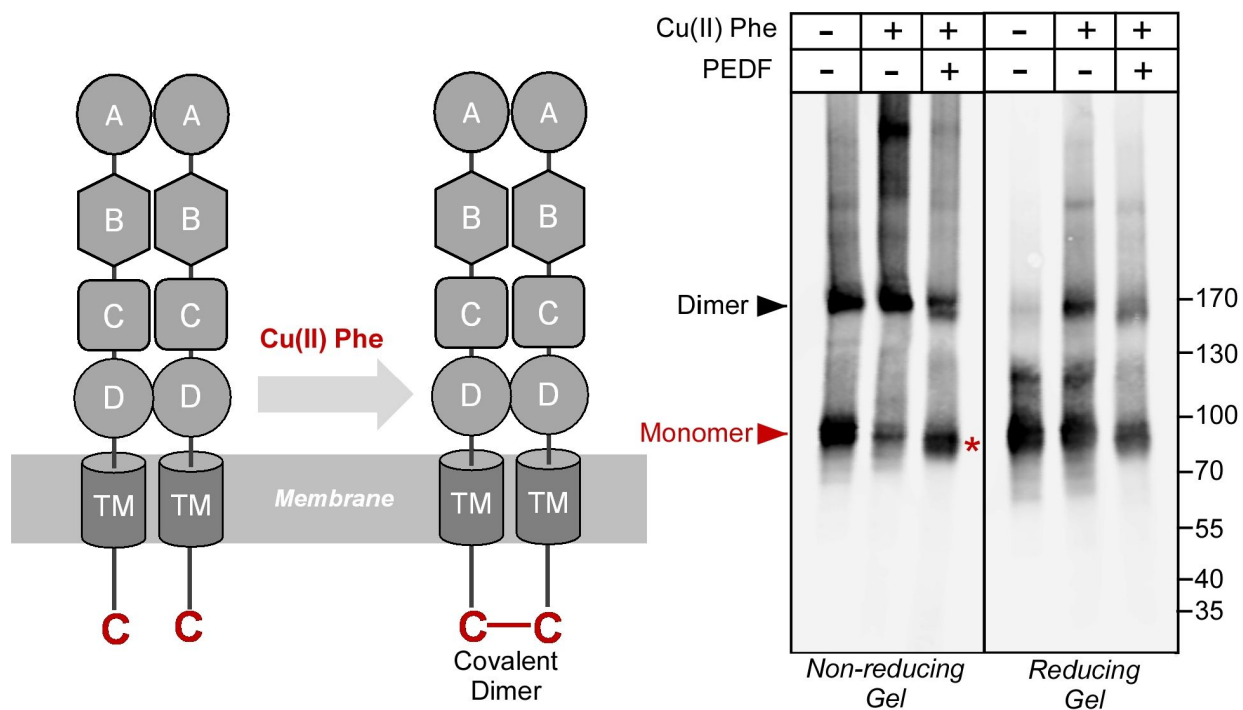
Figure 3-6. PEDF inhibits disulfide bond formation induced by oxidizer

Copper phenanthroline [Cu (II) Phe] treatment creates covalent receptor dimer through oxidation of the free cysteine residue on the cytoplasmic tail (schematic diagram on the left). Cu (II) Phe oxidation creates disulfide bond-linked covalent PLXDC1 dimer, as indicated in the Western blot for the receptor. PEDF inhibits dimer formation as shown by increased monomer band on a non-reducing gel after Cu (II) Phe oxidation (red asterisk). The disulfide bond-linked dimers are sensitive to DTT treatment as shown in the reducing gel on the right. Molecular weight markers are in kD.
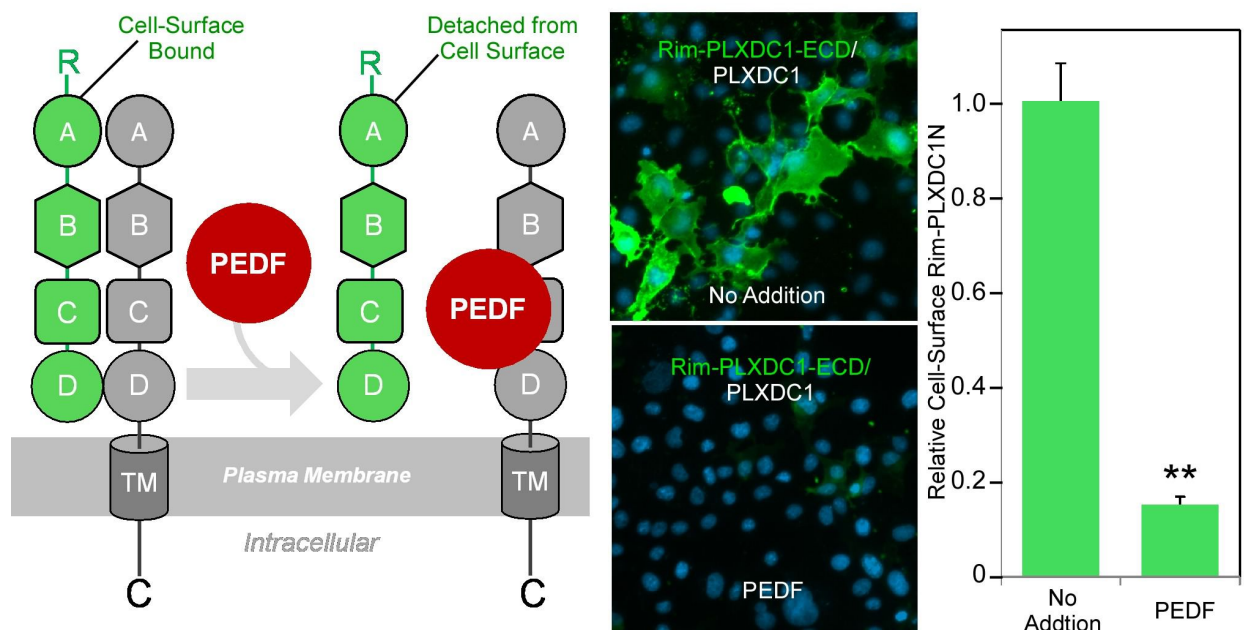
Figure 3-7. PEDF-mediated receptor dissociation on the cell surface

Schematic diagram is on the left. PEDF displaces Rim-tagged PLXDC1 extracellular domain (Rim-PLXDC1-ECD, green) bound to cell surface PLXDC1 (gray) to cause detachment of the extracellular domain. Immunostaining of Rim-PLXDC1-ECD, (cotransfected with PLXDC1) on live cell surface is shown in the middle two pictures (green signal). Blue color is nucleic acid stain DAPI. Upper picture: control (no PEDF). Lower picture: PEDF treated. Quantitation of bound Rim-PLXDC1-ECD on the cell surface with or without PEDF treatment is shown on the right.
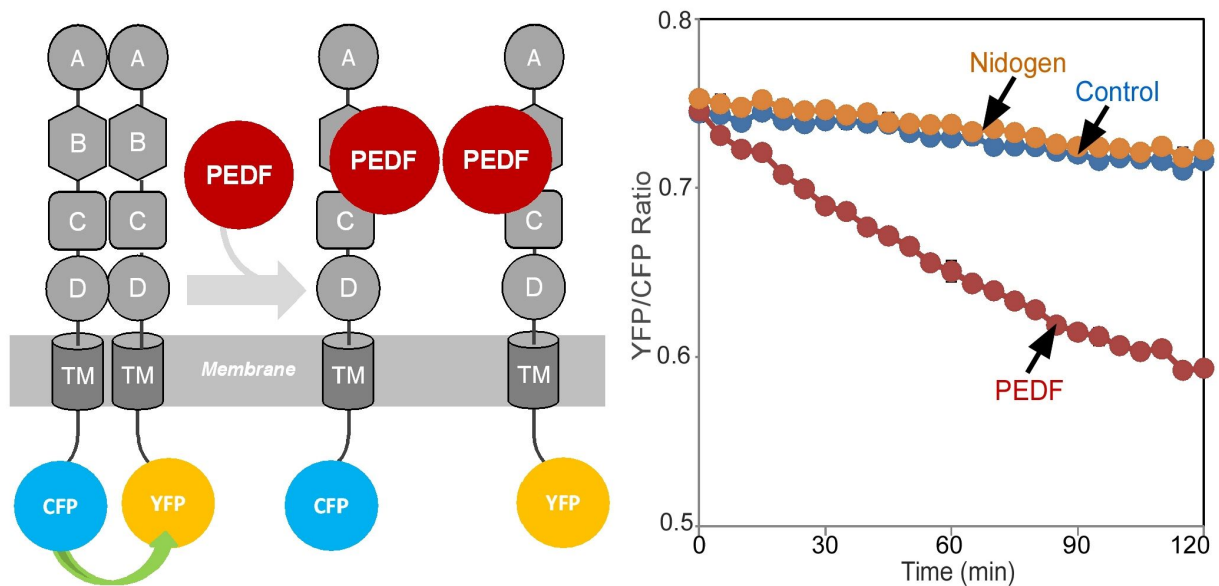
Figure 3-8. PEDF-mediated receptor dissociation in real time

Schematic diagram of the experimental design is shown on the left. The cytoplasmic tail of

PLXDC1 is linked to CFP or YFP, which are in close proximity due to receptor dimerization.

PEDF suppresses the FRET signal between CFP and YFP if it disrupts the association of the

receptor dimer. Right panel: PEDF, but not a control protein (Nidogen) causes a time-dependent

decrease in FRET signal between PLXDC1-CFP and PLXDC1-YFP. Both PEDF and nidogen

were added at time 0.
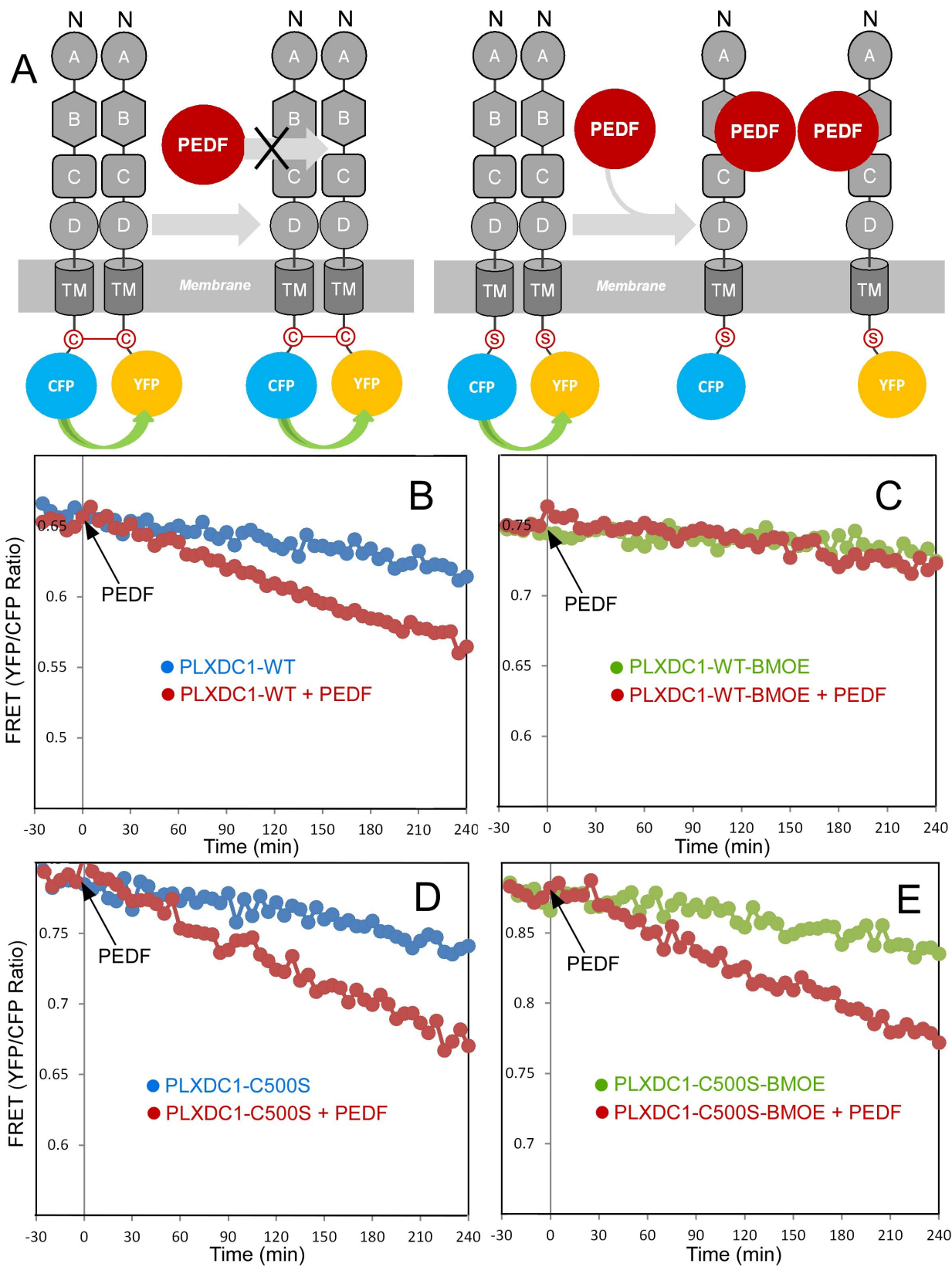
Figure 3-9. Terminal cysteine crosslinking of PLXDC1 prevents PEDF-mediated dissociation.

(**A**) Schematic diagrams of the experimental design. 'C' indicates the cysteine residue located at the C-terminus of PLXDC1. 'S' indicates mutation of this residue to serine. (**B** and **C**) Crosslinking of the cysteine on the cytoplasmic tail of wild-type PLXDC1 (PLXDC1-WT) by sulfhydryl-specific crosslinker BMOE prevents the PEDF-dependent decrease of FRET signal between PLXDC1-CFP and PLXDC1-YFP. (**D** and **E**) BMOE has no effect on PEDF-dependent decrease of FRET signal between PLXDC1-CFP and PLXDC1-YFP if the C-terminal cysteine is mutated to serine (PLXDC1-C500S).
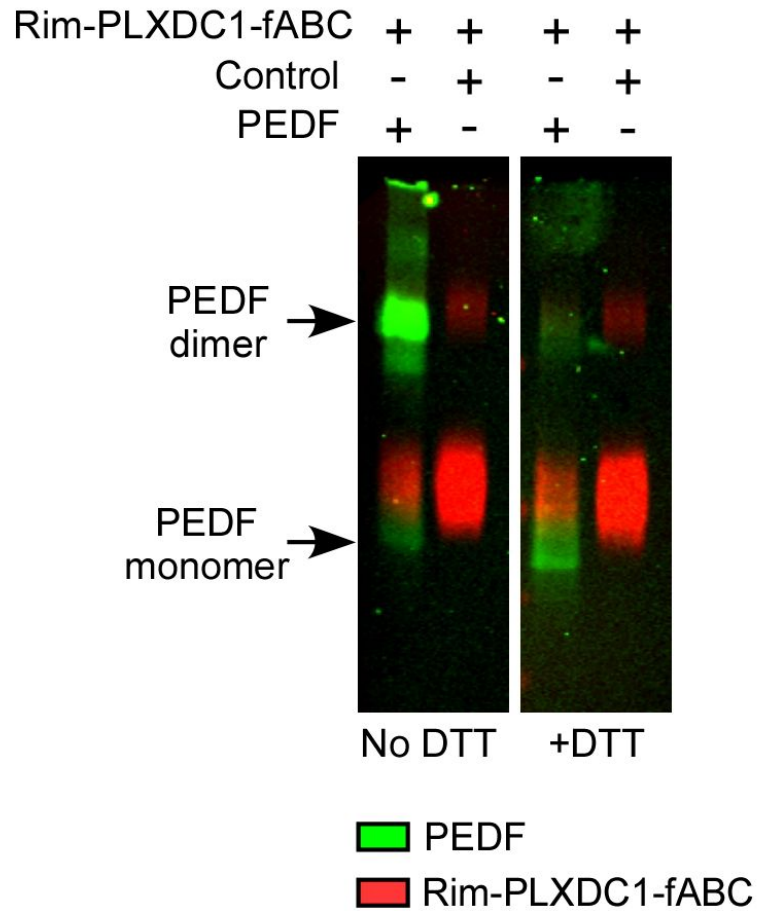
Figure 3-10. PEDF forms dimer during the interaction with PLXDC1.

Rim-PLXDC1-fABC is coexpressed with untagged PEDF or control protein. Proteins are purified by antibody against Rim tag. Purified proteins are resolved in both non-reducing and reducing SDS-PAGE gels. Rim-PLXDC1-fABC and PEDF are probed by anti-Rim antibody and anti-PEDF antibody respectively. The Western blot is developed using Li-Cor Infrared Imager. Both Rim-PLXDC1-fABC (red) and PEDF (green) signals are displayed simultaneously in the image in a color-coded manner. Protein samples are treated without DTT in the non-reducing gel and with DTT in the reducing gel. PEDF dimer and monomer bands are pointed by arrows.

PEDF is copurified primarily as dimer which is sensitive to DTT. PEDF monomer and

Rim-PLXDC1-fABC become undetectable by the antibodies when they copurify with each other.

A

Cysteine 261

B

Rim-PLXDC1-fABC

PEDF
PEDF-C261S
PEDF-D299N
PEDF-His
HA-PEDF
Control

170
130
100
70
55
40
35
20
15
10

PEDF WB
Non-reducing

Rim-PLXDC1-fABC

PEDF
PEDF-C261S
PEDF-D299N
PEDF-His
HA-PEDF
Control

170
130
100
70
55
40
35
20
15
10

PEDF WB
Reducing
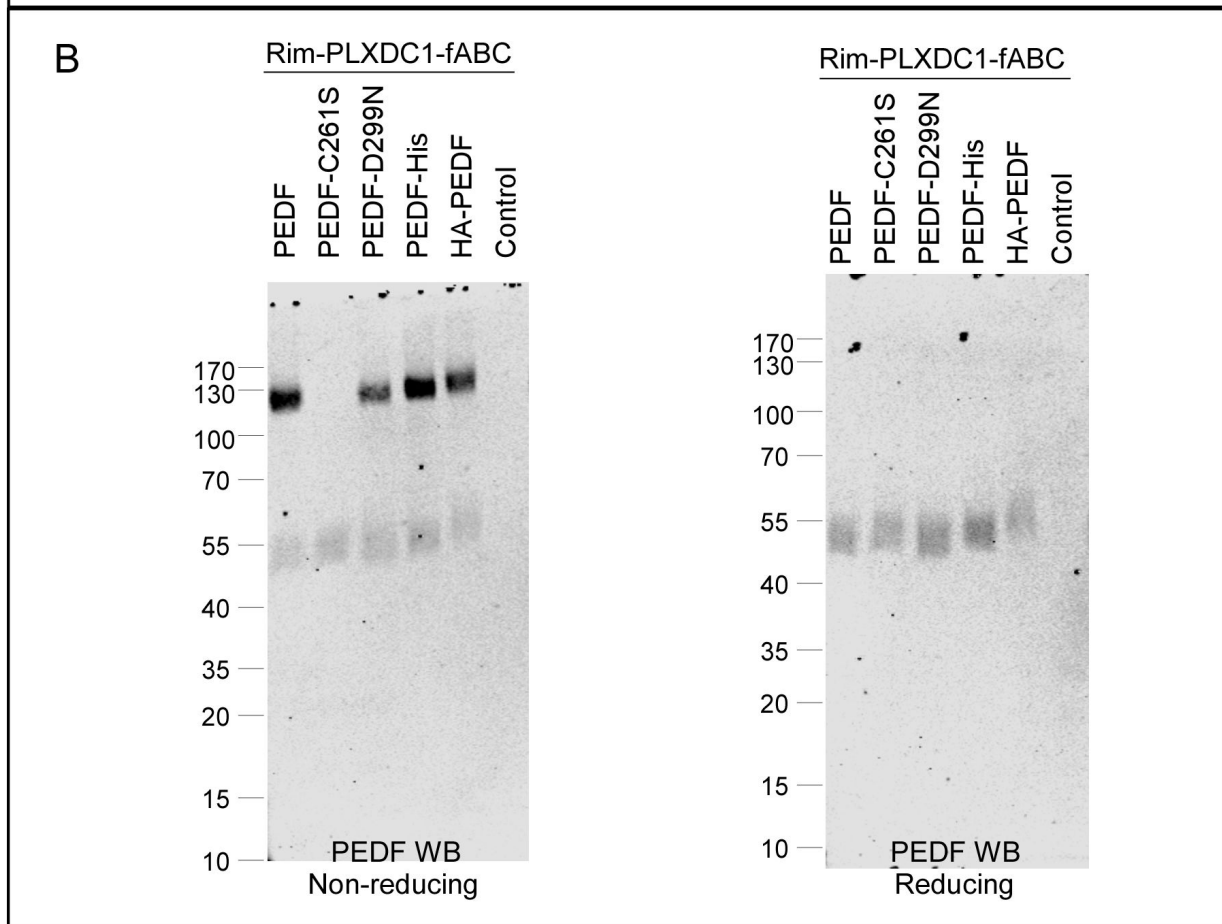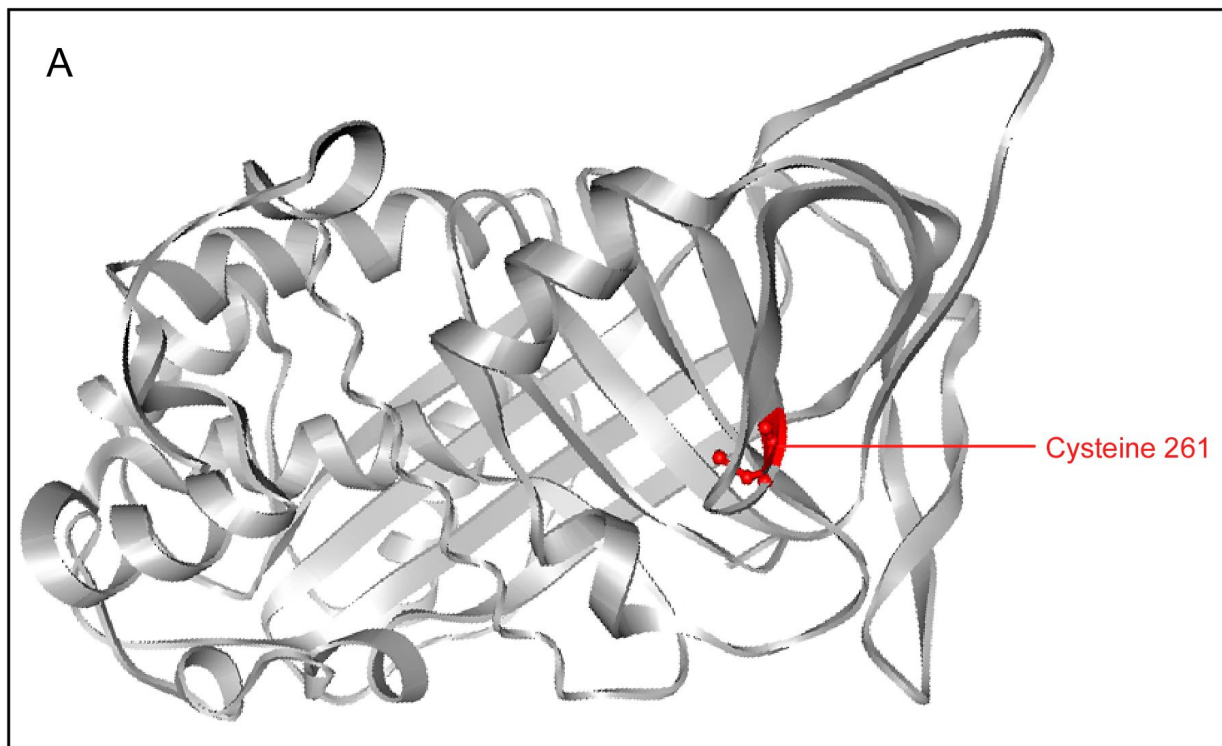
Figure 3-11. PEDF dimerization depends on disulfide bond

(**A**) Crystal structure of PEDF. Cysteine 261 with its side chain is marked in red. (**B**) Rim-PLXDC1-fABC is coexpressed with PEDF-C261S, untagged PEDF, PEDF-D299N, PEDF-His, HA-PEDF and control protein. Proteins are copurified by antibody against Rim tag. All the purified PEDF constructs in non-reducing gel (left) and reducing gel (right) are shown in PEDF Western. PEDF-C261S cannot form dimer as other PEDF constructs upon the interaction with Rim-PLXDC1-fABC.
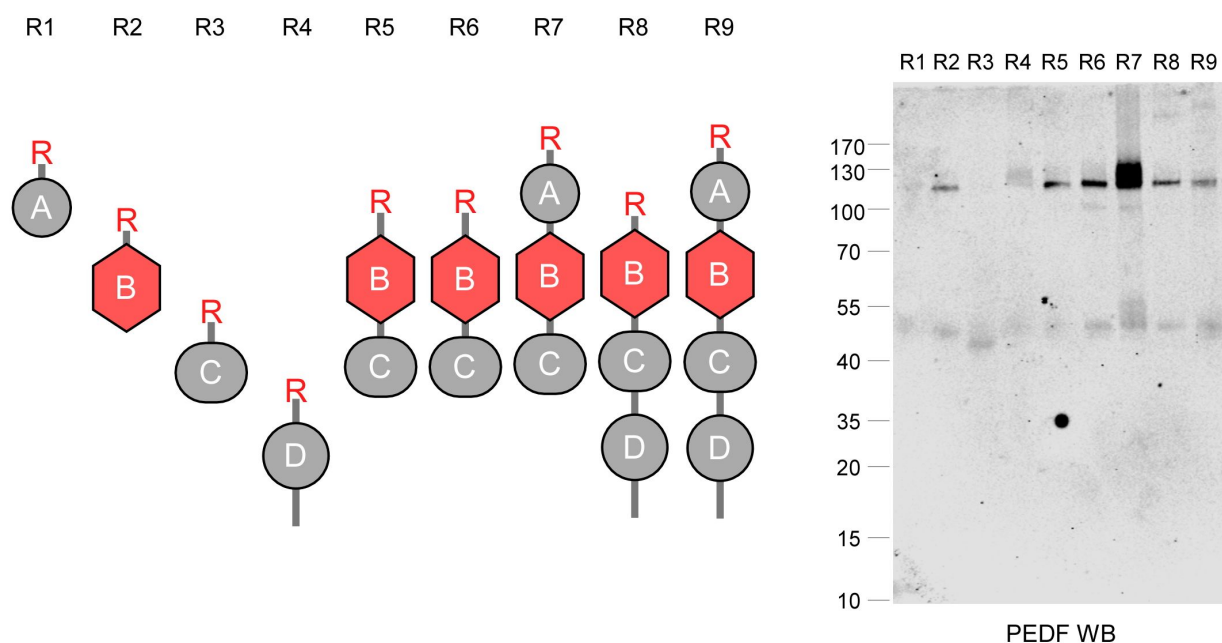
Figure 3-12. PLXDC1 domain B is sufficient and necessary to induce PEDF dimer

Rim-tagged, extracellular fragments of PLXDC1 with different domain deletions (as shown in the diagram on the left, R1 to R9) are coexpressed with PEDF and purified by antibody against Rim tag. Purified proteins are resolved in a non-reducing gel. PEDF dimer is detected by anti-PEDF antibody shown by Western on the right.
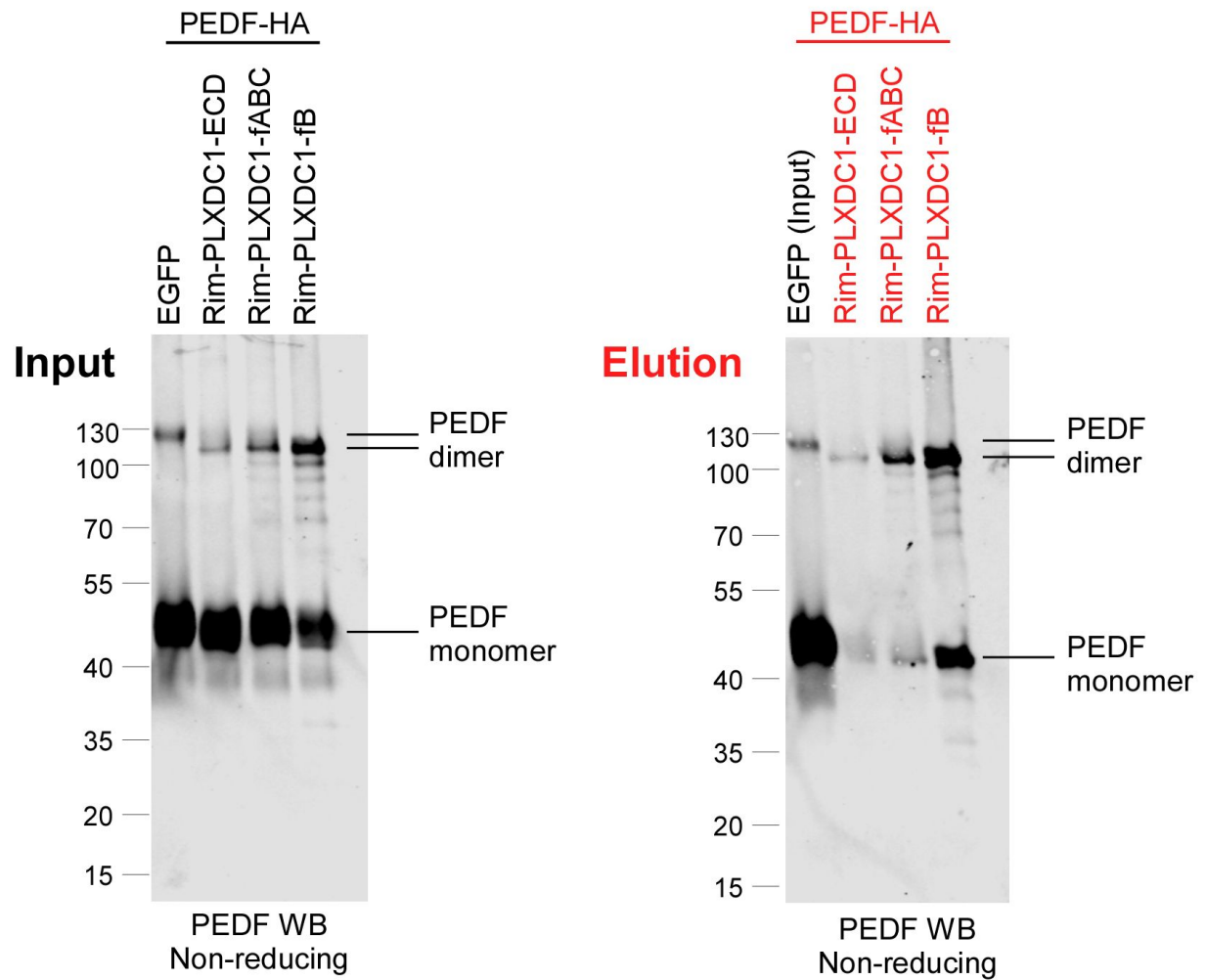
Figure 3-13. PEDF cleavage depends on PLXDC1

PEDF-HA and different Rim-tagged PLXDC1 extracellular constructs are coexpressed respectively in 293T cells. After incubation for 48 hours, a fraction of the expressed proteins are resolved in SDS-PAGE non-reducing gel as "Input" (Left). The rest of proteins are purified by antibody against Rim tag. Copurified proteins were resolved in non-reducing SDS-PAGE gel as "Elution". Both "Input" and "Elution" are probed with anti-PEDF antibody. In the input, the majority of PEDF-HA remained as monomer with a small fraction formed dimer. A downward

shift of dimer band is specifically dependent on the presence of PLXDC1 extracellular constructs

but not EGFP control. PEDF-HA is copurified with PLXDC1 extracellular constructs primarily

as dimer rather than as monomer. Copurified PEDF-HA dimer also shows a smaller molecular

weight compared to the PEDF-HA coexpressed with EGFP in the input.
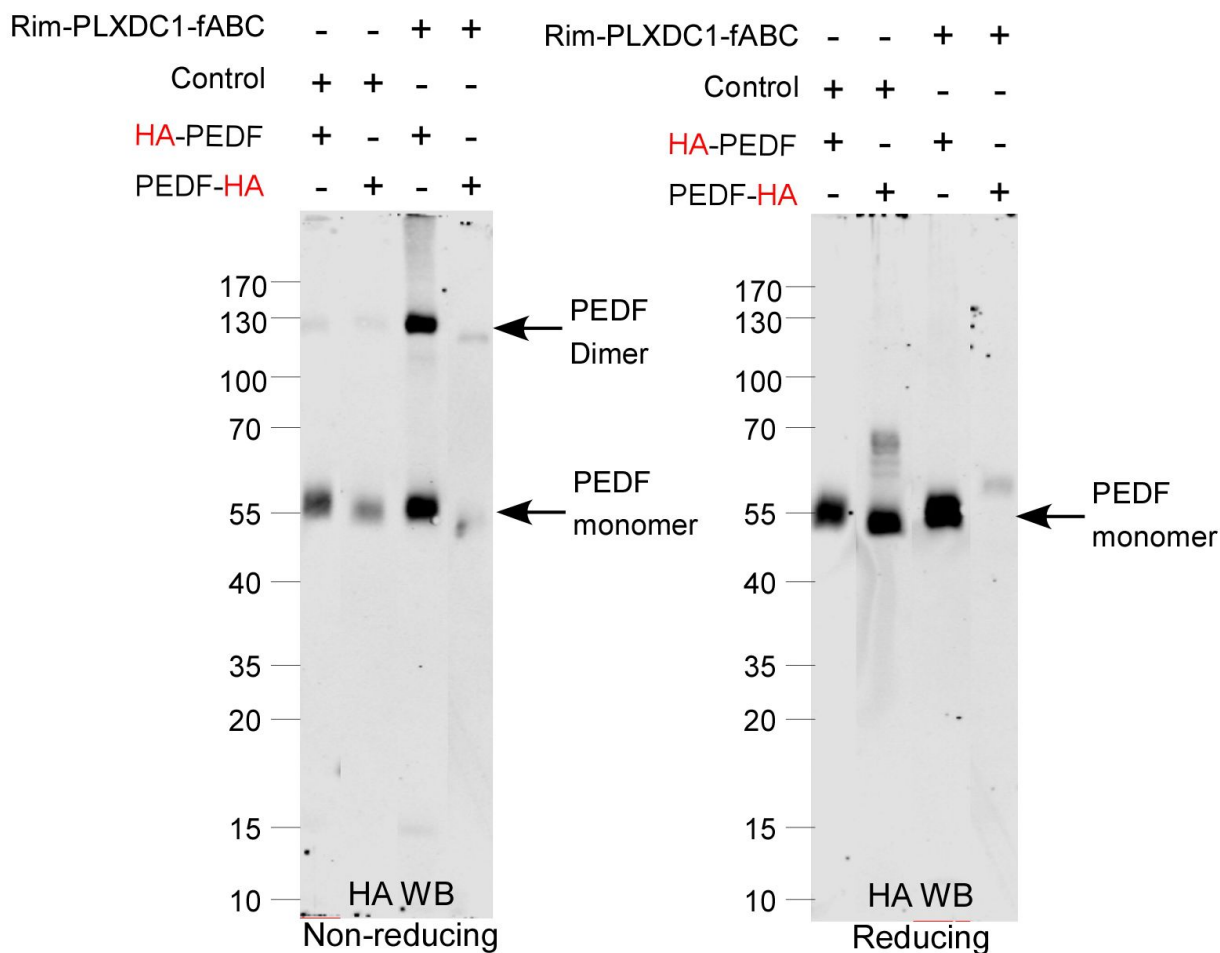
Figure 3-14. PEDF loses its C-terminal tail during the interaction with PLXDC1

PEDF with an N-terminal HA tag (HA-PEDF) and PEDF with a C-terminal HA tag (PEDF-HA) are incubated with Rim-PLXDC1-fABC or a control protein and resolved in the non-reducing (left) or reducing gel (right). HA-PEDF or PEDF-HA is probed by anti-HA antibody. HA-PEDF shows a dimer band in the presence of Rim-PLXDC1-fABC but only a monomer band with control. PEDF-HA is only visible as a monomer after its incubation with control but is completely invisible either as a dimer or as a monomer after its incubation with Rim-PLXDC1-fABC.

A

Exposed Loop

LT

B

```
1    MQALVLLLCI  GALLGHSSCQ  NPASPPEEGS  PDPDSTGALV  EEEDPFFKVP
51   VNKLAAAVSN  FGYDLYRVRS  STSPTTNVLL  SPLSVATALS  ALSLGAEQRT
101  ESIIHRALYY  DLISSPDIHG  TYKELLDTVT  APQKNLKSAS  RIVFEKKLRI
151  KSSFVAPLEK  SYGTRPRVLT  GNPRLDLQEI  NNWVQAQMKG  KLARSTKEIP
201  DEISILLLGV  AHFKGQWVTK  FDSRKTSLED  FYLDEERTVR  VPMMSDPKAV
251  LRYGLDSDLS  CKIAQLPLTG  SMSIIFFLPL  KVTQNLTLIE  ESLTSEFIHD
301  IDRELKTVQA  VLTVPKLKLS  YEGEVTKSLQ  EMKLQSLFDS  PDFSKITGKP
351  IKLTQVEHRA  GFEWNEDGAG  TTPSPGLQPA  HLTFPLDYHL  NQPFIFVLRD
401  TDTGALLFIGKILDPRGP
```

C

Rim-PLXDC1-fABC   Rim-PLXDC2-fABC

HA-PEDF   HA-PEDF-LTAA   HA-PEDF-dcatil   HA-PEDF   HA-PEDF-LTAA   HA-PEDF-dcatil

HA WB

dimer

monomer

Non-reducing   Non-reducing

Figure 3-15. PEDF mutant and Rim-PLXDC1-fABC copurification

(**A**) Crystal structure of PEDF with the reactive loop and potential cleavage site LT (marked red) indicated. (**B**) Human PEDF protein sequence with reactive loop highlighted and LT labeled in red. HA-PEDF-LTAA is made by mutating LT to AA; HA-PEDF-dctail is made by deleting the C-terminal 35 amino acids after LT. (**C**) HA-PEDF, HA-PEDF-LTAA and HA-PEDF-dctail are copurifed with Rim-tagged PLXDC1-fABC (left) or with Rim-tagged PLXDC2-fABC (right) by antibody against Rim tag. All three PEDF constructs are copurified predominantly as dimer as shown in HA Western. HA-PEDF-LTAA dimer (pointed by red arrows) migrates to a slightly higher position than HA-PEDF and HA-PEDF-dctail.

References

Beaty, R. M., Edwards, J. B., Boon, K., Siu, I. M., Conway, J. E., and Riggins, G. J. (2007) PLXDC1 (TEM7) is identified in a genome-wide expression screen of glioblastoma endothelium, *Journal of Neuro-Oncology 81*, 241-248

Becerra, S. P., Sagasti, A., Spinella, P., and Notario, V. (1995) Pigment epithelium-derived factor behaves like a noninhibitory serpin: neurotrophic activity does not require the serpin reactive loop, *Journal of Biological Chemistry 270*, 25992-25999.

Carrell RW, Pemberton PA, Boswell DR. (1987) The serpins: evolution and adaptation in a family of protease inhibitors. *Cold Spring Harb Symp Quant Biol.* 52:527-35.

Cheng, G., Zhong, M., Kawaguchi, R., Kassai, M., Al-Ubaidi, M., Deng, J., Ter-Stepanian, M., and Sun, H. (2014) Identification of PLXDC1 and PLXDC2 as the transmembrane receptors for the multifunctional factor PEDF, *eLife 3:*e05401.

Croix, B. S., Rago, C., Velculescu, V., Traverso, G., Romans, K. E., Montgomery, E., Lal, A., Riggins, G. J., Lengauer, C., Vogelstein, B., and Kinzler, K. W. (2000) Genes expressed in human tumor endothelium, *Science* 289 1197-1202

Illing, M., Molday, L. L., and Molday, R. S. (1997) The 220-kDa rim protein of retinal rod outer segments is a member of the ABC transporter superfamily, *Journal of Biological Chemistry 272*, 10303-10310.

Lu, C., Bonome, T., Li, Y., Kamat, A. A., Han, L. Y., Schmandt, R., Coleman, R. L., Gershenson, D. M., Jaffe, R. B., Birrer, M. J., and Sood, A. K. (2007) Gene alterations identified by expression profiling in tumor-associated endothelial cells from invasive ovarian carcinoma, *Cancer Research 67*, 1757-1768.

McMurray, H. R., Sampson, E. R., Compitello, G., Kinsey, C., Newman, L., Smith, B., Chen, S.-R., Klebanov, L., Salzman, P., Yakovlev, A., and Land, H. (2008) Synergistic response to oncogenic mutations defines gene class critical to cancer phenotype, *Nature 453*, 1112-1116.

Minkevich, N. I., Lipkin, V. M., and Kostanyan, I. A. (2010) PEDF - A noninhibitory serpin with neurotrophic activity, *Acta Naturae 2*, 62-71.

Steele, F. R., Chader, G. J., Johnson, L. V., and Tombran-Tink, J. (1993) Pigment epithelium-derived factor: neurotrophic activity and identification as a member of the serine

protease inhibitor gene family, *Proceedings of the National Academy of Sciences of the United States of America 90*, 1526-1530.

Tombran-Tink, J., Aparicio, S., Xu, X., Tink, A. R., Lara, N., Sawant, S., Barnstable, C. J., and Zhang, S. S.-M. (2005) PEDF and the serpins: Phylogeny, sequence conservation, and functional domains, *Journal of Structural Biology 151*, 130-150.

Yamaji, Y., Yoshida, S., Ishikawa, K., Sengoku, A., Sato, K., Yoshida, A., Kuwahara, R., Ohuchida, K., Oki, E., Enaida, H., Fujisawa, K., Kono, T., and Ishibashi, T. (2008) TEM7 (PLXDC1) in neovascular endothelial cells of fibrovascular membranes from patients with proliferative diabetic retinopathy, *Investigative Ophthalmology & Visual Science 49*, 3151-3157.

Zhou, Y., Nie, Y., and Kaback, H. R. (2009) Residues gating the periplasmic pathway of lacY, *Journal of Molecular Biology 394*, 219-225.

Chapter 4 High Throughput Screening (HTS) of Compounds Targeting PLXDC1 and PLXDC2

4.1 Introduction

A fruitful approach to develop small molecule-based therapeutics is to target receptors. Small molecules targeting receptors account for more than half of all prescription drug sales in the world. There are many reasons why receptors are among the most successful therapeutic targets in medicine. First, they naturally perceive extracellular signals and are accessible on the cell surface. Second, because receptors naturally function to initiate ligand-specific cellular responses, small molecules that mimic or block the natural ligand by targeting receptors can be used to precisely control their cellular responses. For example, caffeine, a widely consumed small molecule in human populations, functions as a selective adenosine receptor antagonist. In disease treatment, small molecule drugs can be developed to mimic or block the action of an extracellular ligand. These small molecules can act on the receptor with better specificity and pharmacokinetics than the original ligand, which can be multifunctional. Here I describe our effort to develop small molecule-based drugs against PEDF receptors.

4.1.1 Broad therapeutic value of PEDF

PEDF has attracted increasing attention from both academia and industry since its identification in 1991. It has been reported to play multiple roles in diverse physiological and pathological

processes. PEDF has been recognized as a neurotrophic factor, a stem cell niche factor, a anti-inflammatory factor, a anti-angiogenic factor and a tumor inhibitor. As a result, targeting PEDF pathway potentially benefits the treatment of a variety of diseases ranging from blinding retinal diseases to many kinds of cancer. However, the therapeutic value of PEDF is greatly impeded by the lack of knowledge on PEDF signaling mechanism. Especially, the identity of PEDF receptor identity has remained obscure for many years. As described in previous chapters, our lab identified PEDF cell surface receptors as PLXDC1 and PLXDC2. In order to transform the high therapeutic value of PEDF to a handy clinical approach, we decided to screen small molecules that targets PEDF receptors.

4.1.2 Two general strategies in drug discovery

Classical pharmacology and reverse pharmacology are two major strategies in drug discovery. In classical pharmacology, drugs are selected by its biological activity in intact cells or organism without the knowledge of its biological targets. Drugs can be obtained by purifying from natural products or extracts, by screening chemical library or even by serendipitous discovery. One great example is the 2015 Nobel Prize awarded achievement. Youyou Tu identified and extracted artemisinin from Chinese traditional medicine Artemisia annua and brought the currently most effective cure for malaria. Yet, the mechanism of artemisinin in curing malaria and its drug target still remain unclear. On the opposite, reverse pharmacology is performed on the basis of a

well characterized target specifically linked to diseases. Drugs are obtained via screening candidates against an isolated biological activity that mimics a disease process. This is a more advanced strategy aided by human genome sequencing and high throughout screening. Examples of drugs developed this way include Imatinib, a small molecule targeting BCR/ABL fusion protein to treat chronic myeloid leukemia, and Bevacizumab, an antibody against vascular endothelial growth factor (VEGF) to inhibit angiogenesis in age-related macular degeneration (it works poorly in cancer due to systemic toxicity). The reverse pharmacology is more currently used in drug development because of its specificity and efficiency (Takenaka., 2001).

4.1.3 Our Screening strategy

Reverse pharmacology is more efficient than classical pharmacology, especially when the target is recognized as in the case PEDF, whose functions and receptors are characterized. To screen compounds that target PEDF receptors, it is required to develop a robust and reproducible assay that mimics a specific PEDF biological activity. In collaboration with Dr. Robert Damoiseaux's lab, we developed a novel strategy based on a cellular assay and high throughput screening (HTS) to identify small molecules by targeting PEDF receptors. The strategy is to screen compounds that lead to cell death or cell survival specifically through PLXDC1 or PLXDC2. This is achieved by a tri-color system whereby we color-coded PLXDC1-expressing, PLXDC2-expressing, and untransfected cells with green, red and blue respectively. Then we

used automated, high-content facility to monitor the change of cell number of each color upon compound treatment. Compounds that specifically target PLXDC1 or PLXDC2 expressing cells are selected. **Figure 4-1** is a schematic diagram of the tri-color system.

The tri-color system has a few advantages. First, it allows direct visualization and tracking of receptor expressing cells, thus allows evaluation at single cell resolution. Second, it provides two internal controls that exclude false positive. For example, red and blue signals serve as two internal controls if green signal is evaluated. A drug that targets PLXDC1 will change green cell number but will not affect the numbers of red, PLXDC2 expressing cells and blue, untransfected cells. However, drugs with general toxicity or pro-survival effect will affect cells of all three colors. Third, tri-color system is able to efficiently screen compounds targeting PLXCD1 and compounds targeting PLXDC2 at the same time, which reduces time, labor and material cost. The strategy will generate a few possible outcomes which are depicted in **Figure 4-2**. After primary screening using the tri-color system, interesting compounds were further tested in our lab using luciferase assay and cell model based assays for validation.

4.2 Materials and Methods

4.2.1 Materials and equipment

The materials, reagents, cells and equipment used in the experiments described in this chapter are listed in **Table 4-1**.

4.2.2 Description of the compound libraries

We screened the compound collection provided by the academic high-throughput screening (HTS) facility led by Dr.Robert Damoiseaux at UCLA. Dr. Damoiseaux's group has applied extensive filtering against liabilities such as reactive groups and aggregators to select compounds for the library collections (Damoiseaux R., 2011). We screened four libriaries: 1) Pharmacological validation and repurposing libraries, 2) Lead-like libraries (DL), 3) the diverse libraries (UCLA), and 4) the diverse/smart libraries (EAM and LS). All the compounds are at least 90% pure or better. More detailed characteristics of each library are depicted in **Figure 4-3**.

4.2.3 Cellular model

We used monkey kidney fibroblast-like cell COS-1 as screening model after testing many cell lines. COS-1 cell is easily transfected. It also grows robustly at a large scale with regular culturing condition. Lastly, but most importantly, COS-1 cell, when heterologously express

PLXDC1 or PLXDC2, undergo cell death upon PEDF treatment. It suggests that COS-1 cells respond to PEDF treatment in a receptor-dependent manner. In contrast, the effect is absent in HEK293T cells as shown in **Figure 4-4**. In another word, COS-1 cell possesses downstream proteins to transduce receptor signals that are responsible for PEDF mediated cell death. Therefore, COS-1 cell is an good model for our large scale screening as it is easily transfected, suitable for large scale culturing and responds to PEDF in a PEDF receptor-dependent manner.

4.2.4 Establishing the tri-color system for high-throughput screening

In the tri-color system, we require COS-1 cell to be color coded and express receptor in an inducible manner. To achieve this goal, we created several doxycycline (Dox)-inducible cDNA constructs. The Dox-inducible construct iPLXDC1-EGFP allows constitutive expression of EGFP and Dox-induced expression of PLXDC1; another construct iPLXDC2-mCherry allows constitutive expression of mCherry and Dox-induced expression of PLXDC2. The structures of the inducible systems are shown in **Figure4-5**. Establishing the tri-color system is a key step of screening. After transfecting individually into cells, iPLXDC1-EGFP and iPLXDC2-mCherry transfected cells are mixed and treated with Dox and Hoechst. Upon Dox treatment, iPLXDC1-EGFP transfected cells will show green fluorescence and express PLXDC1; iPLXDC2-mCherry transfected cells will show red fluorescence and express PLXDC2. Hoechst makes all the cells fluorescent blue by staining nuclear DNA. Thus the untransfected cells are

fluorescent blue with the cell number easily calculated by subtracting the green cell number and the red cell number from the total blue cell number. In summary, in the established tri-color system, all PLXDC1 expressing cells are green coded, all PLXDC2 expressing cells are red coded and all the untransfected cell are blue coded.

4.2.5 Primary compound selection using HTS

Each round of primary screening took 10 days and screened around 14,000 compounds. The workflow of each round is sketched in **Figure 4-6.** Each step of the workflow is described in details below.

In day 1, we split COS-1 cells at 1:3 ratio and grew them with Dulbecco's Modified Eagles Medium (DMEM) and 10% fetal bovine serum (FBS) at 37°C with 5% CO_2 for 16 hours before transfection. Cells would reach around 50% confluency at transfection.

In day 2, transfection was performed using jetPRIME following protocol. 40 plates were transfected with iPLXDC1-EGFP and the other 40 plates were transfected with iPLXDC2-mCherry. 6 hours after transfection, cell medium was changed to fresh DMEM medium with 10% FBS.

In day 3, iPLXDC1-EGFP and iPLXDC2-mCherry transfected cells were harvested, mixed and replated onto 384-well plate with different compound in each well. Each well contains around 5000 cells in 50 μl serum free-, phenol-red free DMEM medium with doxycyclin (3 ng/ml), Hoescht (0.5 μg/ml), and a specific compound (10 μM). The 384-well plates we used are black and have flat and clear bottom wells for fluorescent signal acquiring. To prepare this plate, we added cell culture medium, Dox, Hoescht and compounds to the 384-well plate before harvesting and replating COS-1 cells to the plate. We first made 450 ml of serum free-, phenol-red free DMEM medium with Dox (6 ng/ml), Hoescht (1 μg/ml) and dispensed 25 μl of the medium into each well of 40 plates using Manifold Cell Plating robot in Dr. Robert Damoiseaux's lab. Compounds from libraries were pinned to each 384-well plate by collaborators from Dr. Robert Damoiseaux's lab. Compounds were pinned to reach a final concentration of 10 μM in 50 μl. The first and last column of each 384-well plate were pinned with DMSO at the same concentration as compound to serve as blank control. To replate transfected COS-1 cells, we trypsinized the cells by 0.5 ml 0.05% trypsin for 5 min after medium removal and phosphate buffer saline (PBS) wash. After cell were detached, 0.5 ml trypsin inhibitor and 1 ml of PBS was added and cells were collected from each plate. Cells were spun down for 5 min at 1200 rpm and resuspended in serum free- and phenol-red free DMEM medium. iPLXDC1-EGFP and iPLXDC2-mCherry transfected cells were mixed in a total volume of 450 ml. And 25 μl of cell suspension was dispensed into each well of forty 384-well plate by Manifold Cell Plating robot.

Cells were constantly and gently stirred during replating for homogeneous dispensing among wells. A breathable bio-membrane was applied to seal each plate before it was loaded on Cytomat incubator. The COS-1 cells were incubated with compounds at 37°C with 5% CO_2 for 72 hours. **Figure 4-7** shows a schematic design of a 384-well plate.

In day 6, green, red, and blue fluorescence in each well of each 384-well plate was captured by fluorescent camera in green, red and blue channel respectively. Focusing plane and exposure time in each channel was determined using a random control well from a random plate and were applied to all the plates during image acquiring. The image taking was performed by an automated system which was programmed by Dr. Robert Damoiseaux. Image acquiring parameters were defined in Metaexpress software which was incorporated in the automation.

In day 7, fluorescent signals representing cell count were extracted from each image using Metaexpress software and UCLA super computer. The threshold of each channel is configured using a random control well in a random plate and applied to all the wells.

In day 9, data was downloaded from the UCLA super computer. Each data point was annotated and uploaded onto Collaborative Drug Discovery (CDD) website. In day 10, we analyzed the data on CDD website to identify interesting compounds. Compounds that changed the green cell

number (or red cell number) by at least 40% but changed blue cell and red cell number (or green cell number) by less than ±10% were selected. The interesting compounds were further validated by other assays.

4.2.6 Luciferase assay

Because of the potential artifact of fluorescence-based screening due to the autofluorescence of some compounds, we developed a validating assay using luciferase as the reporter. We made cDNA constructs that constitutively express luciferase and expresses PLXDC1 (iPLXDC1-Luc) or PLXDC2 (iPLXDC2-Luc) upon Dox treatment (**Figure 4-5**). Construct that only expresses luciferase (Luc) was used as control. COS-1 cells were transfected with Luc, iPLXDC1-Luc or iPLXDC2-Luc using jetPRIME and cultured in DMEM medium with 10% FBS at 37°C with 5% CO_2. After transfection for 24 hr, COS-1 cells were replated in SFM with 3ng/ml Dox onto transparent flat bottom 96-well plates at a 1:1 ratio. Meanwhile, 10 μM of compound was added. Drugs were tested in triplicates. Luciferase activity reflecing cell survival was measured by commercial kit and POLARstar Omege 72 hours after compound treatment. Taking PLXDC1 as an example, luciferase activity of compound treated iPLXDC1-Luc COS1 cells was compared with that of DMSO treated cells, which would reveal if the tested compound affects cell survival. Luciferase activity of compound treated iPLXDC1-Luc expressing COS1 cells was also

compared with that of Luc expressing COS-1 cells subject to the same compound, which would reveal if the compound affects cell survival through PLXDC1.

4.2.7 Endothelial cell death assay

Mouse endothelial cell SVEC4-10 was used for this assay. The survival of SVEC4-10 with or without compound treatment was analyzed by the MTT assay. Briefly, SVEC4-10 cells were grown in DMEM medium containing 10% FBS, penicillin and streptomycin at 37°C with 5% CO_2 until confluence. During splitting, SVEC4-10 were detached from the petri dish by 0.05% trypsin for 5 min at room temperature (RT). Trypsin was neutralized by equal volume of trypsin inhibitor. Detached cells were collected and spun down at 1200 rpm for 2min. Cells were then resuspended with serum-free DMEM medium (SFM) containing 0.5mg/ml bovine serum albumin (BSA) and plated at 1:10 ratio. Compound was added to 1 or 5 μM at the same time as cell replating. Cell viability was assessed 24 hours after cell replating by MTT assay.

MTT assay was done by incubating cells with 100μl 100 μg/ml MTT reagent in SFM for 3 hours at 37°C with 5% CO_2. DMSO (50 μl) was added to each well after MTT reagent was removed. The absorbance of the purple color from the formazan formed was measured and quantified using POLARstar Omega at 570 nm. DMSO in empty well was used as blank control.

4.2.8 Copurification assay

HEK293T cells were co-ransfected with N-terminal Rim tagged PLXDC1 extracellular domain (Rim-PLXDC1-ECD) and N-terminal HA-tagged PEDF (HA-PEDF) by jetPRIME. Six hours after transfection, cells were washed once with Hank's Balance Salt Solution (HBSS). Culturing medium was changed to SFM with 5 μM DL-12 or DL-60. Cells were grown for 48 hours at 37°C with 5% CO_2. Then cell conditioned medium was harvested and purified by sepharose beads coated with anti-Rim antibody. Purification was done at RT for 2 hours before washing the beads with HBSS twice. Proteins bound to the beads were eluted with 0.1 M glycine pH=2.3 at room temperature for 10 min. Elution was neutralized by 1M Tris-HCl buffer, pH 9.1, mixed with 5X SDS and boiled. Purified proteins were resolved in SDS-PAGE gel and transferred to nitrocellulose membrane. Western Blotting was performed as described in chapter 2. Monoclonal anti-Rim antibody (1:10,000) and polyclonal anti-HA antibody (1:1,000) were used to probe Rim-PLXDC1-ECD and HA-PEDF respectively. The signals were amplified by Dylight 680 α-mouse antibody and IRDye 800CW α-rabbit antibody and acquired by Infrared Imager.

4.3 Results

4.3.1 Primary selection of compounds by HTS

The final step in primary screening is to analyze how an individual compound affects the blue, green and red signals in each well compared to the signals in DMSO treated control wells. This

was done using the computer aided system on CDD website. **Figure 4-8** shows an example of a plate displayed as heat maps generated by CDD and an example of computer aided compound selection. The heat maps provide an overview of a 384-well plate where cell numbers changed in each well due to different compounds treatment. A compound was selected for further study if it changed green cell number (or red cell number) by at least 40% but changed blue cell and red cell number (or green cell number) by less than ±10%. Selected compounds were subject to further validation.

4.3.2 Second round of screening

The primary screening based on fluorescent signals can potentially introduce false positive results due to the intrinsic fluorescence of the compounds. To overcome the limitation of fluorescence-based screening, we tested the selected compounds from the first round by a luciferase-based assay. iPLXDC1-Luc or iPLXDC2-Luc and Luc transfected cells were treated with compound candidates, and the luciferase activity reflecting cell survival were measured. We selected the compound that suppressed (or increased) the luciferase activity in PLXDC1 (or/and PLXDC2) expressing cells compared to DMSO control but did not change the luciferase activity in the Luc expressing cells treated with the same compound. **Figure 4-9** shows an example of second round screening of 70 compound candidates. Compound DL-60 (orange column) selectively suppressed the luciferase activity of PLXDC1 and PLXDC2 expressing cells but not

that of Luc expressing cells. DL-60 thus, passed the second round of screening. On the contrary, another compound (grey column), suppressing the luciferase activity all three kinds of cells, was excluded due to the general toxicity. We have, so far, selected two top compounds DL-60 and DL-12 and are still in the process of verifying the activity and specificity of more compound candidates.

4.3.3 Two top compounds induce endothelial cells death

After showing that DL-12 and DL-60 induce COS-1 cell death in PLXDC1 or PLXDC2 specific manner, we asked if those drugs induce endothelial cell death as PEDF does. To answer the question, we plated endothelial cell SVEC4-10 in SFM and incubated them with 1 or 5 μM compounds. SVEC 4-10 cell death was evaluated by MTT assay. As shown in **Figure 4-10**, both DL-12 and DL-60 induced SVEC 4-10 cell death in a dose-dependent manner, while neither the control compound nor DMSO had the effect.

4.3.4 Two top compounds interfere with PEDF and receptor interaction

Since DL-12 and DL-60 induce COS-1 cell death in a PEDF-receptor dependent manner, we went on to study if those two drugs interact with PEDF receptor, PLXDC1 or PLXDC2. Direct visualizing the compound-receptor interaction is technically difficult as it requires labeling the compounds with a detectable probe, such as radioactive isotope. We hypothesize that DL-12 and

DL-60 could affect the binding of PEDF to its receptors if the compounds also interact with the receptors. Therefore, we studied how PLXDC1 interacts with PEDF in the presence of DL-12 or DL-60. We cotransfected HEK 293T cells with Rim-PLXDC1-ECD and HA-PEDF and added 5 μM DL-12 or DL-60 to the cell culture medium. Forty-eight hours after compound addition, cell medium was harvested and purified against anti-Rim antibody. We found that HA-PEDF was copurified with Rim-PLXDC1-ECD efficiently in the presence of DMSO. However, both DL-12 and DL-60 significantly reduced the amount of HA-PEDF that was copurified as shown in **Figure 4-11**. The result suggests that DL-12 and DL-60 interferes with the interaction between PEDF and its receptor. Therefore, DL-12 and DL-60 likely interact with the extracellular domain of PEDF receptors directly.

4.4 Discussion

We developed a cell-based high-throughput screening to select the compounds that target on PEDF receptors.The automatic, high-throughput facilities in Dr. Robert Damoiseaux's lab and the tri-color coding system are the powerful tools in this strategy. We particularly screen chemical compounds that lead to cell death or cell survival specifically through PLXDC1 or PLXDC2. The cell based assay creates a neat system that allows evaluation of receptor-mediated specific effect while excluding confounding variables commonly seen in animal based assays. It

is also cost-effective and permits large library screening. In addition, cell-based assay can provide rich information that rules out false positive, false negative or toxicity.

In the large scale screening we identified two interesting compounds DL-12 and DL-60. Using the luciferase-based assay, we further verified that both DL-12 and DL60 induce COS-1 cell death on a PLXDC1 or PLXDC2 dependent manner. They also interfere with PEDF binding to its receptors probably due to its direct interaction with the receptors. We also show that both DL-12 and DL-60 induce SVEC 4-10 endothelial cell death at the same condition as PEDF does. In Chapter 2, we demonstrated that PEDF induces SVEC 4-10 cell death in a PLXDC2 dependent manner. Similarly, DL-12 and DL-60 selectively kill PLXDC1 or PLXDC2-expressing COS-1 cells. It is worth noting that DL-12 and DL-60 induce SVEC4-10 cell death at an identical condition (applied to cells as the cells are plated in SFM) as PEDF does. Thus, we wonder if those compounds induce SVEC 4-10 cell death through PEDF receptors. To answer this question, we will evaluate how the DL-12 and DL-60 affect the survival of SVEC4-10 with gain of function (PLXDC1 or PLXDC2 overexpressing) and with loss of function (endogenous PLXDC1 or PLXDC2 knocked-down). It is also important to know if other endothelial cells respond to DL-12 and DL-60. Primary endothelial cells such as human retinal micro-endothelial cells (HRMEC) and human umbilical vein endothelial cells (HUVEC) will be tested. We will also test if DL-12 and DL-60 inhibit angiogenesis *in vivo*, such as in cornea angiogenesis model and matri-gel transplantation model.

The compounds that show activity specifically through PEDF receptors in the above assays will be strong candidates for future therapy targeting PEDF pathway. In fact, targeting receptors is the most successful strategy in drug discovery. Receptors are key regulators of cell response to the environment because they initiate signal transduction into cells upon ligand presence. Besides, cell-surface receptors are easily accessible to drugs. In fact, according to an analysis on Drug Bank database and human genome, cell-surface receptors make the largest group of drug targets in human (44% of all human drug targets) (Rask-Andersen et al., 2011).

Small molecule has several advantages over PEDF as an option for therapy. First, small molecules have better pharmacokinetics than PEDF itself, which will facilitate its clinical usage. Second, PEDF, as a whole protein, has multiple functions on various types of cells and will generate off-target effect as a drug. On the contrary, small molecules can be selected or/and modified to mimic a specific activity of PEDF on a particular cell type without affecting irrelevant pathways and cells. In addition, small molecules can be modified to be more potent than PEDF itself. Small molecules can be produced in large scale at a relatively low cost than protein reagent. The high stability compared to protein allows easy packaging, transporting and clinical administration. Actually, small molecules are the most common agents acting on novel targets, compromising 60% of new drugs in drug development (Rask-Andersen et al., 2011).

We are in the process of identifying compounds that mimic PEDF in inducing endothelial cells death by targeting PLXDC1 or PLXDC2. The compounds can serve as handy tools in mechanistic research on PLXDC1 and PLXDC2. Moreover, the compounds will potentially be therapeutic valuable to correct aberrant angiogenesis in diseases such as various tumors, diabetic retinopathy and age-related macular degeneration.

Table 4-1. List of reagents, cell lines, and equipment

|	Materials/Equipment	Description	Manufacturer
Cell Lines	COS-1 Cell	Monkey kidney fibroblast cells	ATCC
	HEK293T Cell	Human embryo kidney 293 cell with T-antigen	ATCC
	SVEC4-10 Cell	Mouse endothelial cell	ATCC
Reagents	Anti-Rim Ab	Monoclonal anti-Rim antibody	N/A
	DMEM	Dulbecco's Modified Eagles Medium	Hyclone, GE Healthcare Life Sciences
	DMSO	Dimethyl sulfoxide	BDH solvent
	Doxycyclin	N/A	Sigma
	Dylight 680 Ab	Dylight 680-conjugated goat anti-mouse antibody	Pierce, Thermo
	FBS	Fetal Bovine Serum	Hyclone, GE Healthcare Life Sciences
	HBSS	Hank's Balanced Salt Solution	Thermo Scientific
	Hoeschst	Hoeschst stain solution	Sigma
	IRDye 800CW Ab	IRDye 800-conjugated goat anti-rabbit antibody	Li-Cor
	JetPRIME	DNA transfection reagent	Polyplus-transfection
	Luciferase assay kit	N/A	Promega
	MTT reagent	N/A	Life Science Research Products
	Nitrocellulose membrane	N/A	Maine manufacturing
	PBS	Phosphate Buffered Saline	Corning cellgro
	Phenol red free DMEM	N/A	Hyclone, GE Healthcare Life Sciences
	pAnti-HA Ab	Polyclonal anti-HA antibody	Genemed Synthesis
	Sepharose beads	CNBr-activated Sepharose 4 Fast Flow beads	Amersham, GE Healthcare
	Triton X-100	Triton X-100 surfactant	Omnipur, Millipore
	Trypsin	0.05% trypsin	Hyclone, GE Healthcare Life Sciences
	Trypsin Inhibitor	DTI, defined trypsin inhibitor	Gibco, Life Technology
Equipment	384-well plate	Black, 384-well, flat and clear bottom	CELLSTAR, Greiner Bio-One
	Breathable biomembrane	Breathable sealing biomembrane	Sigma
	Infrared Imager	N/A	Li-Cor
	POLARstar Omega	N/A	BMG Labtech
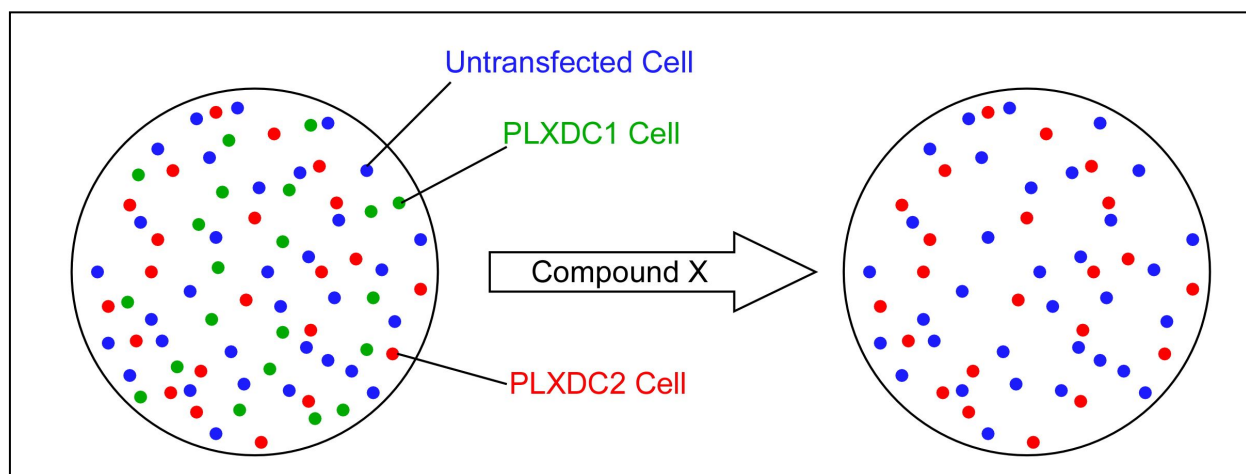
Figure 4-1. Schematic diagram of the experiment design

Each well used in the high-throughput screening has three kinds of cells as shown in the left.

Each colored dot represents a cell. Cells expressing PLXDC1 are labeled in green and cells

expressing PLXDC2 are labeled in red. Untransfected cells are neither green nor red, but have

blue color due to nuclear staining. The example on the right is a well that has its PLXDC1 cells

being selectively killed due to the addition of compound X, which is a candidate compound that
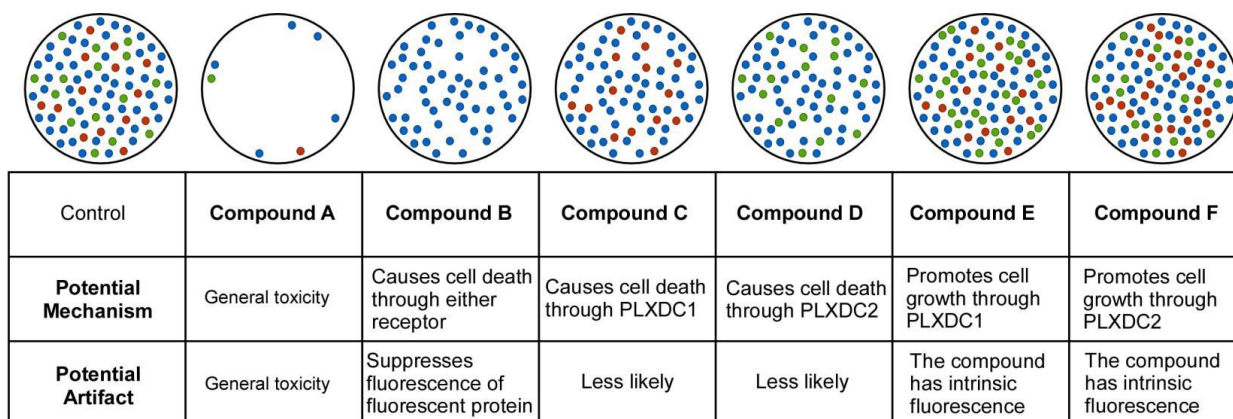
specifically targets PLXDC1.

	Control	Compound A	Compound B	Compound C	Compound D	Compound E	Compound F
Potential Mechanism		General toxicity	Causes cell death through either receptor	Causes cell death through PLXDC1	Causes cell death through PLXDC2	Promotes cell growth through PLXDC1	Promotes cell growth through PLXDC2
Potential Artifact		General toxicity	Suppresses fluorescence of fluorescent protein	Less likely	Less likely	The compound has intrinsic fluorescence	The compound has intrinsic fluorescence

Figure 4-2. Possible outcomes of the high-content screening.

Schematic diagrams of the wells that result from treatment by different compounds (compound A to F). Each colored dot represents a cell. Green cells represent cells expressing PLXDC1 and red cells represent cells expressing PLXDC2. Blue cells represent untransfected cells. Potential mechanisms and potential artifacts are listed below in the table for each category of compounds.
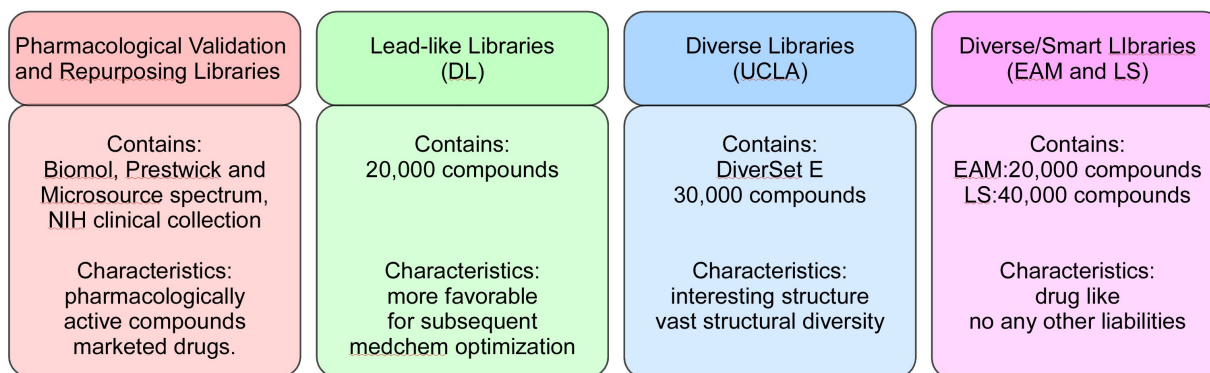
Pharmacological Validation and Repurposing Libraries	Lead-like Libraries (DL)	Diverse Libraries (UCLA)	Diverse/Smart LIbraries (EAM and LS)
Contains: Biomol, Prestwick and Microsource spectrum, NIH clinical collection	Contains: 20,000 compounds	Contains: DiverSet E 30,000 compounds	Contains: EAM:20,000 compounds LS:40,000 compounds
Characteristics: pharmacologically active compounds marketed drugs.	Characteristics: more favorable for subsequent medchem optimization	Characteristics: interesting structure vast structural diversity	Characteristics: drug like no any other liabilities

Figure 4-3. Compound libraries

Pharmacological validation and repurposing libraries (Biomol, Prestwick and Microsource spectrum, NIH clinical collection) contains pharmacologically active compounds and marketed drugs. The Lead-like libraries (DL) is a set of 20,000 compounds which are selected from a set of about 250,000 compounds with more favorable properties for subsequent medchem optimization. The diverse libraries (UCLA) is the DiverSet E from Chembridge. It is a well-established 30,000 compound set selected from 1,100,000 compounds and contains a vast structural diversity. The diverse/smart libraries (EAM and LS) were selected from two large sets of 600,000 and 250,000 compounds by filtering the drug-like compounds that did not have any other liabilities.
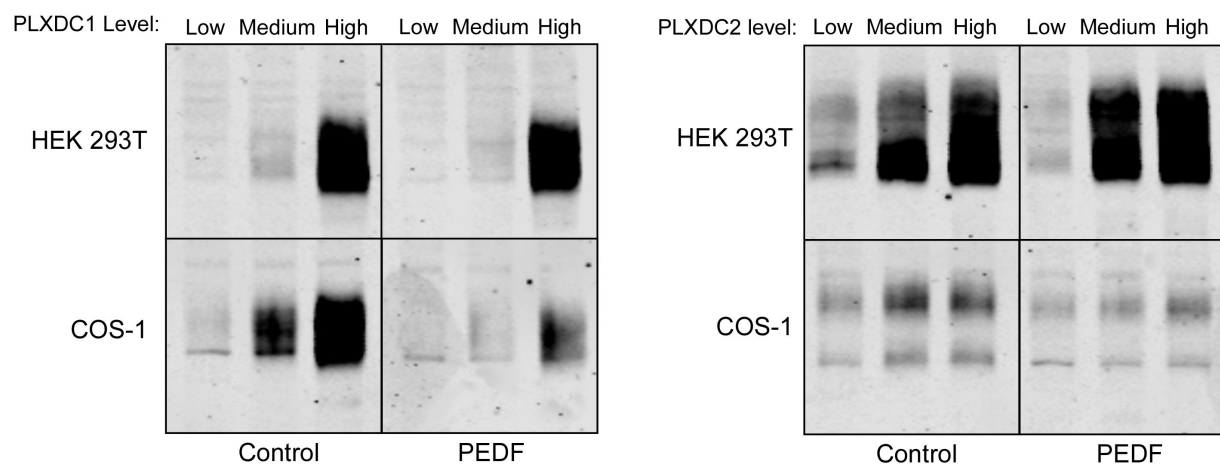
Figure 4-4. Cell type specific response to PEDF

COS-1 cells and HEK 293T cells were heterologously coexpressing PEDF receptor (PLXDC1: left panel; PLXDC2: right panel) with PEDF or a control protein. PLXDC1 or PLXDC2 is expressed in a Dox inducible manner. By applying different doses of Dox, the receptor expression was controlled to low, medium or high level as shown by the Western signal. The signal reflects the survival of cells expressing the receptors. In COS-1 cell, the presence of PEDF caused severe cell death when PLXDC1 (or PLXDC2) was expressed at medium and high levels, which was manifested by the significantly reduced Western signals compared to control. However, the presence of PEDF did not induce obvious cell death compared to control in PLXDC1 or PLXDC2 expressing HEK 293T cells.
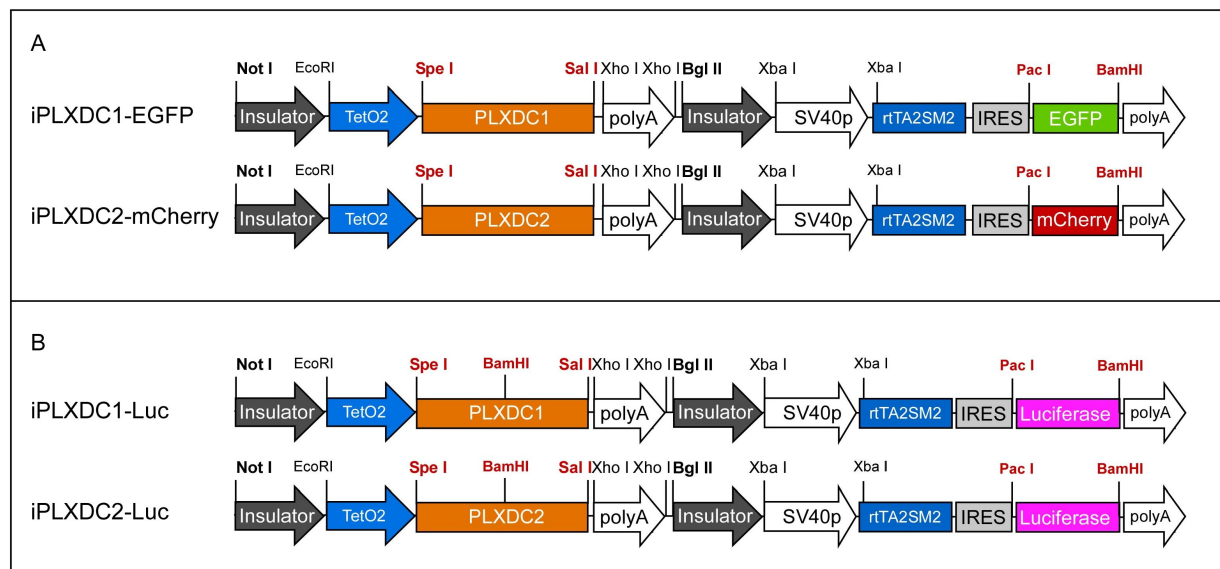
Figure 4-5. Structures of Dox inducible constructs

(**A**) Two Dox inducible constructs with fluorescent reporters. Take the construct iPLXDC1-EGFP as an example, Dox inducible transactivator rtTA2SM2 and EGFP are driven by SV40P promoter and are constitutively expressed. Dox added to the cells will bind to transactivator rtTA2SM2 which in turn binds to Tetracyclin-On (TetO2) operator. The process will eventually leads to the expression of receptor PLXDC1 in the cell. Thus, COS-1 cells transfected by iPLXDC1-EGFP will constitutively express EGFP and express PLXDC1 upon Dox treatment. In our screening system whereby iPLXDC1-EGFP transfected cells and iPLXDC2-mCherry transfected cells are mixed, all PLXDC1 expressing cells will be green, and all PLXDC2 expressing cells will be red. (**B**) Another two Dox inducible constructs whose

fluorescent reporters are replaced by luciferase. A Dox inducible expression of receptor is shown
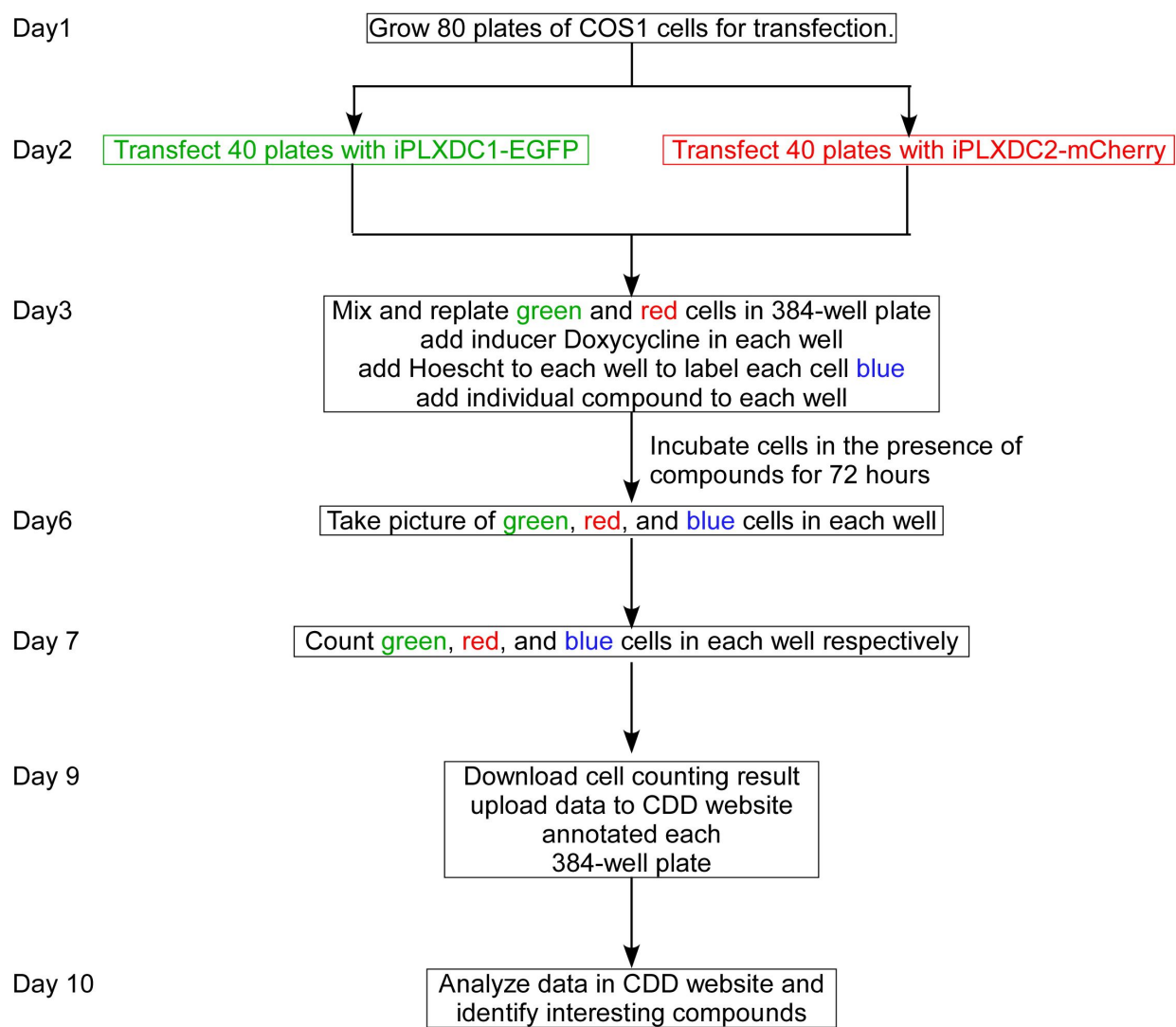
as Western signal in Figure 4-4.

Day1　　　　　　　　　　Grow 80 plates of COS1 cells for transfection.

Day2　　　Transfect 40 plates with iPLXDC1-EGFP　　　　　Transfect 40 plates with iPLXDC2-mCherry

Day3　　　　　Mix and replate green and red cells in 384-well plate
　　　　　　　　　add inducer Doxycycline in each well
　　　　　　　　　add Hoescht to each well to label each cell blue
　　　　　　　　　add individual compound to each well

　　　　　　　　　　　　　　　　　　Incubate cells in the presence of
　　　　　　　　　　　　　　　　　　compounds for 72 hours

Day6　　　　Take picture of green, red, and blue cells in each well

Day 7　　　Count green, red, and blue cells in each well respectively

Day 9　　　　　　　Download cell counting result
　　　　　　　　　　upload data to CDD website
　　　　　　　　　　annotated each
　　　　　　　　　　384-well plate

Day 10　　　　　Analyze data in CDD website and
　　　　　　　　　identify interesting compounds

Figure 4-6. The workflow of each round of screening
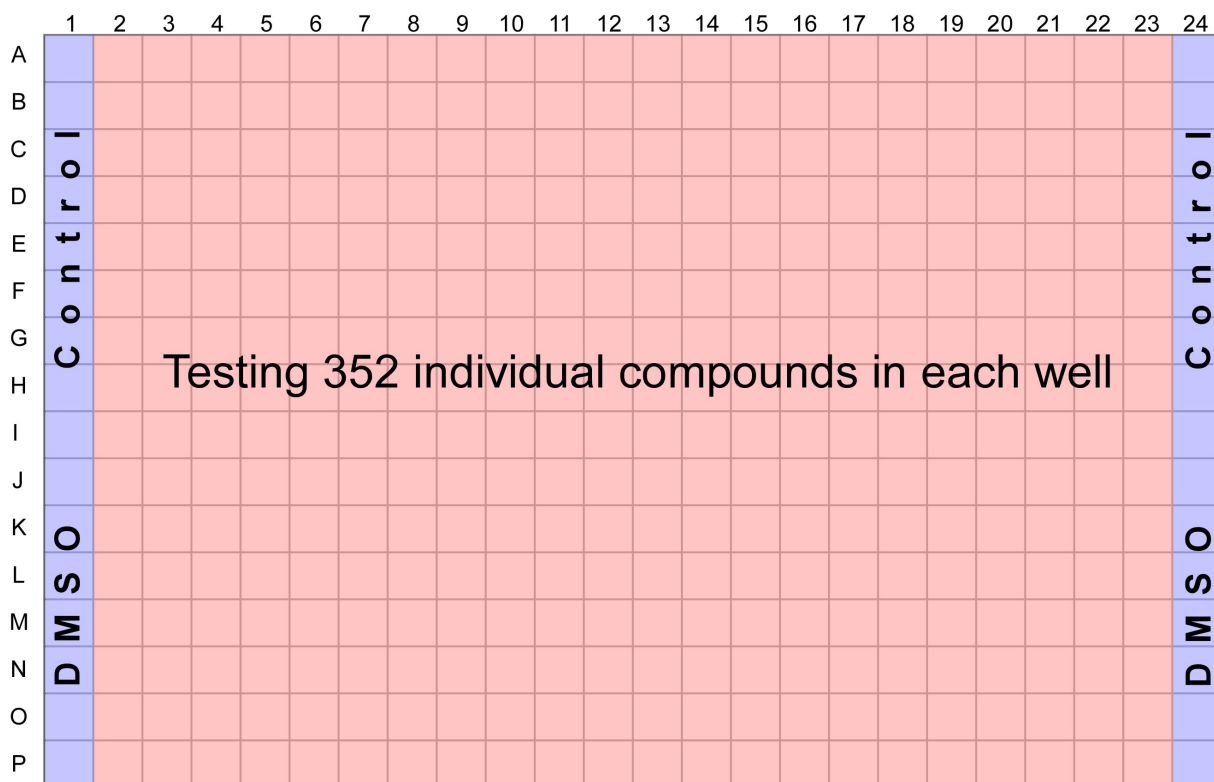
Figure 4-7. A sketch of the design for a 384-well plate

Different compounds were applied to each of the middle 352 wells. The first and last column of 384-well plate were pinned with DMSO at the same concentration as compound to serve as blank control.
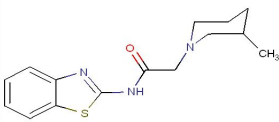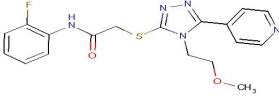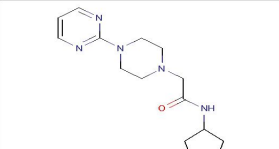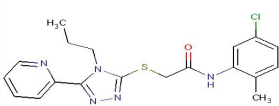
A

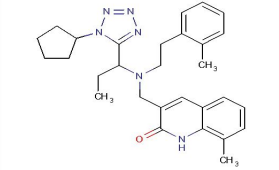Blue Channel   Green Channel   Red Channel
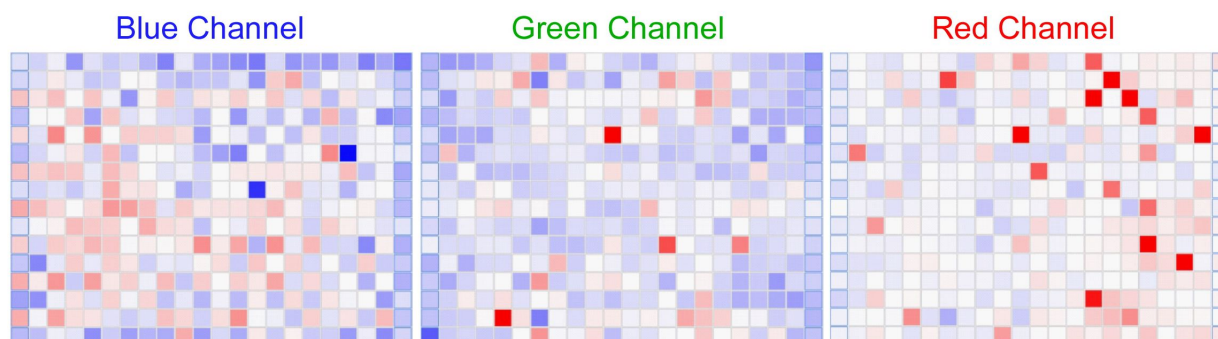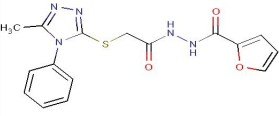

B

Molecule Name	Structure	Plate Name	Plate Well	Green % negative control (%)	Green z score	Red % negative control (%)	Red z score	Total number of cells % negative control (%)	Total number of cells z score
AST 6977948		TAR-13	B08	52	-3	79	-1	100	0
AST 04025382		TAR-5	B08	65	-4	92	0	95	-1
ASN 08245362		DL-52	B08	73	-3	110	1	102	0
ASN 05944572		DL-45	B08	68	-4	90	0	105	0
ASN 05305314		DL-11	B08	56	-4	98	0	95	-1
ASN 03016914		DL-12	B08	47	-4	80	-1	94	0

Figure 4-8. Display of screening results in CDD

143

(**A**) Screening results of a plate shown as heat maps in CDD. Heat map was generated by color coding the fluorescent signal in each channel. Basically, blue color represents a decrease in signal compared to average and red color represents an increase in signal compared to average. Heat maps showing fluorescent signals from untransfected cells (blue channel, left), PLXDC1 expressing cells (green channel, middle) and PLXDC2 expressing cells (red channel, right) were displayed. (**B**) An example of computer aided compound selection. A filter was applied to select compounds that decrease green cell number by at least 40%, but changed blue cell and red cell number by less than ±10%. Compound ID number, structure were listed.
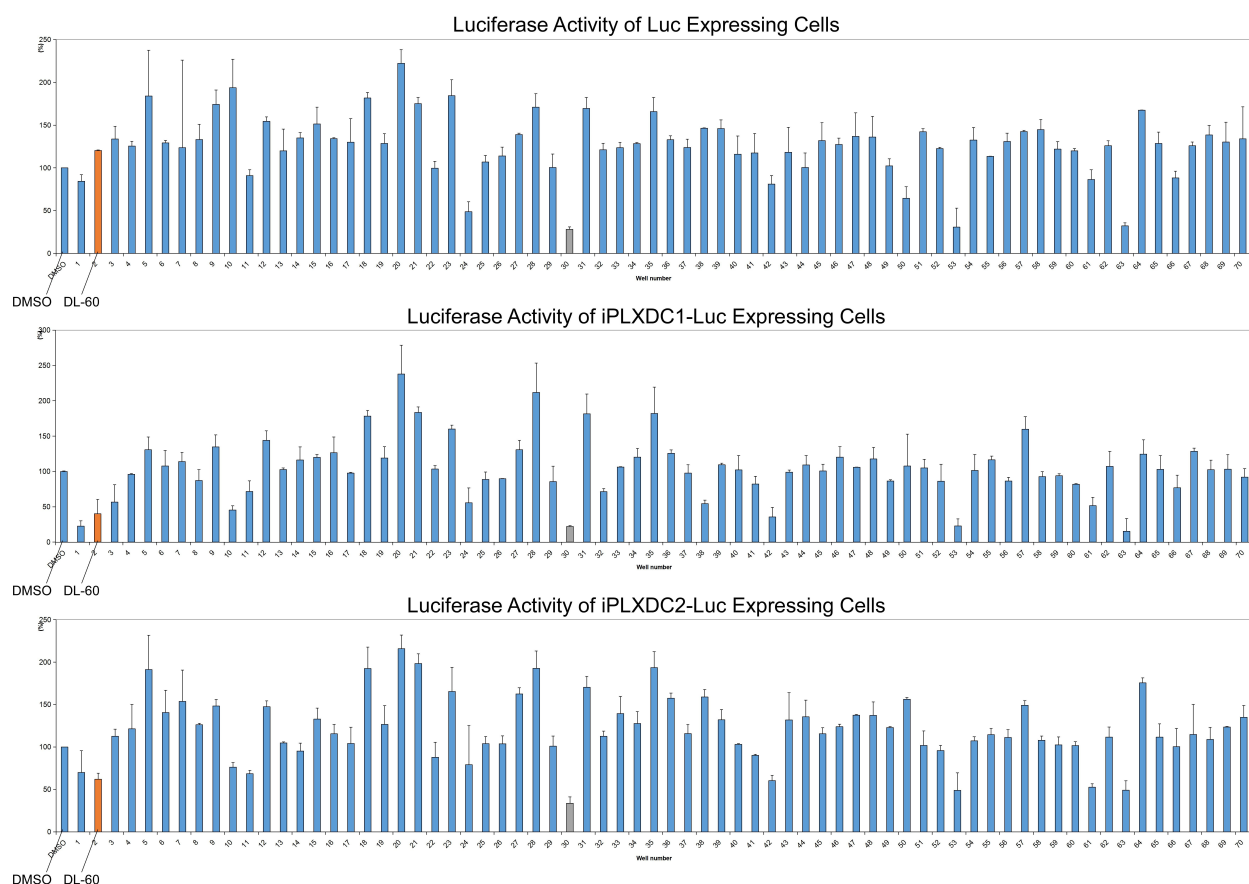
Figure 4-9. An example of luciferase-based verification of 70 compounds

Seventy compounds selected from fluorescence-based screening were tested with DMSO as control. The luciferase activity was compared among control (Luc transfected), PLXDC1-(iPLXDC1-Luc transfected) and PLXDC2- (iPLXDC2-Luc transfected) expressing cells. Compounds were tested in triplicates. As shown in the figure, compound DL-60 (orange column) suppressed the luciferase activity of PLXDC1 and PLXDC2 expressing cells by more than 60% and 40% respectively, but slightly increased the luciferase activity of control cell. However, compound marked as grey column non-specifically suppressed the luciferase activity of all

PLXDC1 expressing-, PLXDC2 expressing- and control cells. Luciferase activity of DMSO
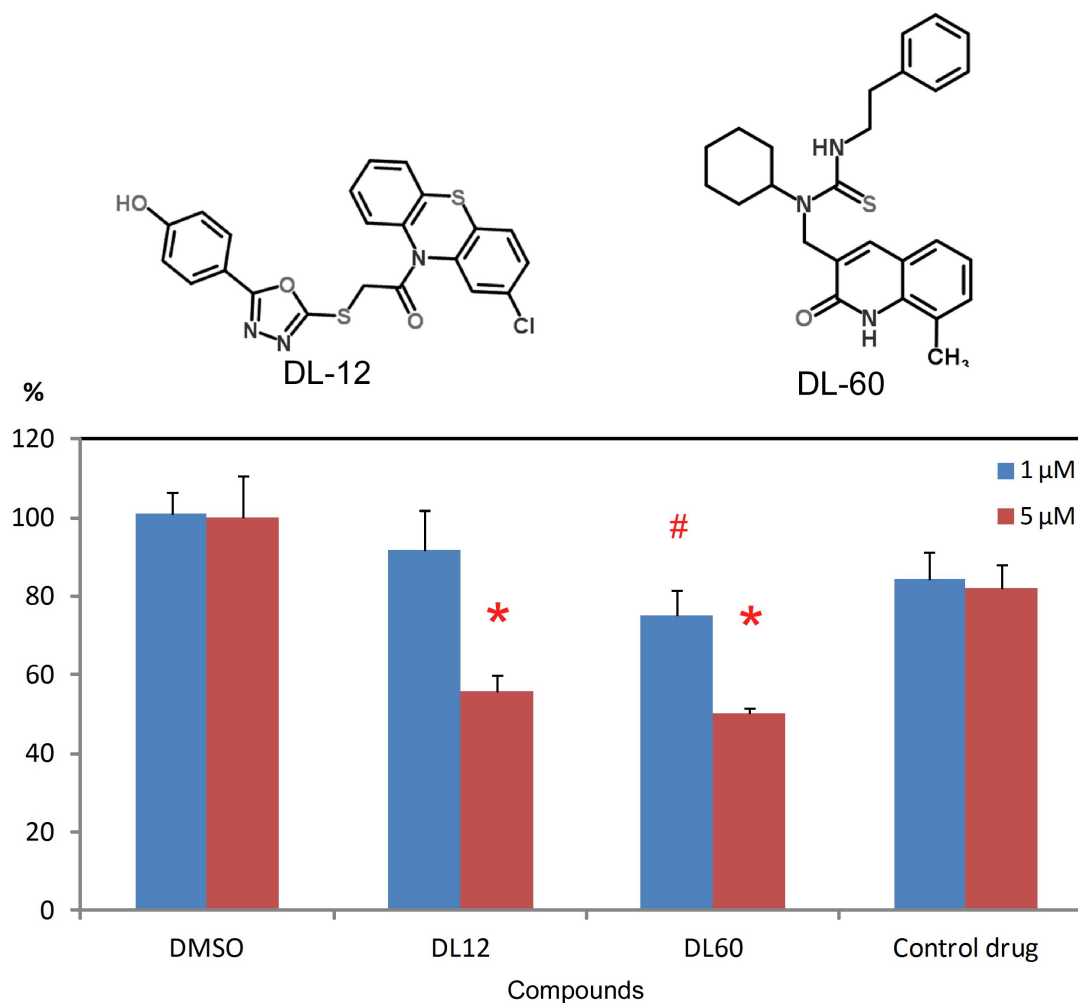
treated cells were regarded as 100%.

Figure 4-10. SVEC4-10 cell death induced by DL-12 and DL-60.

Endothelial cell SVEC 4-10 were plated in SFM with 1 or 5 μM compounds and cultured for 72 hours before evaluation of cell death by MTT assay. DMSO and a random compound served as control. Both DL-60 and DL-12 caused almost 50% cell death at 5 μM, and DL-60 caused 20% cell death at 1μM compared to DMSO control. #: $p < 0.01$ vs. 1 μM DMSO; *: $p < 0.01$ vs. 5 μM DMSO. Drugs were tested in triplicates. The structures of DL-12 and DL-60 are shown above the graph.
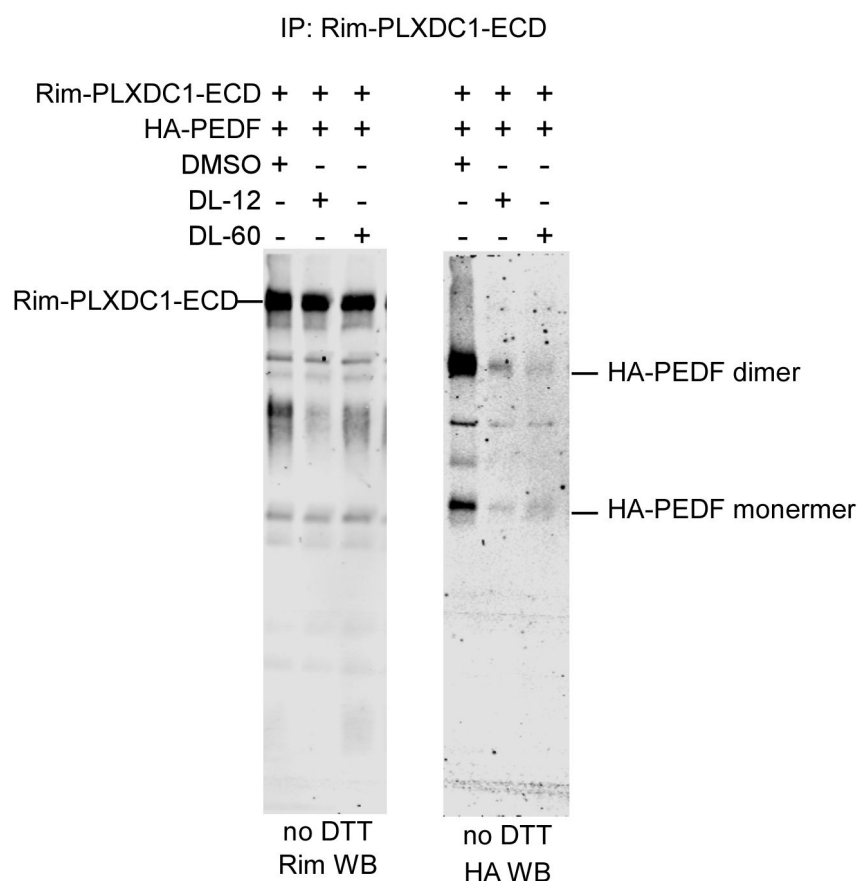
Figure 4-11. DL-12 and DL-60 interfere with the interaction of PLXDC1-ECD and PEDF

DL-12 or DL-60 or DMSO were added to the medium of HEK293T cells secreting Rim-PLXDC1-ECD and HA-PEDF. Final compound concentration was 5 µM. After 48 hours of incubation, cell conditioned medium were harvested and purified using anti-Rim antibody. Purified proteins were eluted and resolved in SDS-PAGE gel in a non-reducing condition. Anti-Rim antibody (left) and anti-HA antibody (right) were used to probe the purified proteins. HA-PEDF was copurifed mostly as dimer. DL-12 or DL-60 dramatically reduced the HA-PEDF copurified compared to DMSO control.

References

Damoiseaux R. Molecular Screening for Therapeutic Agents. Gad SC, editor. Hoboken, NJ: John Wiley & Sons, Inc.; 2011.

Rask-Andersen, M., Almen, M. S., and Schioth, H. B. (2011) Trends in the exploitation of novel drug targets, *Nat Rev Drug Discov 10,* 579-590.

Takenaka, T. (2001) Classical vs reverse pharmacology in drug discovery, *Bju Int 88 Suppl 2, 7-10; Discussion* 49-50.